The Republic of Iraq
Ministry of Higher Education
and Scientific Research
University of Anbar
College of Engineering
Mechanical Engineering Department

Enhancement of Hydrothermal Performance of Pinned Plate – Fin Heat Sinks Using Nanofluids

A thesis

Submitted to the council of the college of engineering - University of Anbar in partial fulfillment for the requirements of the master degree of science in mechanical engineering

By
Ahmed Mufeed Fadhil
(B.Sc. in Mechanical Engineering - 2014)

Supervised by:
Dr. Wissam H. Khalil
Dr. Amer J. Shareef

Rabi al-awwal 1441 **November 2019**

Copyright

Student Name: Ahmed Mufeed Fadhil

Address: University of Anbar, Collage of Engineering, Mech. Eng. Dep.

The Title of Thesis: Enhancement of Hydrothermal Performance of Pinned Plate – Fin Heat Sinks Using Nanofluids

Abstract

The heat dissipation from electronic devices, transformers, IC engine etc., is one of the most critical challenges facing modern industries. High temperature causes a problem in devices and sometimes cause damage. Thus, it is favourable keeping these devices at a limited temperature and take care to cool it to enhance devices work life. The heat sink is one of the common ways to cool electronic components and remove heat generation.

This research uses pinned flat plate heat sinks with SiO_2-water nanofluids to enhance the hydrothermal performance and entropy generation of heat sinks. The computational investigation and simulation of pinned flat plate heat sinks are performed by using ANSYS-Fluent V.14.5. The equations of conjugate heat transfer and laminar convective fluid flow are solved using the finite volume method with a SIMPLE technique. The Pinned Plate – Fin heat sinks include three different pin cross sections; circular (PCP), square (PSP), and elliptic (PEP) as well as flat fins heat sinks as a traditional Case. SiO_2-water nanofluids as base fluid with various nanoparticle volume fraction of 0, 1, 2, 3, 4 and 5% and nanoparticles diameters 20nm have been examined for Reynolds number range between 100-1000. The number of pins (1, 2 and 3) is considered with different locations as well as different pins diameters (1, 2 and 3mm) at constant base wall heat flux at 10^5 W/m^2.

The main data display that the highest average Nusselt number is for PCP around 93% and 100% for pure water and 5% for SiO_2-water, respectively compared with plate fins heat sink. The PCP and PSP have the lowest base temperature, nearly 25% for pure water and 5% nanofluids. Furthermore, the highest hydrothermal performance is for PEP at 1.44 and 1.52 for water and SiO_2-water, respectively of *Re* =1000. While, at *Re*=800, the most magnificent hydrothermal performance is for PCP at 1.44 and 1.50 for water and SiO2-water, respectively. Three pins with 2mm of pins diameter have the largest hydrothermal performance. Moreover, the PCP and PSP have the smallest total entropy generation, approximately 42% for pure water and 5% SiO2-water among other heat sinks. Thus, it is recommended to use this kind of heat sinks with nanofluids instead of traditional coolant for cooling an electronic system.

Acknowledgments

Firstly, thank Allah for giving me the force, motivation and patience to complete this thesis.

Foremost, I would like to express my extreme gratefulness to my supervisors, (*Dr. Wissam H. Khalil*) and (*Dr. Amer J. Shareef*) for encouragement and advise me that has provided throughout my time as a student. I have been fortunate to have supervisors who cared very much about my work, and who responded to my questions and queries very politely and immediately.

Last but not least, I wish to thank everyone who has been involved in any way with this research endeavor.

Ahmed …

Dedication

This thesis is dedicated to....

First and foremost, I have to thank my parents for their love and support throughout my life.

To my brothers and sister.

To my best friends.

To the spirit of my late friend Amer Karim.

Finally, this project is dedicated to all everyone who has taught me.

Ahmed…

List of Contents

Table of Symbols

A_c	[m^2]	cross section area
A_T	[m^2]	total Surface Area
BCs	-	boundary conditions
d_c	[mm]	circular pin diameter
de/De	-	Small diameter/large diameter for elliptic pin
D_h	[mm]	Hydraulic diameter
d_p	nm	particle diameter
d_f	[m]	Molecular diameter of water
M	[kg/mol]	Molecular weight of base fluid
N	[mol^{-1}]	Avogadro number
H	[mm]	Heat sink height
h_{ave}	[$W/m^2.^oC$]	Average heat transfer coefficients
H_b	[mm]	Heat sink base height
H_c	[mm]	Height of the channel
H_p	[mm]	pin height
HTP	-	Hydrothermal performance
k	[W/m.K]	Thermal conductivity
L	[mm]	Length of the heat sink channel
L_s	[mm]	Sides square pin
$\overline{Nu}$	-	Average Nusselt number
P	[Pa]	Pressure
p	[m]	wetted perimeter of CHS channel
Q	[W]	Heat source

Re	-	Reynolds number
R_{th}	[K/W]	thermal resistance
S_{gen}	[W/K]	The entropy generation
T	[ºC]	Temperature
u, v ,w	[m/s]	Velocities components
W	[mm]	Heat sink width
W_c	[mm]	Width of Channel
x, y, z	[m]	3D Cartesian coordinates
Z_1,Z_2,Z_3	-	Pins location
z_1,z_2,z_3	[mm]	Distant of pins from heat sink channel edge

Greek symbols

μ	[N.s/m^2]	Dynamic viscosity
ρ	[kg/m^3]	Density of fluid
C_p	[J/kg K]	Specific heat
Φ	-	Volume fraction
β	-	Fraction of the liquid volume traveling with a particle
α	[m^2/s]	Thermal diffusivity

Subscripts

f	-	Base fluid zone
s	-	Solid zone
n	-	Nanofluids
in	-	Inlet
out	-	Outlet

b	-	Base heat sink
w	-	Wall
eff	-	effect

Abbreviations

CFD	-	Computational Fluid Dynamics
FPHS	-	Flat Plate heat sink
FPHSs	-	Flat-Plate Heat Sinks
GIT	-	Grid Independence Test
GNPs	-	Graphene Nano-Platelets nanofluids
HSs	-	Heat Sinks
JF	-	Performance evaluation criterion
MCHSs	-	Microchannel Heat Sinks
Mini-CHSs	-	Mini-Channel Heat Sinks
PCP	-	Plate-circular pins heat sink
PEP	-	Plate-elliptic pins heat sink
PHSs	-	Pinned Heat Sinks
PSP	-	Plate-square pins heat sink

List of Figures

Number Figure **Page**

List of Tables

CHAPTER ONE

Introduction

1.1 Background

Heat dissipation elimination is one of the most important factors, which affected the performance of electronic equipment. More than 50% of the electronic devices failure are linked to the effect of overheat temperature, as shown in Figure 1.1. The recent trends of electronic industries are to achieve tiny components and more heat removal. Besides, a significant request on the system reliability and high performance has been increased due to the needs for optimum thermal management of electronic devices. Consequently, one of the most critical areas for the application of heat transfer techniques achieves the control and optimal thermal shape of electronic devices using heat sinks. The improvements in the thermal shape have become possible after the development of heat transfer techniques, tools and the solutions of computational methods. Mainly, the modern advancement in the subject of computational fluid dynamics (CFD) significantly improves the ability to achieve the mission of thermal system shape [1].

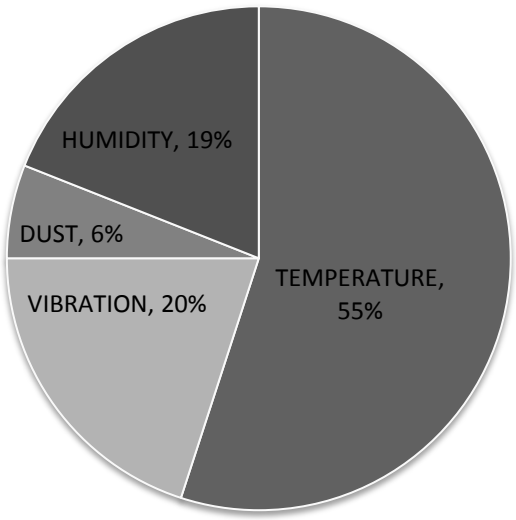

Figure1-1: Major failures reasons of electronic devices [1]

Heat Sinks are one of the most critical applications to enhance heat transfer capability in electronic devices. After the development of electronic devices and today's smaller size and high thermal performance, the challenges of dispersing a large amount of heat have been considered. Over the last three decades, various tests have been achieved for improving the hydraulic-thermal performance of heat sinks to obtain the highest heat dissipation with smaller heat sinks. Heat dispersion from heat sink may be enhanced by different ways such as coolant type (nanofluids and others), the behaviour of flow and geometrical modification. Among many proposed techniques to augment heat transfer, the coolant type with geometrical modifications has been noticed remarkably [2]. Figure 1-2 shows the different cross sectional geometries of microchannel used by researchers, note that more than 58% of researchers used rectangular microchannel geometry compared to other shapes. The Pinned Plate – Fin heat sink is one kind of many heat sinks shapes, which includes flat plate fins and pins, as shown in Figure 1-3.

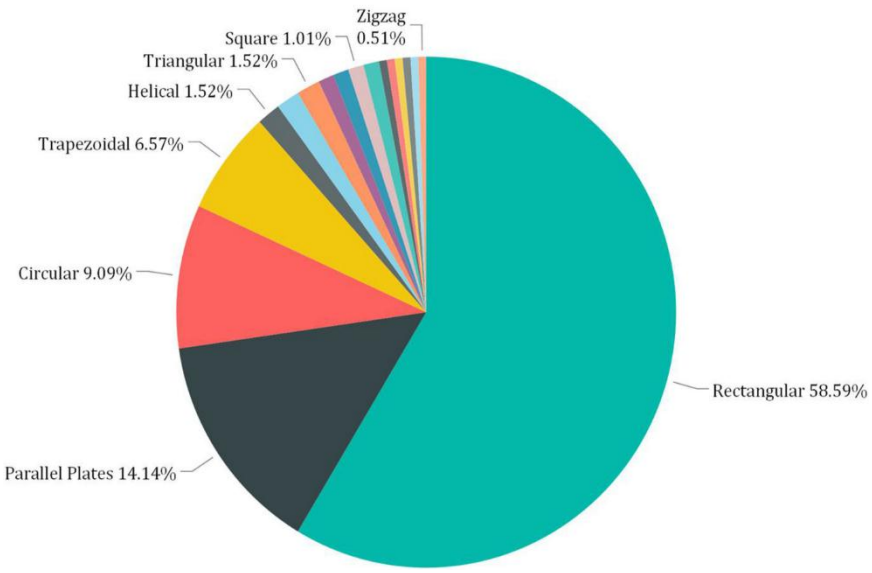

Figure 1-2: Microchannel shapes in the previous publications [3]

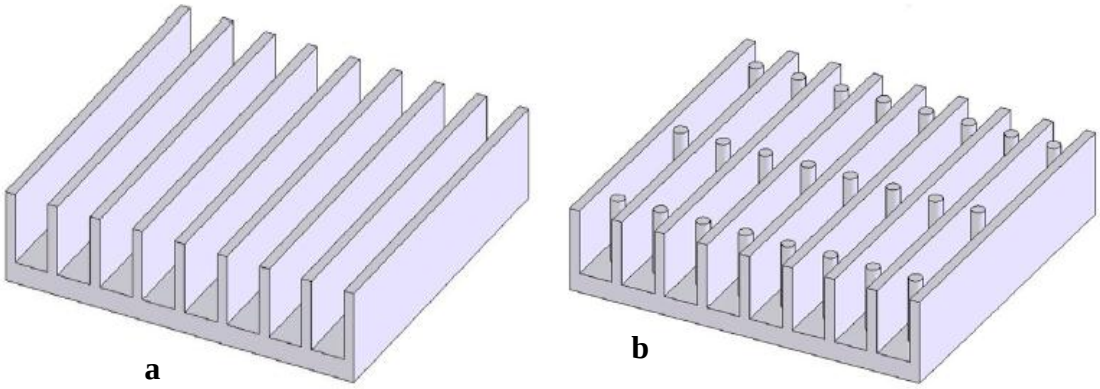

Figure1-3: Schematic diagrams of (a) plate fins heat sink and (b) plate-pin fin heat sink [4]

1.2 Nanofluids

From the viewpoint of coolant type, the low specific heat and thermal conductivity of the traditional thermal fluids such as (oil, ethylene glycol and water) are considered because they play as one of the obstacles to enhance the heat sinks performance. To overcome this issue, the thermal conductivities of thermal liquids can be improved by adding nanoparticles to these base liquids, with particles sizes less than 100nm. Thus, the nanofluids thermophysical properties of viscosity, thermal conductivity, specific heat and density depend on the various parameters such as the size of the nanofluids particles, the concentration of the solid particle, and type of nanoparticles. Based on the 2^{nd} thermodynamics law, heat transfer and fluid flow behaviour in heat sinks are irreversibility process that generates the entropy inside system owing to collision between fluids particles. Hence, these particles have high cohesion force and kinetic energy results in a reduction of system valuable energy. The optimal value of the 2^{nd} thermodynamics relies on the entropy generation minimization with enhancement in the hydrothermal performance [5]. In 1995, the first achievement for the nanofluids was by Chio. Many types of nanoparticles such as SiO2, Al, Cu, Al_2O_3, ZnO, TiO_2, etc. were used with solvents such as water, ethylene, oil, etc. It is preferable to use oxidized metals in nanofluids because minerals alone are susceptible to corrosion and aggregation. The researchers found that nanofluids provide a significant improvement in heat transfer by enhancing of the thermal conductivity and the base fluid properties. Brownian motion, nanolayer and

the volume fraction of nanoparticle are the most important factors that lead to these improvements in base fluid properties. In addition, using nanofluids causes an increase in the friction factor and pumping power loss compared with pure water due to increasing the viscosity and density of water base fluid [6].

1.3 Problem Statement

The heat sink is one of the techniques, which used to enhance the heat transfer and heat dissipation. The enhancement of heat sink performance includes two ways to obtain the preferable shape and find the superior base fluid. In the beginning, it was used the simple shape and air as a coolant. Since heat generation of the electronic device increases, the researchers used a new shape of heat sink and water as a coolant, which gave the superior result compared with simple shape and air [7]. The heat dissipation using water-based fluid is limited to some extent. Thus, the nanofluids made a large development in the heat removal, which prompting researchers to use it as a base fluid for coolant. The small size and superior performance become necessary in the new electronic device shape. It obtains the preferable shape with the superior fluid cooling, which is a goal for researchers in the latest research to achieve the preferred thermal performance with attention to the cost and the possibility of manufacturing.

The current study tries to answer to the following questions:

1. What is the effect of different cross-section shapes of pins (circular, square and elliptic) with flat plate fins as a combined heat sink on hydraulic-thermal performance and the total entropy generation?

2. What is the effect of SiO_2-water nanofluids on the hydraulic-thermal performance and the total entropy generation compared with pure water?

1.4 Aim and Objectives

The main aim of the present investigation is to enhance the hydrothermal performance and reduce the base temperature of the heat sink and the total entropy generation as the flowing :

1. Investigate the effect nanoparticles volume fraction on the characteristics of heat transfer and fluid flow and the total entropy generation.
2. Studying the effect of different pins cross-section shapes (circular, square and elliptic) on the characteristics of heat transfer and fluid flow and the total entropy generation.
3. Assess the effect of locations and number of pins on the characteristics of heat transfer and fluid flow and the total entropy generation.
4. Studying the effect of pin hydraulic diameter on the characteristics of heat transfer and fluid flow and the total entropy generation.

1.5 Scopes of the Research

The scope of the present study is represented by the following:

1. Three different shapes of cross-section pins, which are circular, square and elliptic have been investigated in this study for laminar flow with Reynolds number range between 100-1000.
2. SiO_2-water nanofluids as base fluid with the nanoparticles volume fraction of 0, 1, 2, 3, 4 and 5 % and nanoparticles diameters 20 nm have been examined.
3. The number of pins (1, 2 and 3) is considered with different locations (Case 1 , Case 2 and Case 3) as well as the different hydraulic diameter of pins (1, 2 and 3mm) as constant heat flux at 10^5 W/m^2 (176.5W).

1.6 Outlines of Thesis

Explained briefly, there are five chapters of this thesis as follows:

1. Chapter one consists of the brief background of the heat sinks, problem statement, aim, objectives and the scope of the current study.

2. Chapter two presents some previous studies of experimental and numerical of the effect of different heat sinks shapes on the hydrothermal performance and entropy generation.

3. Chapter three reviews the steps of the numerical study of the current study by use ANSYS-FLUENT 14.5. It is included a research approach, computational domain, assumptions, boundary conditions and numerical procedure.

4. Chapter four explains the results and discussion of the current study. It is included the effect of nanoparticles volume fraction, Reynold number, the geometry of pins, the locations and number of circular pins, the diameter of circular pins on the characteristics of heat transfer and fluid flow and the total entropy generation.

5. Chapter five illuminates the main conclusions of the current investigation and highlight some suggested recommendations for future studies.

6. Finally, references, which are used in this study, are listed.

CHAPTER TWO

Literature Review

2.1 Overview

In this chapter, the previous studies presents the characteristics of forced convection heat transfer of heat sinks (HSs) using liquids as working fluid. The numerical and experimental reports of straight flat-plate and pinned heat sinks with liquids (water and nanofluids) are explained in the first part. The second part is provided the numerical and experimental studies of flat plate-pin heat sinks (pin-fin heat sinks) with and without using nanofluids.

2.2 The Flat-Plate Heat Sinks (FPHSs)

In the next articles, microchannel heat sinks were numerically investigated using water and nanofluids for electronic device cooling.

Xie et al. [8] studied the thermal performance of single and double-layer micro-channel heat sinks. Water was a coolant applied with different velocity range from 0.6m/s to 1.4m/s. This study included three types of microchannel heat sink such as rectangular straight channel, wavy single-layer and wavy double-layer. The effect of wave amplitude on pressure drop, heat transfer, and thermal resistance was considered. The results found that theaverage Nusselt number increases as the wavy length increases because the Dean number reduces with increasing wavy length. The thermal performance of the wavy micro-channels is higher than the straight micro-channels with the same cross-section. Furthermore, the single layer was less heat transfer rate and more significant pressure drop compared with double layer wavy micro-channel. **Ahmed and Ahmed [9]** investigated the effect of the different groove shapes on the heat transfer enhancement. The study included three different groove shapes; rectangular, triangular and trapezoidal with variable pitch, the orientation of the cavities and tip lengths. Water was used as a coolant with range of Reynolds number from 100 to 1000 under constant heat flux 1000 kW/m^2. It is explained that the highest value of performance evaluation criterion (JF) was with ratio 0.4 of

groove depth. The maximum JF of groove pitch ratio and the orientation ratio were 3.33 and 0.0, respectively. At the lowest Reynolds number, the thermal performance is the highest. Besides, the optimum shape were for trapezoidal with the ratio of groove tip length, depth, pitch, and orientation were 0.5, 0.4, 3.334 and 0^{o}, respectively. At Reynolds number 200, it is provided 51.6% of enhancement in Nusselt number and friction factor increases about 2.35%.

The effect of nanoparticle on the nanofluids performance in trapezoidal micro-channel heat sink was studied by **Fani et al. [10].** The study included copper-oxide nanofluids with a range of spherical nanoparticle size and volume concentration was between 100-200 nm and 1-4%, respectively. The numerical data showed that the pressure drop enlarges when the nanoparticle size increases and the enhancement in heat transfer reduces. **Chen and Ding [11]** studied the analysis of the effect of Al_2O_3 nanofluids on the micro-channel heat sink performance with mass flow rate between 200-1000 cm^3/min. The study used the Brinkman-Forchheimer-extend Darcy equation model, Navier-Stokes and energy equations. It is indicated the temperature distribution of the channel wall is found to be practically in sensitive to the inertial effect, while the fluid temperature distribution and the total thermal resistance alter noticeably due to the inclusion of flow inertial force.

Hung et al. [12] reported the effect of nanoparticle type, particle size and particle volume fraction on the heat transfer enhancement and pumping power of heat sinks. Six different types of nanofluids (Al_2O_3, CuO, TiO_2, Cu, Ag and Diamond) with water base fluid were considered using 0.5 %, 1%, 2%, and 5% volume fraction. The flow rate range was between 200 and 1000cm^3/min. The findings indicate that alumina-water nanoparticle achieves the greatest heat transfer enhancement compared with other types of nanofluids. The maximum enhancement ratio of heat transfer was around 21.6% as diamond-water and Al_2O_3-water were used. Furthermore, all kind of nanofluids caused reducing in the thermal resistance by growth pumping power. The thermal resistance increases when the particle size increases. The entropy generation of microchannel heat sinks with different geometries with pure water has been investigated by **Alfaryjat et al. [13]**. Geometries of microchannel were three

different sections such as square, circular, and hexagon. This study covered various Reynolds number range between 100 and 1600 and different heat flux 125, 150, 175 and 200kW/m^2. It is found that the entropy generation reduces when the Reynolds number increases and the applied heat flux decreases. The square cross-section has the lowest number of entropy generation and total entropy generation compared with the circular and hexagonal MCHS. **Alfaryjat et al. [14]** investigated the effect of different nanofluids such as SiO_2-water, CuO-water and Al_2O_3-water with different heat flux on the entropy generation of a hexagon microchannel heat sink. The range of Reynolds number and the heat flux were 200-1500 and 125-500 kW/m^2, respectively. They found that the smallest entropy generation is for pure water at minimum heat flux and great Reynolds number. However, for maximum heat flux, the nanofluid is recommended to reduce the total entropy generation. Furthermore, the Al_2O_3-water has the minimum the total and thermal entropy generation while the SiO_2-water has the lowest frictional entropy generation. The thermal entropy generation decreases and the frictional entropy generation increases with increasing the concentration of nanofluids. **Shalchi-Tabrizi and Reza [15]** have investigated the hydrothermal characteristics and the entropy generation of a circular microchannel heat sink with Al_2O_3-water nanofluids. Utilizing Al_2O_3-water nanofluids with different particle diameters and volume fractions were numerically examined. The data indicated that hydrothermal performance was enhanced with the increasing volume fraction of nanofluids. Besides, the total entropy generation is reduced with increasing Reynolds number and nanofluids concentration and declining nanoparticles size.

The following studies have experimentally investigated the hydrothermal performance of microchannel heat sinks.

Microchannel heat sink which was made from copper with a 50 mm length, 800 µm width and 283 µm cross-section area was studied **by Ho et al. [16]** with alumina-water nanofluids. In this study, 25 parallel rectangular micro-channels were used with the range of Reynolds number between 226-1676, nanofluids particle volume fractions 1% and 2% under uniform heat flux. The results presented that the

maximum convection heat transfer coefficient was nearly 70% at the largest flow rate for 1% nanofluids concentration compared with pure water. While the wall temperature and thermal resistance were reduced by 25% and 0.029 K/W, respectively. **Duangthongsuk et al. [17]** studied the effect of the particle concentration and the Reynolds number on the micro-channel heat sink with Al_2O_3-water nanofluids. The rectangular microchannel heat sink was fabricated from aluminum with square dimensions 50mm ×50mm. The Al_2O_3-water of nanoparticle concentration of 1, 2 and 3% was tested with two heaters has capacity 50W for each of them, which is applied on the heat sink bottom. The nanofluids achieve higher convection heat transfer coefficient by approximately 7-15% than that of pure water. The wall temperature of the micro-channel heat sink reduce with increasing Reynolds number for the same nanofluids concentration. Additionally, the increment effect of particle concentration is small on the pressure drop, while the pressure drop increases as Reynolds number grows for nanofluids and water micro-channel heat sink.

The effect of chevron fin interruption on thermo-fluidic transport characteristics of nanofluids-cooled electronic heat sinks was experimentally and numerically studied by **Hassani et al. [18].** Water and Al_2O_3-water nanofluids were utilized with two nanofluids concentration 0.5% and 1% and the range of Reynolds number from 100 to 900 under constant heat flux at 25000 W/m². The length, width and height of channel were 100 mm, 20 mm and 5 mm, respectively. The study included seven different cutting off fins and compared it with the traditional channel heat sink. The findings showed that the pressure drop increases in all Cases with increasing Reynolds number and nanofluids particles concentration. The coefficient of convection heat transfer is also enhanced as Reynolds number increase. Besides, the enhancement in heat transfer of interrupted models occurs due to swirling flows and it has lower fin base temperature compared with the traditional models. **Halelfadl et al. [19]** analytically studied the effect of the aqueous-carbon nanotubes based nanofluids on the pressure drop and thermal performance of the rectangular microchannel heat sink. The aqueous nanotubes based nanofluids were used as coolant with 0.01% concentration. The study examined the effect of aspect ratio and wall ratio of a channel with an inlet temperature effect on the pumping power and thermal

resistance. The findings showed that when the nanofluids are used, the enhancement of heat transfer rate is by 13 % at 40 ºC, 12 % at 30 ºC and 2% at 20 ºC. It is obtained that the thermal resistance of heat sink with nanofluids is lower than that of pure water. Further, the most significant thermal performance is achieved at higher exchange surface area and narrower channel. **Manay et al.** [**20**] have studied the effect of channel height of rectangular microchannel heat sink on the entropy generation with TiO_2-water nanofluids. The channel heights are 200 µm, 300 µm, 400µm, and 500µm are considered in this study. Besides, the Reynolds number was 100-750 with different particle volume fractions at (0.25%, 0.5%, 1.0% and 2.0%) under constant heat flux. It is found that the lowest entropy generation is obtained for the largest height of the channel. The increase in the nanofluids concentration leads to lower entropy generation. Also, the thermal entropy generation is reduced and, the frictional and total entropy generation is improved as the Reynolds number increases.

The following section deals with several numerical and analytical works on the miniature heat sinks (Mini-CHSs).

Ijam et al. [21] analytically investigated the effect of nanofluids types and volume fraction on the heat transfer characteristics. This study used two kinds of such nanofluids as Al_2O_3-water and TiO_2-water with a concentration range between 0.8% and 4% and mass flow rate range from 0.0076 kg/s to 0.127 kg/s. Dimensions of the mini-channel heat sink were 20 mm×20 mm with varying heat flux applied on the heat sink base from 156.2 W/cm^2 to 160.7 W/cm^2. The authors indicated that the maximum enhancement in the thermal conductivity was 12% for Al_2O_3-water and 10% for TiO_2-water at 4% volume fractions compared with pure water. The most significant improvement of cooling was roughly 17.3% as the inlet velocity was 0.1 m/s and 0.8% of Al_2O_3-water nanofluids. While it is about 2.95% as velocity inlet was 1.5 m/s and 4% particle concentration for the same nanofluids. Furthermore, the pumping power and pressure drop for TiO_2-water and Al_2O_3-water were 0.000552W and 73.7Pa at 0.1 m/s of inlet velocity and 0.12437 W and 1105.54 Pa at 1.5 m/s of inlet velocity with 4% volume fraction. **Mohammad et al. [22]** examined the numerical and analytical behaviour of the miniature heat sinks performance using

SiO_2-water nanofluids. The study used the numerical solution for temperature profile and analytical solution for velocity profile. Two equation models have been applied to heat transfer between the liquid and solid material of heat sink, while the Darcy equation was used for fluid flow. The effects of channel aspect ratio and porosity on heat transfer coefficient of the heat sink are studied in detail The heat sink channel length, height, width and fin thickness were 40, 12, 2, 2 mm respectively, under constant heat flux thermal boundary condition. The results explained that when the porosity and aspect ratio of the channel increase, the characteristics of heat transfer improve. The use of SiO_2-water nanofluids instead of water led to enhance the rate of heat transfer.

In the next section, minichannel heat sinks have experimentally tested using water and nanofluids.

Jajja et al. [23] studied the effect of fin spacing of mini-channel heat sinks for microprocessor cooling using water. Five different heat sinks were used with fin spacing of 0.2 mm, 0.5 mm, 1 mm, and 1.5 mm with heater power 325 W. The results showed the lowest heat sink base temperature of 40.5 ºC was achieved by using a heat sink of 0.2 mm fin spacing which was 9% lower than the best reported value of base temperature of 40 ºC by using a nanofluid with a commercially available heat sink. The heat transfer of nanofluids in the mini-rectangular fin heat sinks have been investigated by **Naphon and Nakharintr [24].** TiO_2-water was used and compared with de-ionized water. This study has been conducted three different channel heights 1 mm, 1.5 mm and 2 mm with length, width and base thickness of 110, 60, and 2 mm, respectively. Besides, the Reynolds number was 80-200 at constant particle volume fraction (0.4%) and constant heat flux. The data indicated that the preferable heat transfer enhancement heat sink is at channel heights 2mm. Furthermore, the pressure drop of nanofluids was approximately the same that of de-ionized water.

The following researchers experimentally and numerically investigated the hydrothermal performance of minichannel heat sinks.

Hassani and Mazloumi [25] tested the effect of the pin-fins interruption on the thermal performance of straight and wavy heat sink. Water and Al_2O_3-water nanofluids were used and the range of Reynolds number was between 100 and 900. The nanofluids concentration were 0, 0.1 and 0.4%. The outcomes explained that the closeness between the experimental and numerical study was 9% for the pressure drop and 5% for the heat transfer rate. The largest enhancement of hydraulic-thermal performance was for the interrupted miniature heat sink compared with the traditional miniature heat sink. The hydrothermal performance factor for interrupting small heat sink was higher than that of the straight small heat sink by 1.19-2.32 times for Reynolds number range from100 to 900. While the wavy channel miniature heat sink presented a higher thermal performance by 1.23–2.28 times compared with the straight channel. Furthermore, the nanofluids particle rises the heat transfer rate and pressure drop by 2.2–28.2% and by 1.3–12.7% respectively, compared with pure water. **Fazeli et al. [26]** conducted the characteristics of heat transfer in a miniature heat sink using SiO_2-nanofluids. The circular channel heat sink diameter and length were 4mm and 40mm, respectively. Moreover, 180 W/cm^2 constant heat flux was applied on the base of heat sinks and the Reynolds number range between 400-2000 with 3.5–5% of nanofluids particle concentration. It is observed that SiO_2-nanofluids has provided higher enhancement of the heat sinks performance than water base fluid. The enhancement of thermal performance develops while the thermal resistance reduces as the Reynolds number and particle concentration increase.

The different mini-channel heat sinks with alumina-water nanofluids were investigated by **Saeed and Kim [27]** to enhance the heat transfer rate. The study involved the array effect of channels, the volume fraction and coolant flow rate on the heat transfer enhancement. Four different arrays and two nanofluids concentration volume fraction (1% and 2.5 %) with a flow rate range between 0.5L/min-1.5L/min and also with 325W of constant heat flux. The outcomes indicated that the enhancement of the heat transfer coefficient was around 31%, 27.6%, 25% as the spacing of fins 0.5mm, 1mm and 1.5mm respectively. The improvement of heat sinks performance was about 1.33, 1.29 and 1.28 as fins spacing 0.5mm, 1mm and 1.5mm respectively.

The effect of heat transfer performance on the electronics cooling system using Al_2O_3-water nanofluids has been experimentally performed by **Sohel et al. [28].** The mini-channel heat sink dimensions were 50mm×50mm×10mm and it is fabricated from copper. The volume flow rate and the nanoparticle concentration ranges were 0.5L/min-1.25 L/min and 0.05%-0.2%, respectively. The experimental data found that the base temperature of heat sink reduces when the volume flow rate rises. The entropy generation decreases approximately by 11.5% as nanofluids were replaced by pure water. Furthermore, the increase in the nanofluids concentration and the volume flow rate cause a growth pressure drop and the entropy generation while the base temperature of heat sink reduces. **Ho and Chen [29]** considered the alumina nanofluids effect on the thermal performance in the mini-channel heat sink. The heat sink was made from copper with 50 mm×1 mm×1.5 mm dimensions. Alumina-water nanofluids were used as a coolant with range concentration from 0.5% to 10% and compared it with pure water. The findings showed that in all Cases of cooling, the nanofluids provided the highest cooling performance compared with pure water. The heat transfer coefficient enhancement increases by 35% and 72% as the inlet and bulk temperature increase respectively at 10% of Al_2O_3-water.

2.3 Pinned Heat Sinks (PHSs)

Hasan [30] numerically reported the fluid flow and heat transfer characteristics in micro pins heat sinks. Three pin shapes such as triangular, circular and square have been compared with the flat microchannel heat sink. Diamond-water and Al_2O_3-water nanofluids were used as a coolant as well as pure water. Reynolds number was ranged from 100 to 900 and volumetric concentration was ranged between 1% and 4%. The outcomes showed that the different pins shapes with two types of nanofluids gave rise in the heat dissipation while the pressure drop across heat sinks increases. The performance of heat transfer rate for both nanofluids are higher than that of pure water and the heat transfer rate of diamond-water is the largest number. For both nanofluids types, the circular pins achieved the highest rate of heat dissipation compared with triangular and square pins, whereas the square pins have a higher pressure drop. Optimization of minichannels with short micro pin fins

with utilizing water has been tested by **Tullius et al. [31]**. The numerical study covered six pin-fin geometries; circular, hexagon, square, diamond, triangle, and elliptic which were used in a staggered array. In addition, the spacing and width of fins have been investigated with Reynolds number range between 100-1500. It is found that the highest Nusselt value was approximately 37% for the triangle pins. While, the minimum amount of pressure drop was for circular and elliptic pins compared with other pins shape, both the Nusselt number and the pressure drop increase when the height, width and spacing of pins increase.

In the next works, heat sinks have experimentally considered using water and nanofluids for electronic device cooling.

Duangthongsuk and Wongwises [32] experimentally studied the hydraulic-thermal performance of heat sinks, which is affected by a miniature circular pin fin. SiO_2-water and ZnO-water nanofluids were used in this study. The concentration range of nanofluids was between 0.2-0.6% with pure water. In addition, the inlet temperature of fluid flow was at 15ºC and the heat flux on the base of heat sinks range from 20 to 48 kW/m². The range of mass flow rate was between 0.65-3.32 kg/min. The diameter, pitch, height, and pins number were 1.2mm, 2.4mm, 1.2mm and 143, respectively. The results displayed that the enhancement of the heat transfer increased as the mass flow rate and nanofluids concentration increased. Additionally, the thermal performance was improved by about 3-9% and pumping power increment when SiO_2-water instead of ZnO-water for the same nanoparticle concentration. The nanofluids concentration was a small effect on the pressure drop for both nanofluids type.

The effect of form of mini array pin geometries with nanofluids on the pressure drop and heat transfer characteristics was studied by **Duangthongsuk and Wongwises [33]**. The heat sink dimensions were 33 mm×28 mm. The nanofluids type was SiO_2-deionized water with a concentration range between 0.2-0.6%. The Reynolds number and heat flux range were 700-3700 and 2-5W/cm², respectively. The test included two pin geometries square and a circular cross-section. The data showed that when the Reynolds number and the nanofluids concentration increased, the Nusselt number

improved. When SiO_2-water was used rather than water, the heat transfer rate increases by around 4-14%. Furthermore, the circular pins of miniature heat sink gave a development in the thermal performance by about 6-9% higher than that of the square pins of the miniature heat sink. The pressure drop of square pins heat sink is higher than that of the circular pins heat sinks.

The experimental and numerical studies of the effect of nanofluids and pin fins geometry on the performance of pin fins miniature heat sink were investigated by **Khoshvaght-Aliabadi et al. [34]**. This study was included 20 pins with eight shapes of pin geometry; circular, half circular, trapezoidal, hexagonal, triangular, rhombic, rectangular and square. The base plate of all plate-fin microchannel heat sinks is in a cube geometry with the length,width,height of 100, 20, and 5 mm, respectively. The Reynolds number range between 100-900 and the constant heat flux was 25000W/m² with Al_2O_3-water and pure water. They found that the circulation zone and the separation point of the boundary layer depend on the pin geometry. The highest values of the pressure drop and the heat transfer coefficient were recorded for the half circular pins. When the half circular was used instead of square pin fins, the enhancement of the heat transfer coefficient achieved nearly 85% and the pressure drop increases by 2.5 times. Furthermore, at minimum Re value, the pressure drop and the heat transfer coefficient were nearly 180% and 38%, respectively. While at maximum Re, the pressure drop and the heat transfer coefficient were about 290% and 121.5%, respectively.

The channel angle and water-based graphene nano-platelets nanofluids (GNPs) effect on the heat transfer characteristics of pin fins heat sinks was reported by **Ali and Arshad [35].** The experimental work was performed for the flow rate range of 0.25–0.75 LPM and the volumetric concentration of particles was 9.5%. Three different inclination angles of heat sink channel were applied such as 22.5^o, 45^o and 90^o under constant heat flux. The lowest thermal resistance and the maximum thermal performance are achieved at a 22.5^o. **Vinoth and Kumar [36]** investigated the effect of microchannel heat sinks with oblique micro pinned on heat transfer characteristics. Water and Al_2O_3-water were applied in this study. Three different channel cross

sections (square, trapezoidal and semicircular) were considered. The length and width of microchannel were 48 and 80 mm respectively. Reynolds number was from 325 to 850 and particle concentration 0.25% with varying mass flux from 100 to 450 $kg/m^2.s$. It is found that the nanofluids raise the heat transfer rate by 4.6% compared with pure water. The highest Nusselt number and heat transfer rate were produced by the trapezoidal pins compared with semicircle and square respectively. In addition, the pressure drop of the trapezoidal pins was higher than that of square and semicircular by around 16.8% and 24%, respectively. Thus, the trapezoidal cross-section has preferable thermal performance compared with others.

2.4 Plate–Pin Heat Sinks (PPHSs)

In the following section, several numerical studies have described the hydraulic thermal performance of microchannel heat sinks.

The heat transfer performance of single-phase heat sinks with micro pin-fins structures have been studied by **Shafeie et al. [37]**. Water is used as a coolant fluid with 10mm×10mm of heat sink dimensions. The plate-pin microchannel heat sinks (PPMCHS) and pinned heat sinks (PHSs) were considered with two Cases of pins array; oblique and staggered. Different height of micro plate-pin (500, 180, 90 μm) in MCHSs and PHSs were performed. The pumping power range was from 0.5W to 2W. It is observed that finned heat sinks, the Case with highest depth(500 mm) had the highest heat removal for a specific pumping power. The PFMCHSs have more substantial thermal performance than that of PHSs within the same pumping power. The channels height and fins height effect were more important than the plate-pin distributions on the amount of removed heat from the heat sinks. MCHSs and PHSs were not preferable compared with optimum traditional MCHS for the same pumping power. Moreover, the entropy generation reduces with increase removed heat of the heat sinks. **Ambreen and Kim [38]** investigated the effect of different pins shape with TiO_2-water on the thermal performance of MPFHS. It was used three different cross-section shapes of pins such as square, circular and hexagon with constant pins height and diameter. The in-line arrangement pins were used with constant heat flux

(192 W). Reynolds number was from 250 to 550 and the size and the particle concentration of 30nm and 4.31 vol%, respectively. Higher thermal performance was for the circular pins compared with other pins-shapes heat sinks. While the smallest value of the thermal performance was for square pins. Moreover, the Nusselt number enhances by nearly 26%, 44% and 62% for square, circular and hexagon respectively.

The silicon microchannel with cone pin fin geometry (MCPF) using deionized-water and Reynolds number range 147-637 was reported by **Jia et al. [39]**. This study considered the MCPF location effect on the cooling performance of heat sinks. These locations were included four Cases; up-stream, middle, down-stream and the fixed pin fins number throughout microchannel. The outcomes indicated that the Nusselt number and the friction factor of all Cases were larger than that of the flat rectangular microchannel. The preferable base temperature distribution was for the fixed number pin-fins whereas the middle location produced the preferred thermal performance for the microchannel. In addition, the cooling enhancement of the heat sink and the friction factor increase as the diameter and height of fins increase.

Macrochannel heat sinks have experimentally considered using water and nanofluids in the next section.

Roshani et al. [40] studied the effect of a plate-elliptical pin heat sink on the hydrodynamic and heat transfer characteristics with used TiO_2–water and Al_2O_3–water nanofluids. The sink length, width, and height were 42, 42, 14mm respectively and Reynolds range between 100 and 1100. In addition, the constant heat flux was 124.8 kW/m² and the nanofluids concentration were between 0.5% and 2%. It is found that the temperature on the bottom heat sink decreases by 1.8ºC and 1.4ºC for 2% of Al_2O_3–water and TiO_2–water. The highest values of heat transfer coefficient were about 16% and 14 % for 2% nanoparticle concentration of Al_2O_3–water and TiO_2–water, respectively. **Zirakzadeh et al. [41]** investigated the heat transfer characteristics in Pinned Plate – Fin heat sinks utilize Al_2O_3-water nanofluids with a concentration range between 0.5-2% and Reynolds number range from 200 to 1800. The dimensions of the heat sink were 42 mm length, 42 mm width and 14 mm height.

Five rectangular plate fins with three circular-pins for each channel are performed as constant heat flux is 180W/cm^2. The investigations showed that the thermal resistance of heat sink decreases and the heat transfer improves with increasing Reynolds number. The thermal resistance was around 23% drops while the heat transfer convection enhances by nearly 20% for the plate-pin heat sink compared with the plate fins heat sink.

2.5 Summary

The literature review included the experimental and numerical researches, the first section is about the flat-plate heat sink. The researchers in this section used many ways to obtain desirable shape and fins distribution. The second part was about the plate-pin heat sink, and it included different pins shapes cross-sections. In general, all the above researches used water and nanofluids as a coolant. The Nusselt number, heat transfer rate, pressure drop and hydraulic-thermal performance of the heat sink were discussed. According to the knowledge of authors, the two experimental studies were considered the plate fins and pins in the same heat sink). Thus, the current research will explain in details about the heat transfer and fluid flow characteristics of the plate-pin heat sinks with different pins geometries using water and SiO2-water nanofluids. Furthermore, the hydrothermal performance with entropy generation of this type of heat sink will be investigated to fill this gap. The following **Table 2-1** included the summary of all previous studies, classification according to type of study, geometry, Reynolds (or mass flow rate), type of base fluid, nanoparticle material, nanoparticle concentration and the main findings.

Table 2-1: Summary of literature review

Ref. (years of publication)	Type of Study and geometry	Re / $\dot{m}$	Base Fluid	Nano-particle Material	Nanoparticle Concentration (%)	Findings
Xie et al. [8] (2013)	Numerical, single and double-layer microchannel heat sinks	100-230	water	-	0	Nu ↑ as the wavy length ↑ The thermal performance of the wavy micro-channels is higher compared with the straight channels with the same cross-section.
Ahmed and Ahmed [9] (2015)	Numerical, Grooves shapes	100-1000	water	-	0	Nu ↑ 51.6% f ↓ 2.35%.
Fani et al. [10] (2013)	Numerical, trapezoidal microchannel heat sink	500	water	copper-oxide	1-4	ΔP ↑ nanoparticle size ↑ and the enhancement in heat transfer ↓.
Chen and Ding [11] (2011)	Analysis, micro-heat sink	200-1000 cm^3/min	water	Al_2O_3	0-0.05	The effect of the inertial force on the distribution of T_w < (R_{th} and T_f).
Hung et al. [12] (2012)	Numerical, microchannel heat sink	240-660 cm^3/min	water	Al_2O_3, CuO, TiO_2, Cu, Ag and Diamond	0.5, 1, 2, and 5	Al_2O_3-water achieves the greatest heat transfer enhancement compared with other types of nanofluids. The maximum enhancement ratio of heat transfer is around 21.6% as diamond-water and Al_2O_3-water were used.
Alfaryjat et al. [13] (2016)	Numerical, microchannel were three different section	100-1600	water	-	0	S ↓ Re ↑ and the applied heat flux ↓ . The square cross-section has the lowest number of S_{th} and S_{total} compared with the circular and hexagonal MCHS.
Alfaryjat et al. [14] (2018)	Numerical, hexagon microchannel heat sink	200-1500	water	SiO_2, CuO and Al_2O_3	1-4	S_{th} ↓ and S_f ↑ with Φ ↑.
Tabrizi and Reza[15] (2012)	Numerical, circular microchannel heat sink	50-200	water	Al_2O_3	1-4	HTP enhances with ↑ Φ . S_{total} ↓ with ↑ Re and Φ and ↓ nanoparticles size.
Ho et al. [16] (2010)	Experimental, rectangular micro-channels	226-1676	water	Al_2O_3	1-2	(h ↑ 70% at largest $\dot{m}$ for 1% Φ) > pure water. (T_w and R_{th}) ↓ (25% and 0.029K/W, respectively)
Duangtho-ngsuk et al. [17] (2012)	Experimental, rectangular microchannel heat sink	1600-3000	water	Al_2O_3	1-3	T_w ↑ with Re ↓ for the same Φ. ΔP ↑ with Re ↑
Hassani et al. [18] (2018)	Experimental and numerical, chevron fin	100-900	water	Al_2O_3	0.5 and 1	ΔP ↑ with Re ↑ and ↑ Φ . h ↑ with Re ↑
Halelfadl et al. [19] (2013)	Analytical, rectangular micro-channel heat sink	4.7 cm^3/s	water	aqueous-carbon nanotubes	0.01	At nanofluids heat transfer rate ↑ (13% at 40ºC, 12% at 30ºC and 2% at 20ºC) and ↓ R_{th}
Manay et al. [20] (2018)	Experimental, rectangular microchannel heat sink	100-750	water	TiO_2	0.25, 0.5, 1.0 and 2.0	S_{th} ↓ and S_f ↑with Φ ↑ S_{total} ↓ with ↑ Re
Ijam et al. [21] (2012)	Analytical, mini-channel heat sink	(0.0076- 0.127) kg/s	water	Al_2O_3 and TiO_2	0.8-4	k ↑ (12% for Al_2O_3-water and 10% for TiO_2-water at 4% volume fractions) compared with pure water.
Mohammad et al. [22] (2012)	Numerical and analytical, miniature heat sinks	0-800	water	SiO_2	3.5, 4, 4.5 and 5	(the porosity and aspect ratio) ↑ heat transfer ↑

Ref.	Type of Study and geometry	Re / $\dot{m}$	Base Fluid	Nano-particle Material	Nanoparticle Concentration (%)	Findings
Jajja et al. [23] (2014)	Experimental, mini-channel heat sinks	200-800	water	-	0	(T_b ↓ 9%) other heat sinks at 0.2mm of fins spacing.
Naphon and Nakharintr [24] (2013)	Experimental, mini-rectangular fin heat sinks	80-200	water	TiO_2	0.4	The preferable heat sink is at channel heights 2mm. ΔP of nanofluids ≈ de-ionized water.
Hassani and Mazloumi [25] (2017)	Experimental and numerical, pin-fins straight and wavy heat sink	100-900	water	Al_2O_3	0, 0.1 and 0.4	The wavy channel miniature heat sink performance > (1.23–2.28 times) the straight channel.
Fazeli et al. [26] (2012)	Experimental and numerical, circular mini-channel heat sink	400-2000	water	SiO_2	3.5–5	The thermal performance enhancement develops while the R_{th} ↓ as the Re and Φ ↑ .
Saeed and Kim [27] (2018)	Experimental and numerical, mini-channel heat sinks	(0.5 -1.5) L/min	water	Al_2O_3	1 and 2.5	h ↑ { 31% at 0.5mm; 27.6% at 1mm; 25% at 1.5mm } performance { 1.33 at 0.5mm; 1.29 at 1 mm; 1.28 at 1.5mm }
Sohel et al. [28] (2015)	Experimental and numerical, mini-channel heat sinks	(0.5 -1.25) L/min	water	Al_2O_3	0.05-0.2	(Φ and Re) ↑ (ΔP and S) ↑ while the T_b ↓ .
Ho and Chen [29] (2013)	Experimental and numerical, mini-channel heat sinks	133-1515	water	Al_2O_3	0.5 -10	h ↑ (35% and 72%) as the (T_{in} and T_{bulk}) respectively at 10% of Al_2O_3-water.
Hasan [30] (2014)	Numerical, micro pins heat sinks	100 -900	water	Diamond and Al_2O_3	1 and 4	heat dissipation of the circular pins > (triangular and square pins) ΔP of the square pins > (triangular and circular pins)
Tullius et al. [31] (2012)	Numerical, mini-channels with short micro pin fins	100-1500	water	-	0	Nu of the triangle pins by 37% > other pins shape ΔP of circular and elliptic < other pins shape
Duangtho-ngsuk and Wongwis-es [32] (2015)	Experimental, miniature circular pin fin heat sink	0.65-3.32 kg/min	water	SiO_2 and ZnO	0.2-0.6	when used SiO2-water instead of ZnO-water The thermal performance ↑ (3-9%) pumping power ↑ for the same nanoparticle concentration.
Duangtho-ngsuk and Wongwis-es [33] (2015)	Experimental, mini array pins	700-3700	water	SiO_2	0.2-0.6	When SiO2-water was used rather than water, heat transfer rate ↑ (4-14%) Thermal performance of circular pins ↑ (6-9%) > square ΔP of square pins > circular pin.
Khoshvag-ht Aliabadi et al. [34] (2018)	Experimental and numerical, pin fins miniature heat sink	100-900	water	Al_2O_3	0.3-0.6	ΔP and h of half circular pins > other pins When the half circular was used instead of square pin fins h ↑ 85% and ΔP ↑ 2.5 times

Ref.	Type of Study and geometry	Re / $\dot{m}$	Base Fluid	Nano-particle Material	Nanoparticle Concentration (%)	Findings
Ali and Arshad [35] (2017)	Experimental, pin fins heat sinks	0.25–0.75 LPM	water	GNPs	9.5	at a 22.5^{o} are achieved < R_{th} and > thermal performance
Vinoth and Kumar [36] (2017)	Experimental, micro-channel heat sinks with oblique micro pinned	325 - 850	water	Al_2O_3	0.25	The trapezoidal cross-section has preferable thermal performance compared with others.
Shafeie et al. [37] (2013)	Numerical, heat sinks with micro pin-fins	0.002-0.01 kg/s	water	-	0	MCHSs and PHSs were not preferable compared with optimum traditional MCHS for the same pumping power S ↓with ↑ removed heat of the heat sinks.
Ambreen and Kim [38] (2018)	Numerical, MPFHS	250 - 550	water	TiO_2	4.31	the thermal performance of square pins < other pins. Nu ↑ (26%, 44% and 62% for square, circular and hexagon respectively).
Jia et al. [39] 2018)	Numerical, cone pin fin (MCPF)	147-637	water	-	0	(The cooling enhancement and friction factor) ↑ as the (diameter and height of fins) ↑.
Roshani et al. [40] (2015)	Experimental, plate-elliptical pin heat sink	100 - 1100	water	TiO_2 And Al_2O_3	0.5 and 2	h ↑(16% and 14 %) for 2% Φ of Al_2O_3–water and TiO_2– water, respectively.
Zirakzadeh et al. [41] (2012)	Experimental, Pinned Plate – Fin heat sinks	200-1800	water	Al_2O_3	0.5-2	R_{th} ↓ 23% h ↑ 20% for the plate-pin heat sink compared with the plate fins heat sink.

CHAPTER THREE

Numerical Simulation

3.1 Overview

The computational fluid dynamic (CFD) is widely employed to solve laminar fluid flow and model of conjugate heat transfer in this type of Pinned Plate – Fin heat sinks. The shape of complex shapes, grid generation, simulations and obtaining accurate results became more available and reliable with the various numerical simulation programs such as ANSYS-FLUENT.

3.2 Research Approach

The main reason for using numerical simulation is to reduce the cost, time and effort that will be in the experimental study. The methodology of the current research used ANSYS FLUENT-CFD V.14.5 [42] to solve the governing equations by finite volume method (FVM). The computational domain and boundary conditions are described in detail. In addition, the validation with previous studies is considered to confirm that the current simulation method is reliable and accurate. The grid independence test (GIT), the number and quality of mesh geometry, should be tested to achieve the stability of results. Furthermore, the calculations of numerical data are performed. In general, Figure 3-1 showns the flow chart for the approach of the present study.

Three steps of ANSYS FLUENT-CFD analysis are performed as the following discribsion. Firstly, the pre-process includes building geometry and grid mesh with set the boundary conditions. Secondly, the processing or solver consists of solving the governing equations. Finally, the post-processing involves the results, plots, graphics and animations.

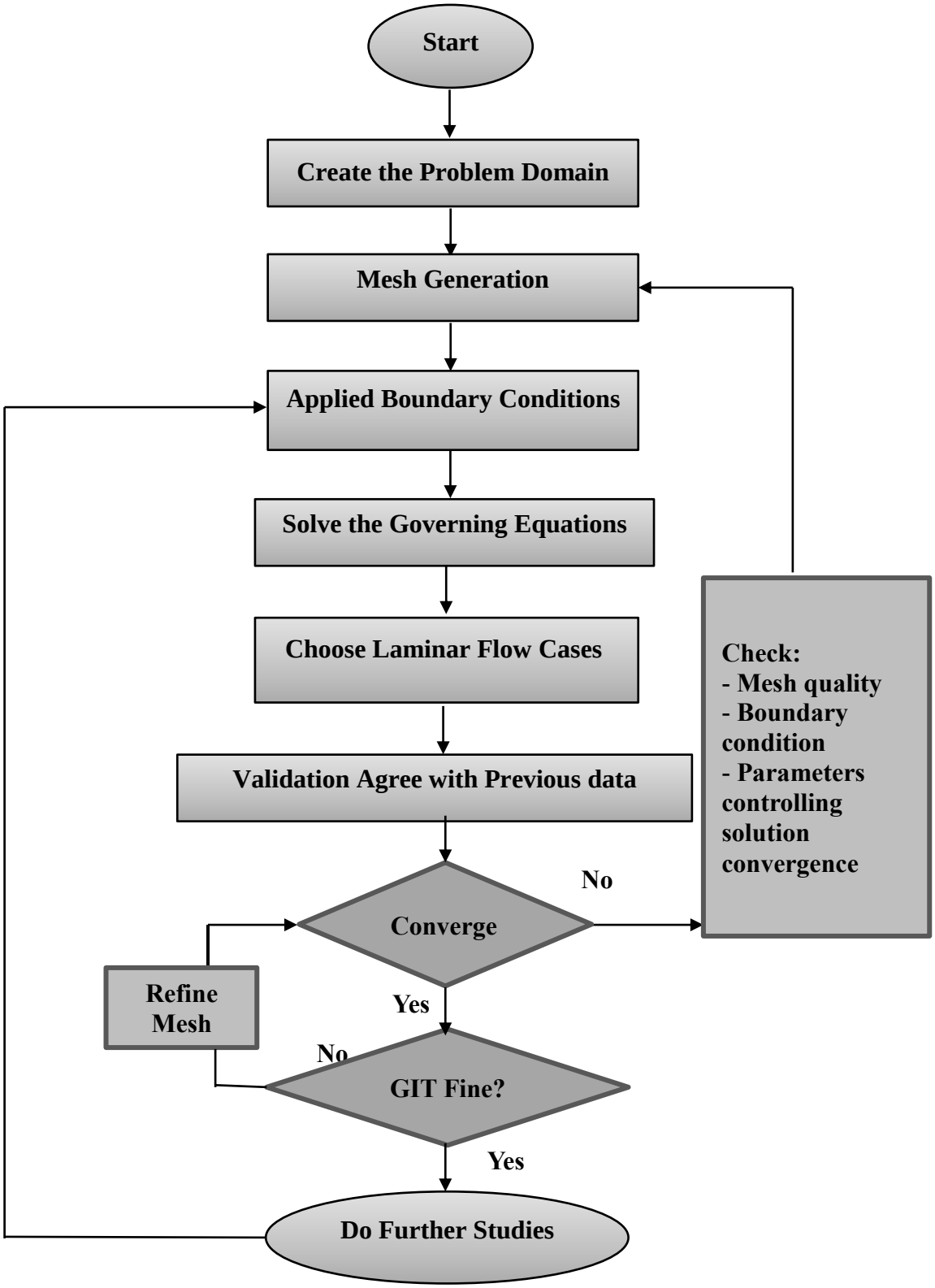

Figure 3-1: Flow chart of the present study

3.3 Computational Domain and Assumptions

The computational model in this study consists of four macro heat sinks configurations, as shown in Figure 3-2. The traditional one is flat plate heat sink (FPHS) while modified shapes are plate-pins heat sinks. The plate-pins heat sinks involve pins among flat plate fins. The cross-section of pins is circular (PCP), square (PSP) and elliptic (PEP), which are used in this investigation to compare with the traditional Case without pins (FPHS). Five channel of heat sink with the dimensions are 42mm in length (L), 42mm in width (W), 14 mm in height (H). The width (W_c) and height (H_c) of the channel are 6 mm and 10 mm, respectively. The pin height (H_p) is 10 mm and circular pin diameter (d_c) is 2 mm, square pin is 2 mm×2 mm (Ls) and 0.46 of aspect ratio (small diameter/large diameter, de/De= 0.7/1.5) for elliptic pin, as presented in Table 3-1. The plate-pins heat sinks have one, two and three pins. Table 3-2 presented pins location at one and two pins in the channel path. While, Z_1 (z_1/L = 7/42), Z_2 (z_2/L = 21/42) and Z_3 (z_3/L = 35/42) are the pins location in the heat sink channel from the edge per length of channel as shown in Figure 3-2 F. The locations of these one pin have been changed at the Case 1, Case 2 and Case 3 of the channel of the heat sink. While, the two pins locations are changed at the Case 1, Case 2 and Case 3 of the heat sink channel, as shown in Figure 3-3. For three pins, the space between the centres of pins is 14mm while the distances from the first pin centre to the edge of the entrance and from the third pin centre to the outlet of the heat sink is 7mm.

The main assumptions of the fluid flow and heat transfer can be defined as the following:

1. 3D and Steady state.
2. The fluid is incompressible, single phase, and laminar flow.
3. The thermal conductivity of the nanofluids are changing with temperature.
4. Constant heat flux is applied on the base wall of the plate-pins heat sinks and no heat generation.

Table 3-1: The dimensions of pinned plate-fin heat sinks.

length (L)	**42mm**	**width of the channel (W_c)**	**6mm**	**pin diameter (d_c)**	**2mm**
width (W)	42mm	**height of the channel (H_c)**	10mm	**sides square pin (Ls)**	$(2\times2)mm^2$
height (H)	14mm	**pin height (H_p)**	10mm	**small diameter/large diameter for elliptic pin (d_e/D_e)**	0.7/1.5
Heat sink base height (H_b)	4mm	**Fin thickness (t)**	2mm	**Heat sink height (H)**	14mm

Table 3-2: One and two pins location in the plate-pins heat sink channel

Location	One pin	Two pins
Case 1	Z_1 (7/42)	Z_1(7/42), Z_2 (21/42)
Case 2	Z_2 (21/42)	Z_1(7/42), Z_3 (35/42)
Case 3	Z_3 (35/42)	Z_2(21/42) , Z_3 (35/42)

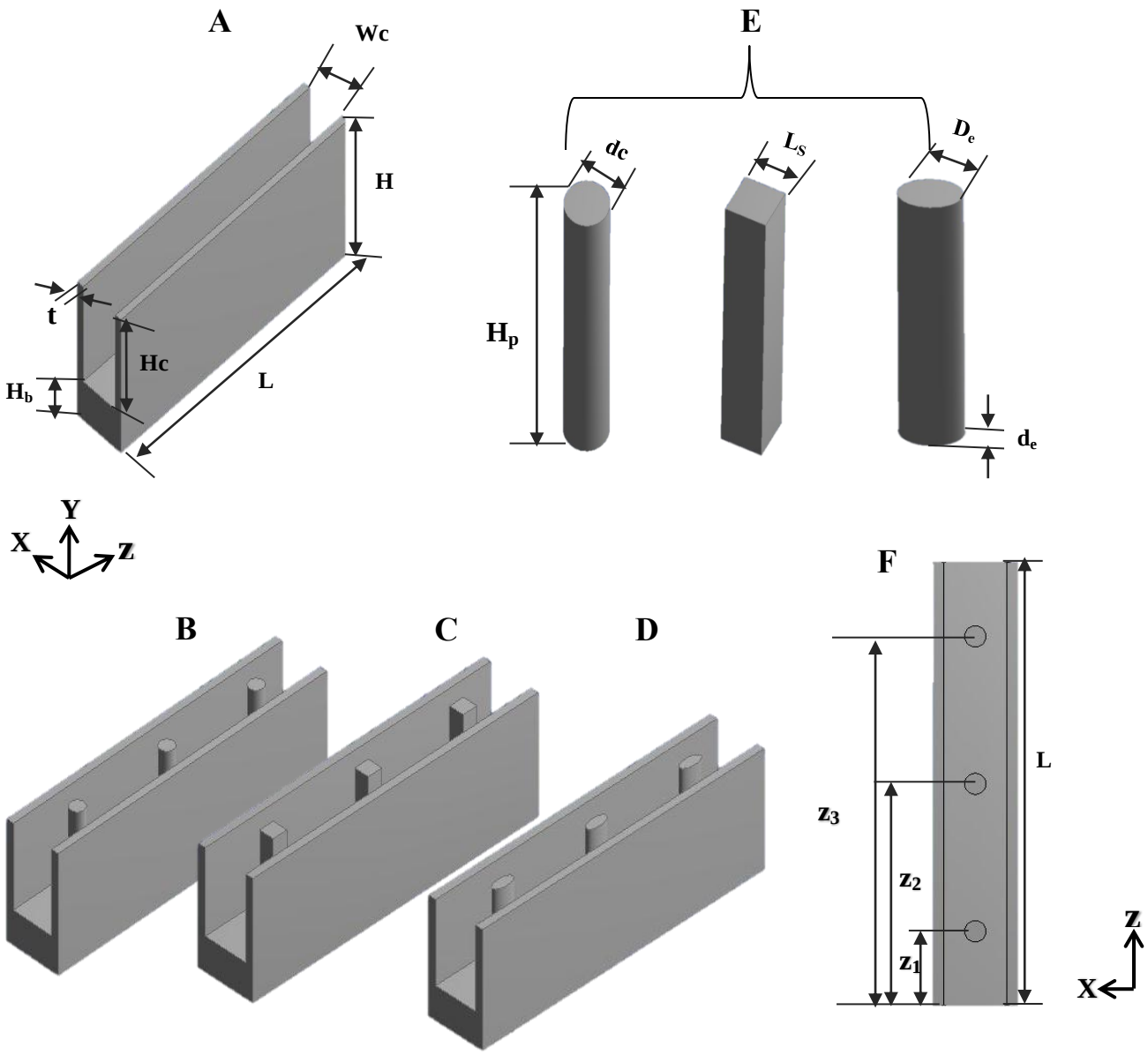

Figure 3-2: Plate-pins heat sinks: (A) Plate-Fins Heat Sink, FPHS (B) Plate-Circular Pins Heat Sink, PCP (C) Plate-Square Pins Heat Sink, PSP (D) Plate-Elliptic Pins Heat Sink, PEP (E) pins dimensions and (F) pins location.

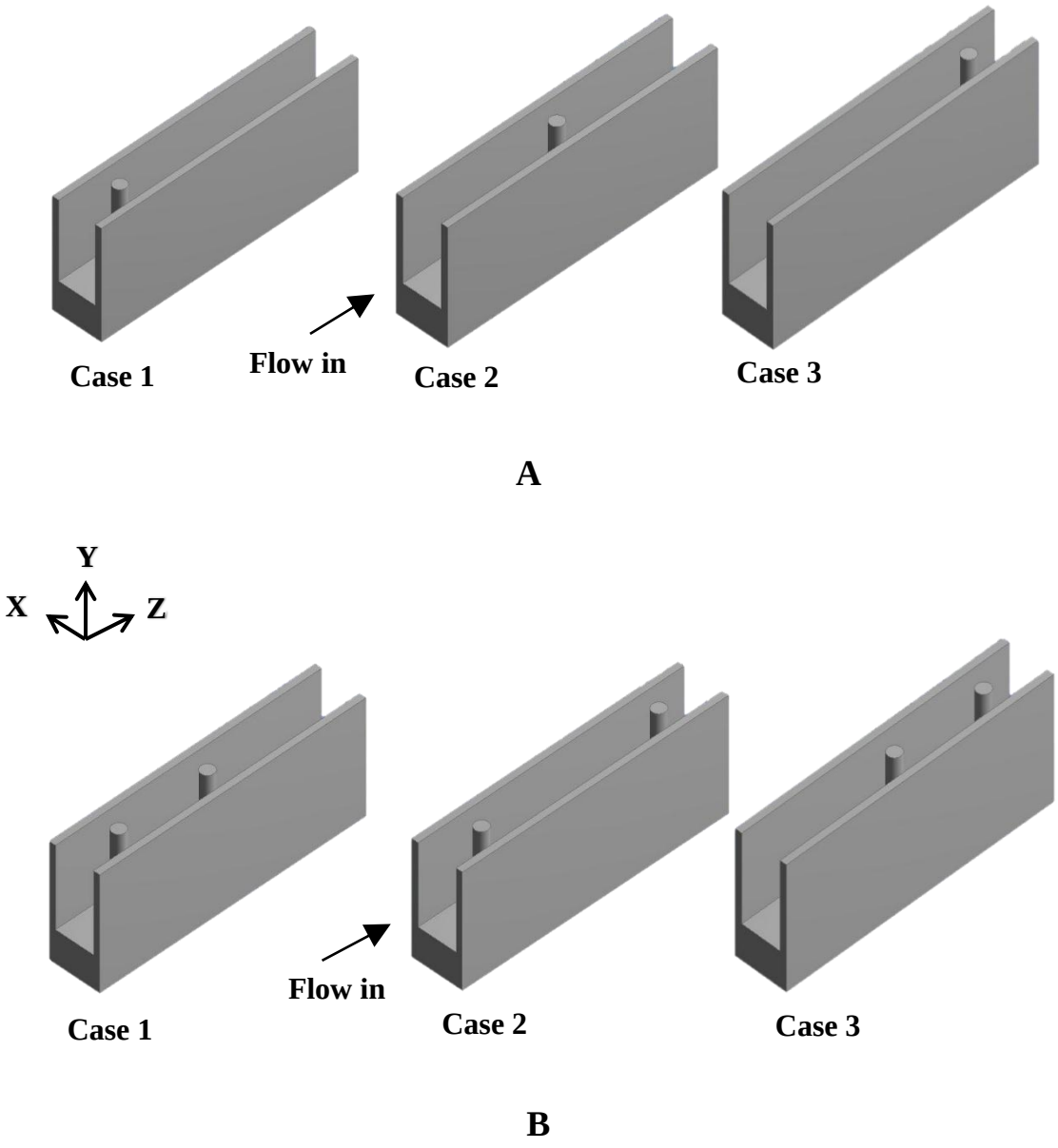

Figure 3-3: The pins location in Pinned Plate – Fin heat sink at (A) One circular pin and (B) Two circular pins

3.4 The Model of Conjugate Heat Transfer and Fluid Flow

The heat transfer rate of conduction could be pressented by the Fourier's law and it is solved to present the temperature field of heat sinks solid [43].

$$\left[\frac{\partial}{\partial x}\left(\frac{\partial T}{\partial x}\right)+\frac{\partial}{\partial y}\left(\frac{\partial T}{\partial y}\right)+\frac{\partial}{\partial z}\left(\frac{\partial T}{\partial z}\right)\right]_{solid}=0 \qquad 3\text{-}1$$

The formula of the continuity, momentum, and energy governing equations in Cartesian coordinates (x, y and z) can be given [44]:

- Continuity Equation

$$\frac{\partial(u)}{\partial x}+\frac{\partial(v)}{\partial y}+\frac{\partial(w)}{\partial z}=0 \qquad 3\text{-}2$$

- Momentum Equation in X-axis

$$u\frac{\partial(u)}{\partial x}+v\frac{\partial(u)}{\partial y}+w\frac{\partial(u)}{\partial z}=\frac{\mu_{eff}}{\rho_{eff}}\left(\frac{\partial^2 u}{\partial x^2}+\frac{\partial^2 u}{\partial y^2}+\frac{\partial^2 u}{\partial z^2}\right)-\frac{\partial P}{\partial x} \qquad 3\text{-}3$$

- Momentum Equation in Y-axis

$$u\frac{\partial(v)}{\partial x}+v\frac{\partial(v)}{\partial y}+w\frac{\partial(v)}{\partial z}=\frac{\mu_{eff}}{\rho_{eff}}\left(\frac{\partial^2 v}{\partial x^2}+\frac{\partial^2 v}{\partial y^2}+\frac{\partial^2 v}{\partial z^2}\right)-\frac{\partial P}{\partial y} \qquad 3\text{-}4$$

- Momentum Equation in Z-axis

$$u\frac{\partial(w)}{\partial x}+v\frac{\partial(w)}{\partial y}+w\frac{\partial(w)}{\partial z}=\frac{\mu_{eff}}{\rho_{eff}}\left(\frac{\partial^2 w}{\partial x^2}+\frac{\partial^2 w}{\partial y^2}+\frac{\partial^2 w}{\partial z^2}\right)-\frac{\partial P}{\partial z} \qquad 3\text{-}5$$

- (Energy Equation)

$$u\frac{\partial(T)}{\partial x}+v\frac{\partial(T)}{\partial y}+w\frac{\partial(T)}{\partial z}=\frac{k_{eff}}{\rho_{eff}\,C_{p_{eff}}}\left(\frac{\partial^2 T}{\partial x^2}+\frac{\partial^2 T}{\partial y^2}+\frac{\partial^2 T}{\partial z^2}\right) \qquad 3\text{-}6$$

3.5 Boundary Conditions

The heat transfer and fluid flow require suitable boundary conditions (BCs) as shown in Table 3-3 and Figure 3-4.

The aluminium flat plate and pins represent the conduction heat transfer rate that equal to the convection heat transfer. Each flat plate and pins have two BCs, one for the solid domain and other for the flow fluid region. The energy balance on the flat plate and pins surfaces are called conjugated heat transfer. At the base wall of heat sink, constant heat flow of 176.4 W. The walls of the heat sink are no-slip conditions, which means the velocity in all directions is zero. The temperature and Reynolds number range of fluid flow at the inlet channel of heat sink are 20 ºC and 100-1000, respectively [40].

At the outlet side, pressure outlet is applied to avoid diverged solution and the reverse backflow. At this condition, gauge pressure is zero. The left and right surfaces of the heat sink channel are a symmetric BC due to the symmetry in the geometry of heat sink and uniform fluid flow. The symmetry of BC saves computer memory and decreases the time of converged solution. On the other surfaces, walls are assumed adiabatic, this means no heat transfers through the walls. In addition, the solid domain is no-slip conditions, due to the rigidity of solid material and fluid flow velocity is zero in all directions [39].

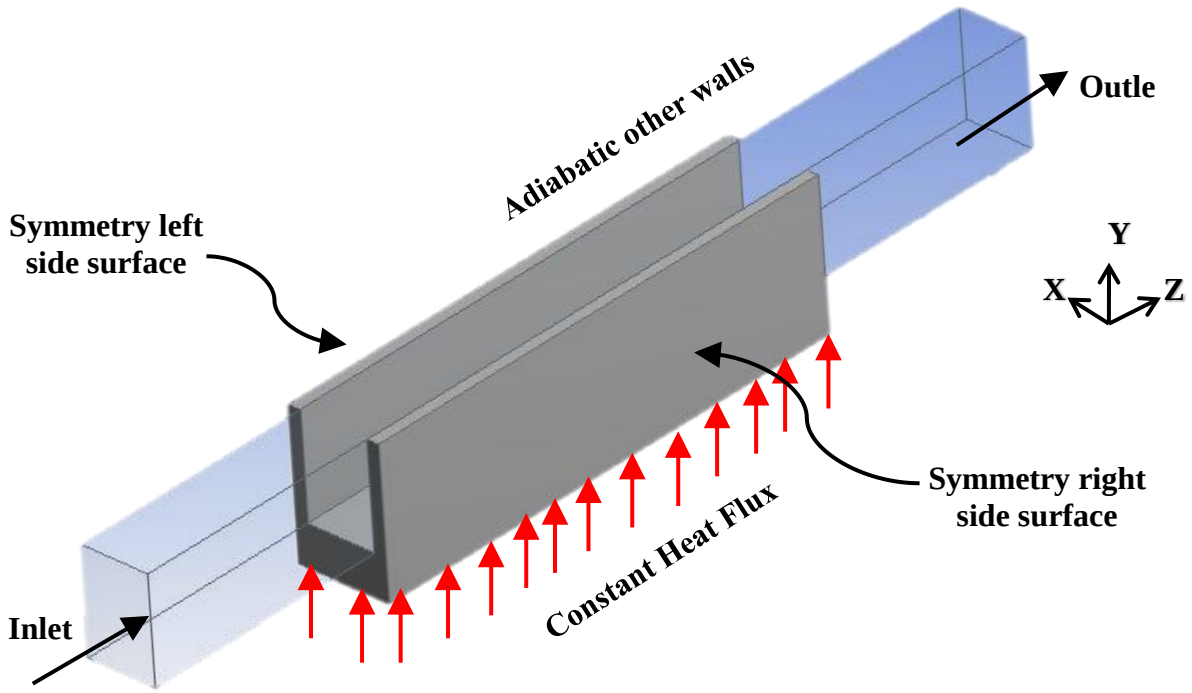

Figure 3-4: Schematic diagram of the physical domain of heat sink

Table 3-3: The boundary conditions of the Pinned Plate – Fin heat sinks model.

Settings	Fluid Conditions	Thermal Conditions	Settings	Fluid Conditi-ons	Thermal Conditions
Inlet	*Re* (100-1000)	T_{in}=20ºC	**The base surface of heat sinks**	$u=v=w=0$	$q''=10^5$ (W/m^2) (176.4 w)
The channel side surfaces (Symmetry)	$du/dx=0$	$dT/dx=0$	**Pressure outlet**	$P_{gauge}=0$	$dT/dz=0$
Other surfaces	$u=v=w=0$	$dT/dn=0$	**Solid heat sinks domain**	$u=v=w=0$	$K_f \frac{dT_f}{dn} = K_s \frac{dT_s}{dn}$

3.6 Thermophysical Properties of Nanofluids

The following equations and Table 3-4 are defined as the thermophysical properties for SiO_2-water nanofluids as incompressible fluid:

- The density of nanofluids is presented by [45]:

$$\boldsymbol{\rho_{eff} = (1-\Phi)\rho_f + \Phi\rho_s} \quad 3\text{-}7$$

- Specific heat of nanofluids is offered by [45]:

$$\boldsymbol{(\rho C_P)_{eff} = (1-\Phi)(\rho C_p)_f + \Phi(\rho C_P)_s} \quad 3\text{-}8$$

- The thermal conductivity of the nanofluids is given by [46]:

$$\boldsymbol{k_{eff} = k_{Static} + k_{Browain}} \quad 3\text{-}9$$

$$\boldsymbol{k_{Static} = k_f \left(\frac{(kp+2kf)-2\Phi(kf-kp)}{(kp+2kf)+\Phi(kf-kp)}\right)} \quad 3\text{-}10$$

$$\boldsymbol{K_{Browinan} = 5\times 10^4 \beta\, \Phi\, \rho_f\, C_{pf} \sqrt{\frac{k_b T}{\rho_p\, d_p}}\, f(T,\Phi)} \quad 3\text{-}11$$

$$\boldsymbol{\beta = 1.9526(100\Phi)^{-1.4594}} \quad \text{at } 298\text{K} \le T \le 363\text{K} \quad 3\text{-}12$$

$$\boldsymbol{f(T,\Phi) = (2.8217\times 10^{-2}\,\Phi + 3.917\times 10^{-3})\left(\frac{T}{T_{in}}\right) + (-3.0669\times 10^{-2}\Phi - 3.91123\times 10^{-3})} \quad 3\text{-}13$$

- The dynamic viscosity of the nanofluids is given by [49]:

$$\boldsymbol{\frac{\mu_{eff}}{\mu_f} = \frac{1}{1-34.87\,(d_p/d_f)^{-0.3}\,\Phi^{1.03}}} \quad 3\text{-}14$$

$$\boldsymbol{d_f = 0.1\left[\frac{6M}{N\pi\rho_f}\right]^{1/3}}$$

where d_f is Molecular diameter of water (m), M is Molecular weight of base fluid (0.01801528 (kg/mol)), N is Avogadro number (6.02 10^{23} (mol^{-1}) and d_p is the particle diameter is taken 20 nm.

Table 3-4: The properties of thermophysical for water, SiO_2 and Aluminium at a temperature of 20^{o}C.

Pure Water		**SiO_2**		**Aluminium heat sinks properties**	
k_f **(W/m .K)**	0.603	k_n**(W/m .K)**	1.4	K_s **(W/m .K)**	202.4
ρ_f **(kg/m^3)**	998.6	ρ_n **(kg/m^3)**	2200	ρ_n **(kg/m^3)**	2719
μ_f **(N.s/ m^2)**	0.001003	μ_n**(N.s/ m^2)**	—	α_s **(m^2/s)**	97.1×10^{6}
C_{pf} **(J/kg.K)**	4182.5	C_{pn}**(J/kg.K)**	745	C_{ps} **(J/kg .K)**	871

3.7 Numerical Procedure

3.7.1 Solution Method

The computational domain of heat sinks are constructed by The ANSYS DesignModeler while the grid generation is performed by ANSYS Meshing. The computational fluid dynamics CFD package solved the dominated equations by applying the boundary conditions and assumptions. Depending on the finite volume method (FVM), ANSYS-FLUENT adopted to solve the equations of conjugate heat transfer and laminar fluid flow. The convective term of 2nd order upwind technique which applied the algorithm of SIMPLE is utilized for pressure and velocity conjugation. The 2nd order upwind is applied to approximate the energy and momentum equations in the diffusion term. The simulation run is convergent when the residuals sum was less than 10^{-4} for momentum and continuity equations and lower than 10^{-6} for energy equation. The effective thermal conductivity of nanofluid is prescribed as a piecewise liner as a function of temperature.

3.7.2 Numerical Calculation

The pressure drop along heat sinks is calculated as follow:

$$\Delta \boldsymbol{P} = \boldsymbol{P_{out}} - \boldsymbol{P_{in}} \qquad 3\text{-}15$$

The coefficient of average heat transfer and the average Nusselt number can be calculated based on the total internal surface area of heat sinks (A_T) respectively [47]:

$$\boldsymbol{h_{ave}} = \frac{\mathbf{Q}}{\boldsymbol{A_T}\left[\boldsymbol{T_s}-\left(\frac{\boldsymbol{T_{out}}+\boldsymbol{T_{in}}}{\mathbf{2}}\right)\right]} \quad 3\text{-}16$$

$$\boldsymbol{Nu_{ave}} = \boldsymbol{h_{ave}}.\boldsymbol{L}/\boldsymbol{k_{eff}} \quad 3\text{-}17$$

where Q, T_{out} and T_{in} are heat flow rate, outlet and inlet temperature of the fluid , respectivily.

The total internal surface area of the heat sink (A_T) is estimated by:

$$\boldsymbol{A_T} = [(\mathbf{2H_c} + \mathbf{W_c})\mathbf{L}\ ] \times 5 \quad 3\text{-}18$$

Where A_T is the total internal surface area of CHSs.

The hydrothermal performance of CHSs can be found by [8]

$$\boldsymbol{HTP} = \left(\frac{\boldsymbol{Nu_{.ave,CHs}}}{\boldsymbol{Nu_{ave,PF}}}\right)\Big/\left(\frac{\boldsymbol{\Delta P_{CHs}}}{\boldsymbol{\Delta P_{PF}}}\right)^{\mathbf{1}/\mathbf{3}} \quad 3\text{-}19$$

The total entropy generation includes two effects; the friction of fluid flow and the heat transfer through heat sinks. It can be estimated by the following question [48]:

$$\boldsymbol{S_{gen}} = \left(\frac{\boldsymbol{Q^2}}{\boldsymbol{T_{in}}\times\boldsymbol{T_b}}\right)\boldsymbol{R_{th}} + \frac{\dot{\boldsymbol{m}}\boldsymbol{\Delta P}}{\boldsymbol{\rho_{eff}}\boldsymbol{T_{in}}} \quad 3\text{-}20$$

Where $\dot{m}$ and R_{th} ($\frac{\Delta T}{Q}$)are mass flow rate and thermal resistance, respectively.

Reynolds number can be calculated as the following formula:

$$\boldsymbol{Re} = \frac{\boldsymbol{\rho_{eff}}.\boldsymbol{U}.\boldsymbol{D_h}}{\boldsymbol{\mu_{eff}}} \quad 3\text{-}21$$

Where D_h has represented the hydraulic diameter of CHSs channel, can be found as follows:

$$\boldsymbol{D_h} = \mathbf{4}\frac{\boldsymbol{Ac}}{\boldsymbol{P}} = \frac{\boldsymbol{4Wc.Hc}}{(\boldsymbol{2Hc}+\boldsymbol{Wc})} \quad 3\text{-}22$$

where A_c and P represent the cross sectional area and wetted perimeter of CHS channel.

3.7.3 Validation with Previous Works

The result of numerical study require a confirm that the main computational data are accurate and reliable that is performed through validation of the current study against several previous experimental and numerical studies.

The first validation is carried out with the experimental study of Zirakzadeh et al. [41] for plate fins heat sinks using pure water and 0.5-2% of Al_2O_3-water nanofluids at Re = 200-1800 under constant wall heat flux. Figure 3-5 presents the comparison of the coefficient of average heat transfer (h_{ave}) across the heat sink of the previous experimental work with the predicted current study. The typical deviation are very acceptable agreed, which are less than 5% for pure water and lower than 6% for 0.05% Al_2O_3-water nanofluids.

The second comparison is the numerical prediction of pressure drop (ΔP) and thermal resistance (R_{th}) of the straight microchannel heat sink Xie et al. [8] with the present simulation study as shown in Figure 3-6. The velocity range of pure water is between 0.6 m/s and 1.4 m/s under constant wall heat flux. The comparison results were found that the maximum deviation of pressure drop and thermal resistance were less than 3% and 1%, respectively.

Additionally, the Nusselt number (Nu_{ave}) and friction factor (f) of the numerical assessment for Jia et al. [39] using micro plate-fins heat sink and micro plate-cone pins heat sink using pure water have been validated with the current computational model. The validation indicated that the deviations between the simulation and previous finding of Jia et al. [39] are less 2% and 3% for micro plate-fins and micro plate-cone pins heat sinks, respectively, as shown in Figure 3-7. Furthermore, the local base temperature distribution ($T_{b,Local}$) along the base surface of the micro plate-fins heat sink of Jia et al. [39] is compared with the present simulation model as Re= 341. It is exposed that the typical percentage deviation is very acceptable agreement, which is less than 2%, as shown in Figure 3-8.

Finally, the average heat transfer coefficient (h_{ave}) data of the experimental investigation for Roshani et al. [40] using macro plate-elliptical pins heat sink with pure water has been compared with the current predictions data. The comparison outcomes indicated that the maximum deviation of h_{ave} was acceptable, which is less than 7% ,as shown in Figure 3-9.

Hence, the present computational work is very compatible with the previous experimental and numerical studies. thus, the current computational assessment can be applied for more parameters investigation for this kind of Pinned Plate – Fin heat sinks.

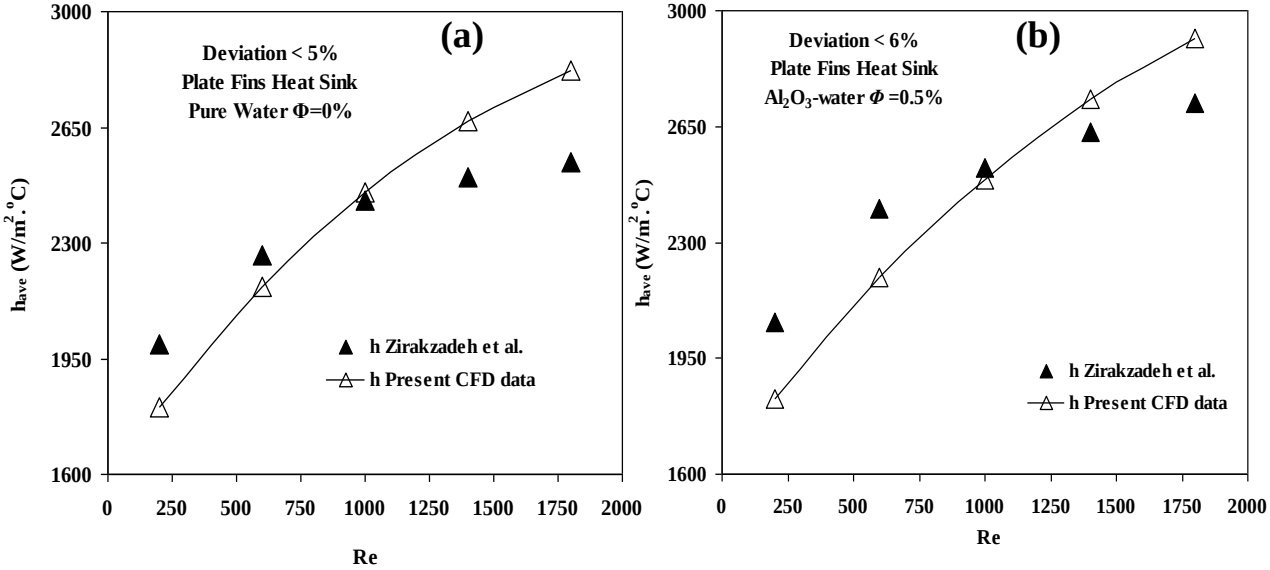

Figure 3-5: Validation of average heat transfer coefficient (h_{ave}) predictions with Zirakzadeh et al. [41] for (a) pure water and (b) 0.5vol.% of Al_2O_3-water

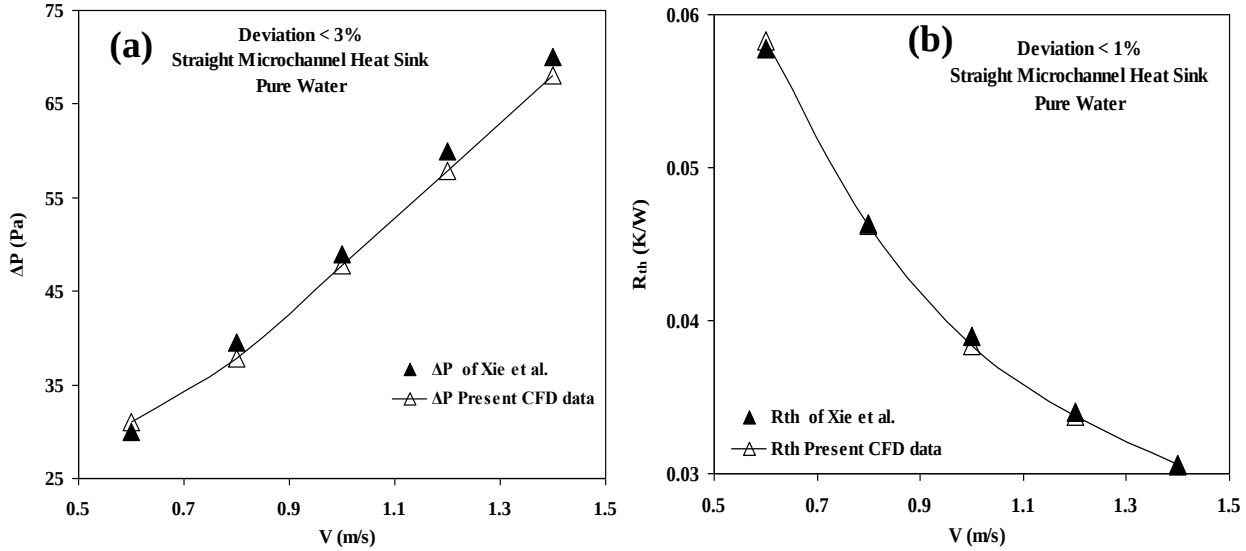

Figure 3-6: Validation of (a) pressure drop (ΔP) and (b) thermal resistance (R_{th}) predictions with Xie et al. [8].

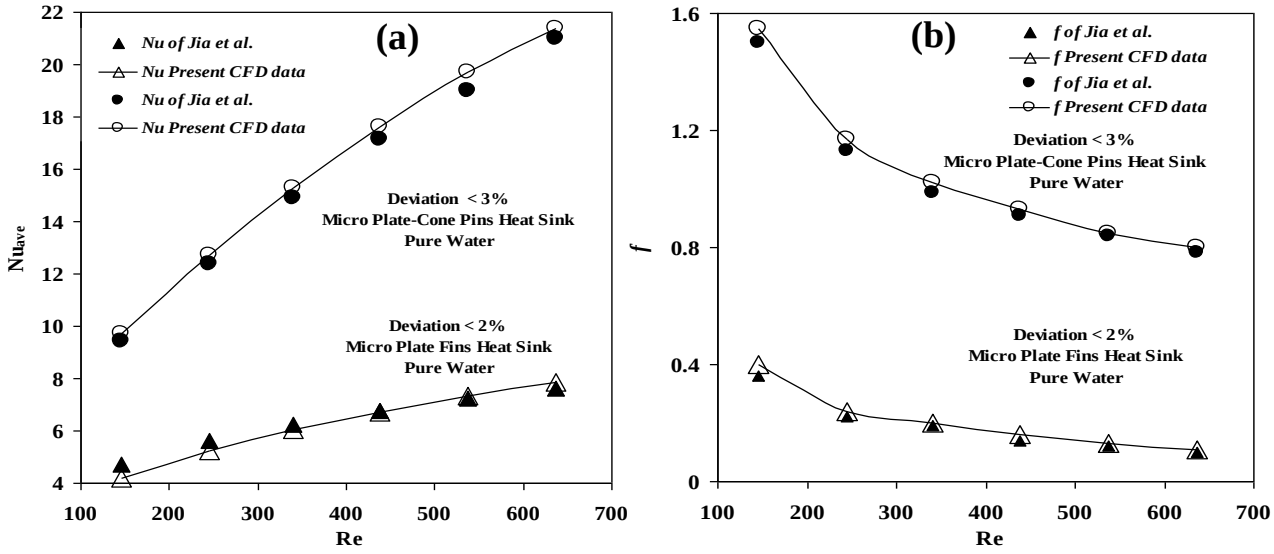

Figure 3-7: Validation of (a) average Nusselt number (Nu_{ave}) and (b) friction factor (f) predictions with Jia et al. [39] for different Reynolds number.

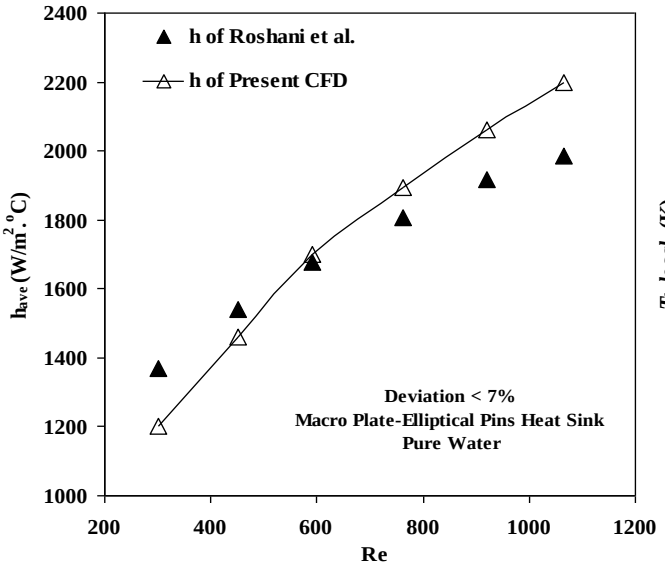

Figure 3-9: Validation of heat transfer coefficient (h_{ave}) of Roshani et al. [40]

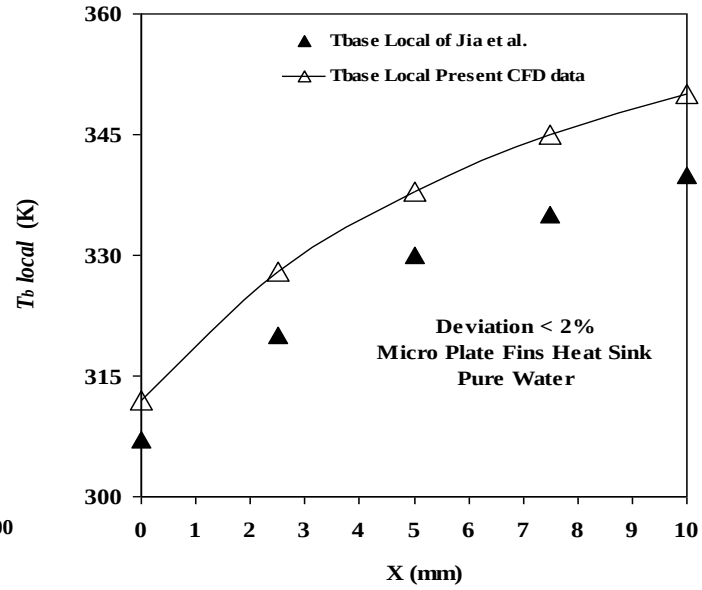

Figure 3-8: Validation of local temperature base (T_{bLocal}) predictions with Jia et al. [39] at Re = 341.

3.7.4 Grid Independence Test (GIT)

In this study, the uniform structured mesh is used in the whole domain except the pins zone, which is an unstructured as finer cells and high density of mesh near internal walls. Meshing, Tetrahedron Hyper mesh and Hexahedral mesh are used for several mesh distributions to confirm that grid independence is achieved and the numerical data is independent for mesh density by ANSYS. Accordingly, mesh cells should be dense enough near pins surface to predict the temperature distributions and fluid flow. Figure 3-10 shows the structure of mesh for the flat plate heat sink (FPHS) and plate-circular pins heat sink (PCP).

The grid size system was tested to estimate the required mesh number for the present study. This technique is used for testing the effect of mesh number increase on the stability of computational data such as the pressure drop (ΔP), base temperature of the heat sink (T_b), and Nusselt number (Nu) for the flat plate heat sink (FPHS), and plate-circular pin (CPH_S). Pure water and 4% of SiO_2-water nanofluids are applied in this test at Re 600. In the Case of the flat plate heat sink (FPHS), six different numbers of mesh were tested from 150×10^3 to 900×10^3 cells, as shown in Figure 3-11. Since the increase of cells number after 300×10^3 led to less than 1% of ΔP, T_b and Nu. Thus, the cells number 300×10^3 is considered as mesh independence for a flat plate heat sink.

Concerning the plate-circular pin heat sink (PCP), six different numbers of mesh from 150×10^3 to 10^6 are considered, as shown in Figure 3-12. It is found that the increase of the cells number after 400×10^3 led to less than 1% of ΔP, T_b and Nu. Hence, the cells number 400×10^3 is required as mesh independence due to presence pins.

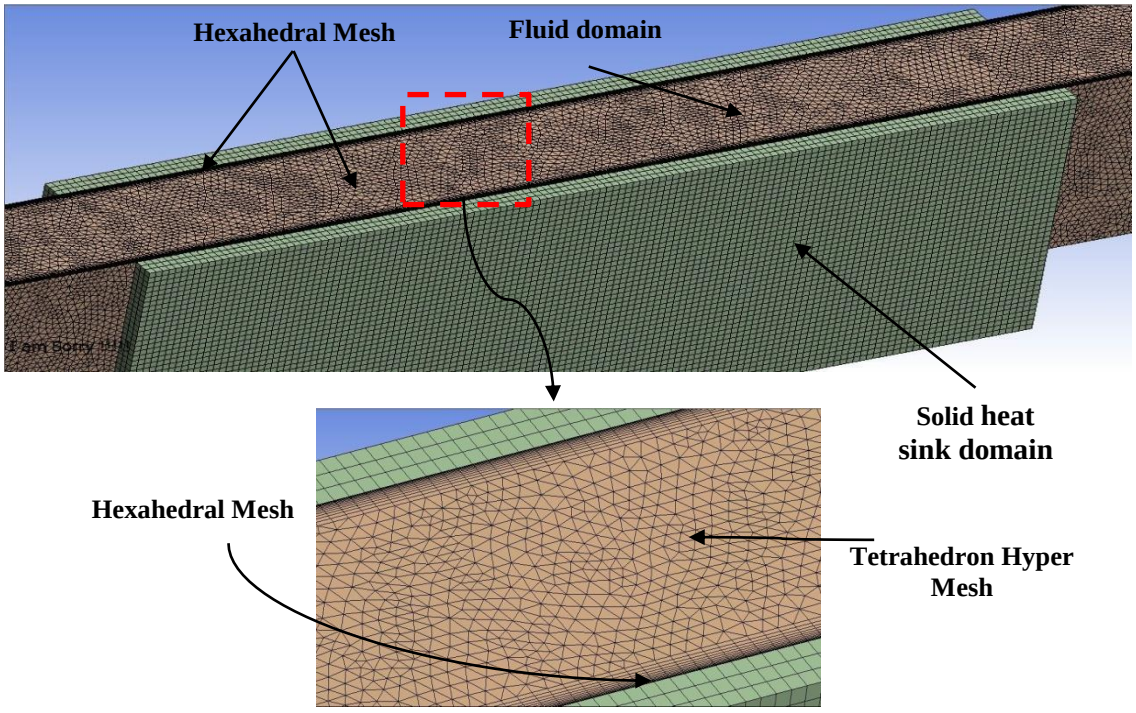

(a)

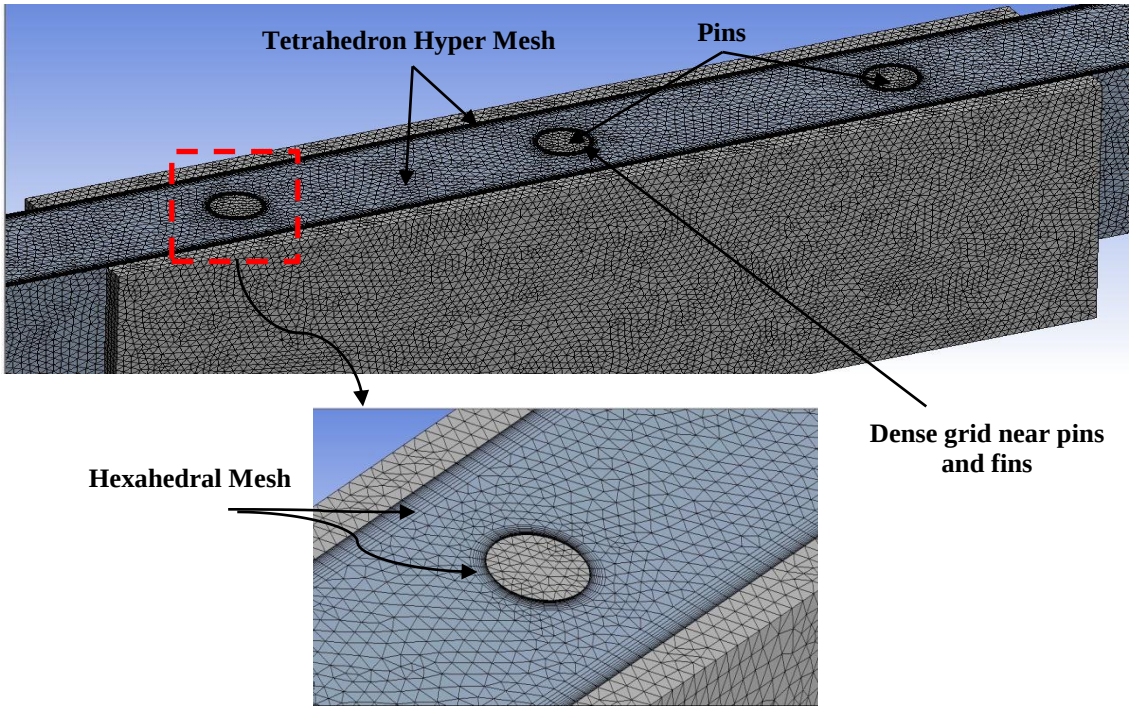

(b)

Figure 3-10: Meshing of generation for (a) FPHS and (b) PCP.

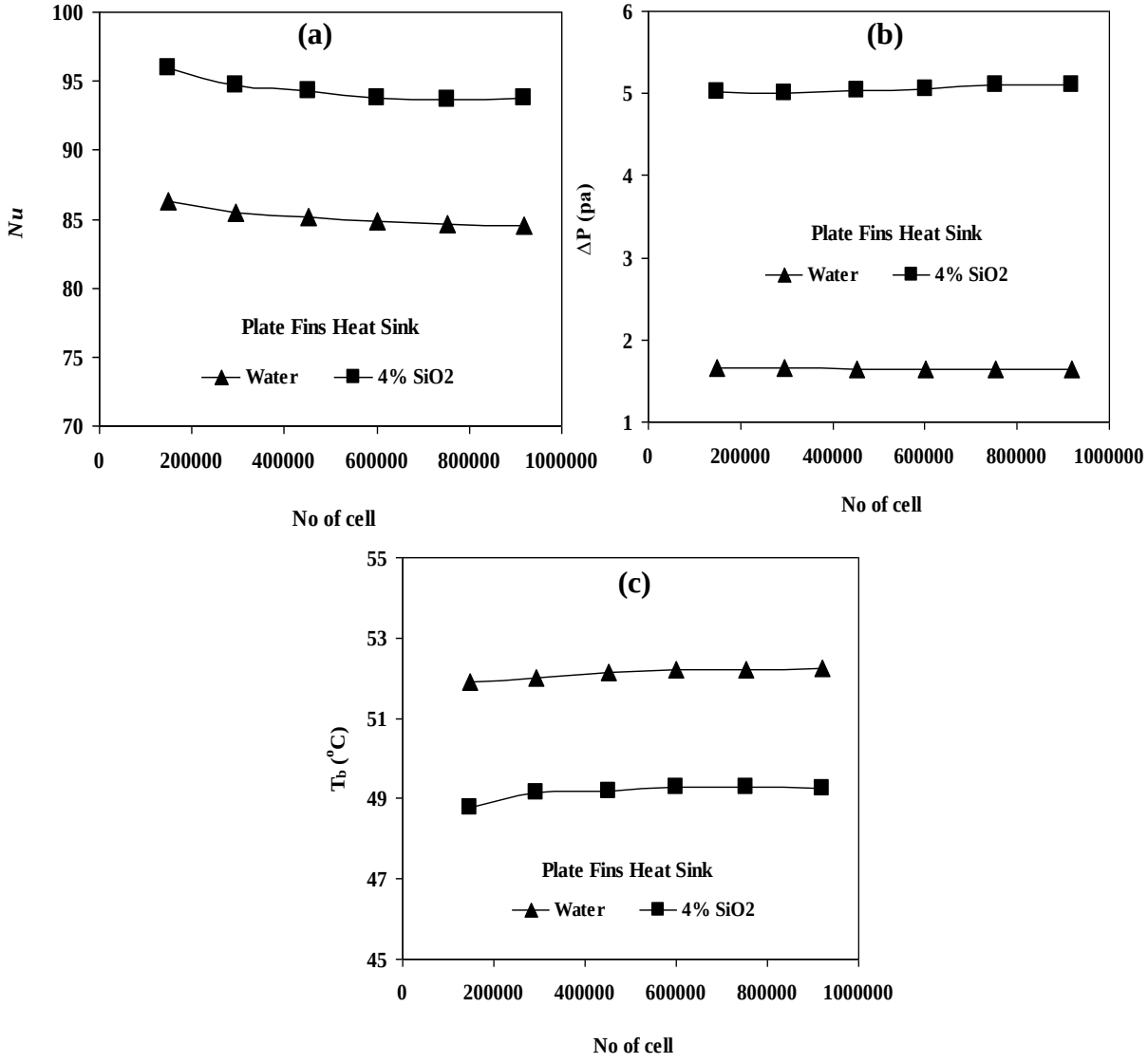

Figure 3-11 Grid independence test of flat plate heat sink shape at Re 600 and with water and 4% of Sio_2-water **(a)** Nusselt number (Nu) **(b)** pressure drop (ΔP) (c) base temperature (T_b).

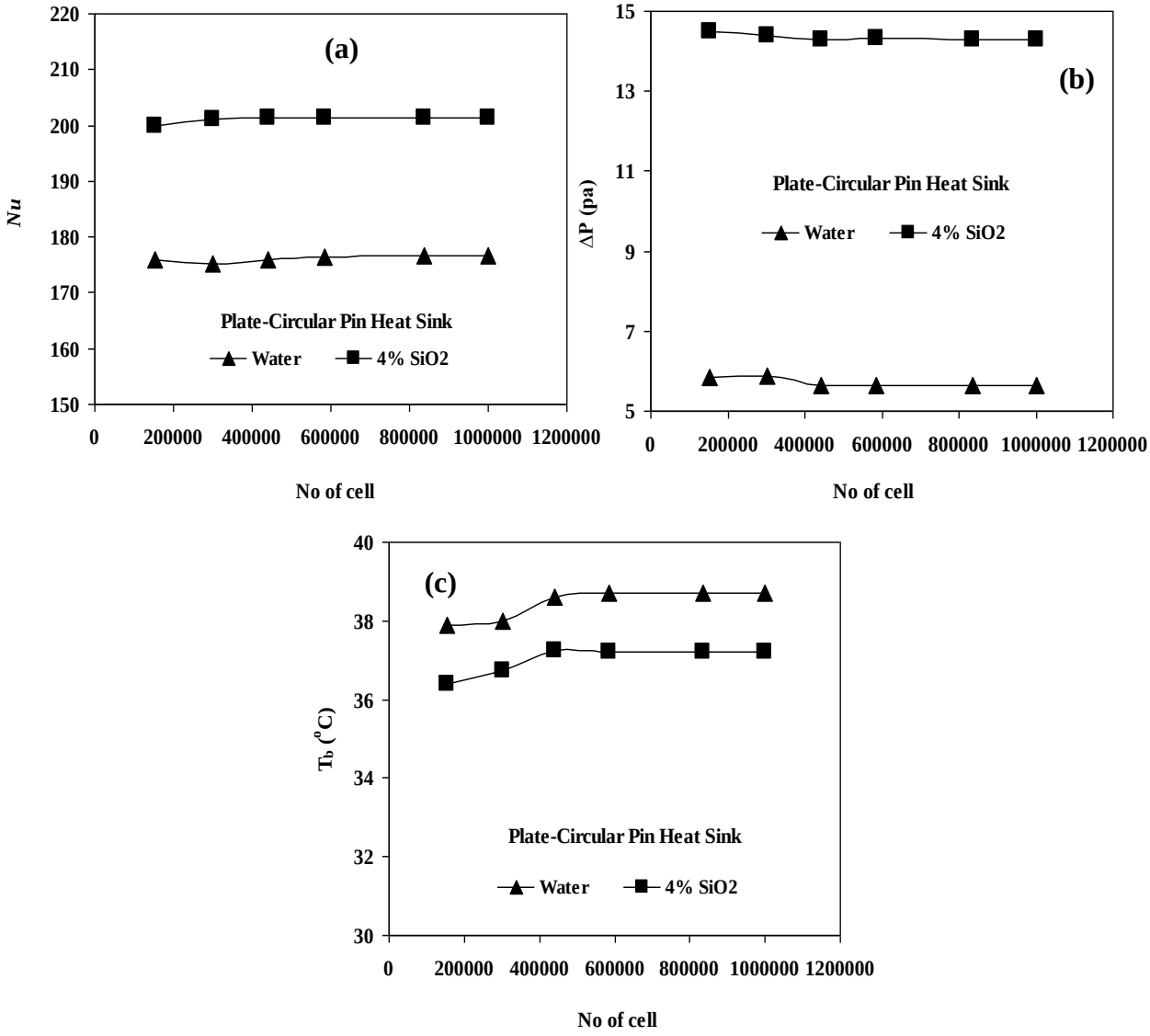

Figure 3-12. Grid independence test of plate-circular pins heat sink shape at Re 600 and with water and 4% of Sio_2-water **(a)** Nusselt number (Nu) **(b)** pressure drop (ΔP) **(c)** base temperature (T_b).

3.8 Summary

The computational solution methods have been employed to simulate laminar fluid flow through Pinned Plate – Fin heat sink designs and the conjugate heat transfer using ANSYS FLUENT. The research approach, physical domain, main assumptions boundary conditions are described in details. Thus, the variable thermophysical properties of fluids are considered in this investigation.

The computational method is explained and validated versus previous results to water and nanofluids flow over Pinned Plate – Fin heat sinks. Additionally, the validations and the grid independence test are considered. Since, a very accepted convergence between the current numerical data and previous experimental and numerical findings with variable properties of water and nanofluids, the simulation conjugate heat transfer with laminar flow model is currently applied to investigate the effect of the number, position of pins, and different shapes of pins cross-section with various concentrations of SiO_2-water nanofluids in the next chapters.

CHAPTER FOUR

Results and Discussion

4.1 Overview

This chapter shows and discusses the numerical results of heat transfer and fluid flow characteristics for different heat sinks shapes using water and SiO_2-water nanofluid in details. These characteristics are represented in terms of pressure drop (ΔP), average Nusselt number (Nu), base temperature (T_b) and the total entropy generation (S_{gen}) of heat sinks. Furthermore, the hydrothermal performance (HTP) is considered in the current study. The temperature and velocity streamline contours are presented as well. Reynolds number range was 100-1000 and applied 10^5 W/m^2 of heat flux on the base of Pinned Plate – Fin heat sinks.

4.2 Fluid flow field behaviour

The effect of different Pinned Plate – Fin heat sinks shapes on the field of liquid flow is shown in Figures [4-1 to 4-6] with Re= 200 and 800 for water and 5% nanofluid concentration. The Pinned Plate – Fin heat sinks with elliptic pins (PEP), square pins (PSP) and circular pins (PCP) are used and compared with a flat plate heat sink (FPHS).

For FPHS, no re-circulation can be seen in the direction of fluid flow field along the heat sink. The velocity profile and velocity vector are smooth with Reynolds number 200 and 800. The highest velocity is at the center of the channel of FPHS. At Re= 200, as shown in Figures [4-1 to 4-3], the re-circulation (vortices) region starts growing behind the pins due to the separation of the boundary layer on the surface of the pin. Thus, the vortices and reversed fluid flow are generated behind the pins especially for velocity vector, as shown in Figure 4-3. The re-circulation means that the fluid flow in this region goes in the reverse direction to the main flow. As Re = 800, as shown in Figures [4-4 to 4-5], the re-circulation and vortices in the PEP, PSP and PCP enlarges behind pins. Note that the re-circulation zones in the PSP are larger than that of PEP and PCP due to the edges of the square pins shape which lead the drag force of PSP is the largest while the PEP and PCP are more aerodynamic shapes.

Thus, the vortices and reversed fluid flow are generated behind the pins, as shown in Figure 4-6. Moreover, since the density and viscosity of nanofluid is larger than that of water for the same Reynolds number (200 and 800), the velocity distribution of nanofluid is higher compare with water.

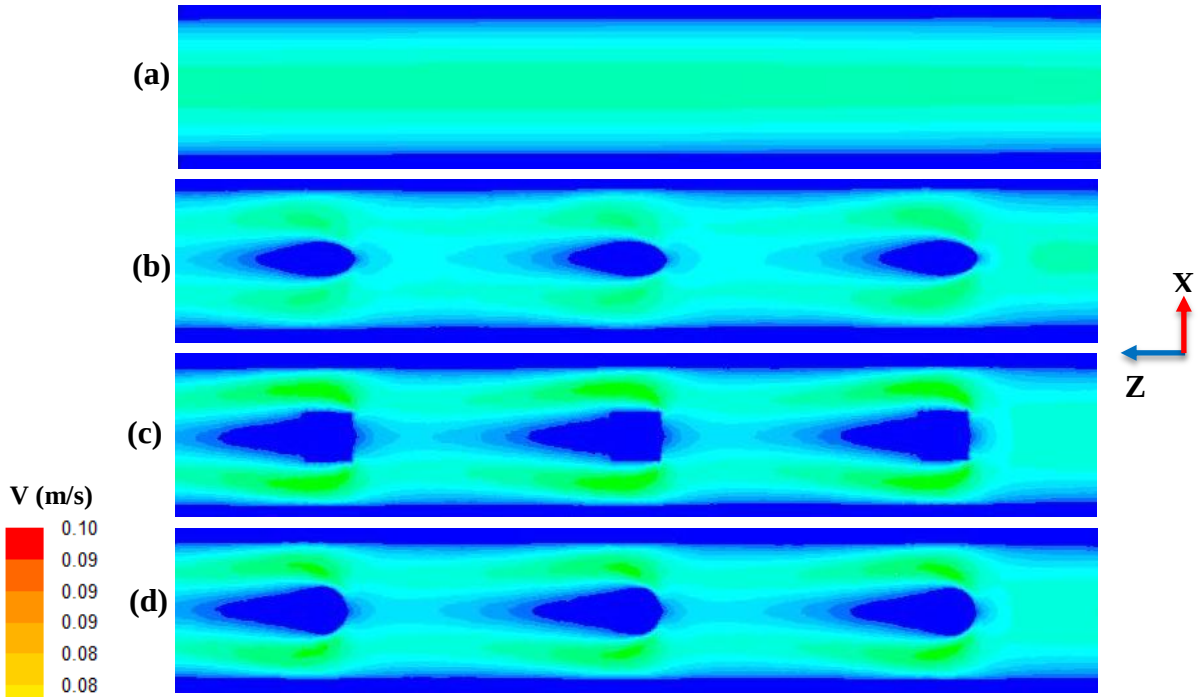

Figure 4-1: Stream wise velocity contour for water flow in Pinned Plate – Fin heat sink with *Re*= 200 and water (a) FPHS (b) PEP (c) PSP (d) PCP

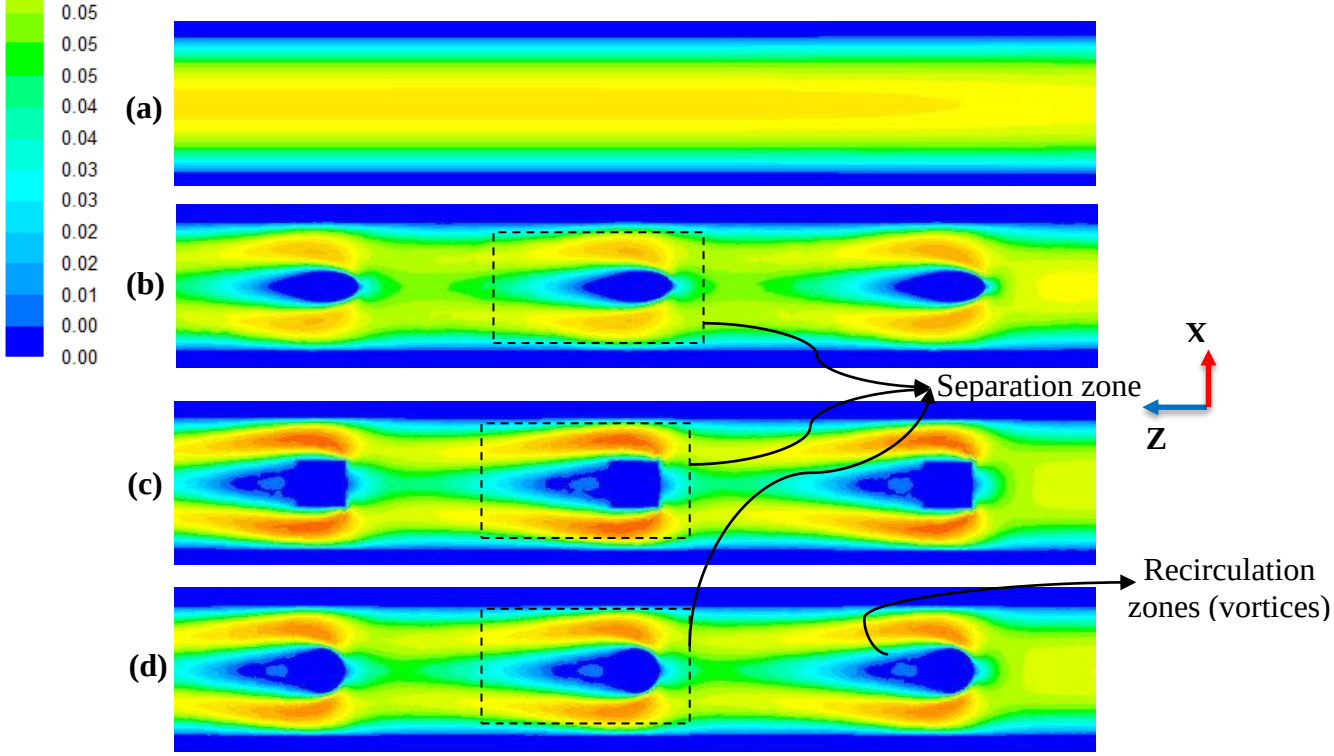

Figure 4-2: Stream wise velocity contour for nanofluid flow in Pinned Plate – Fin heat sink with *Re*=200 and Φ=5% SiO_2-water (a) FPHS (b) PEP (c) PSP (d) PCP

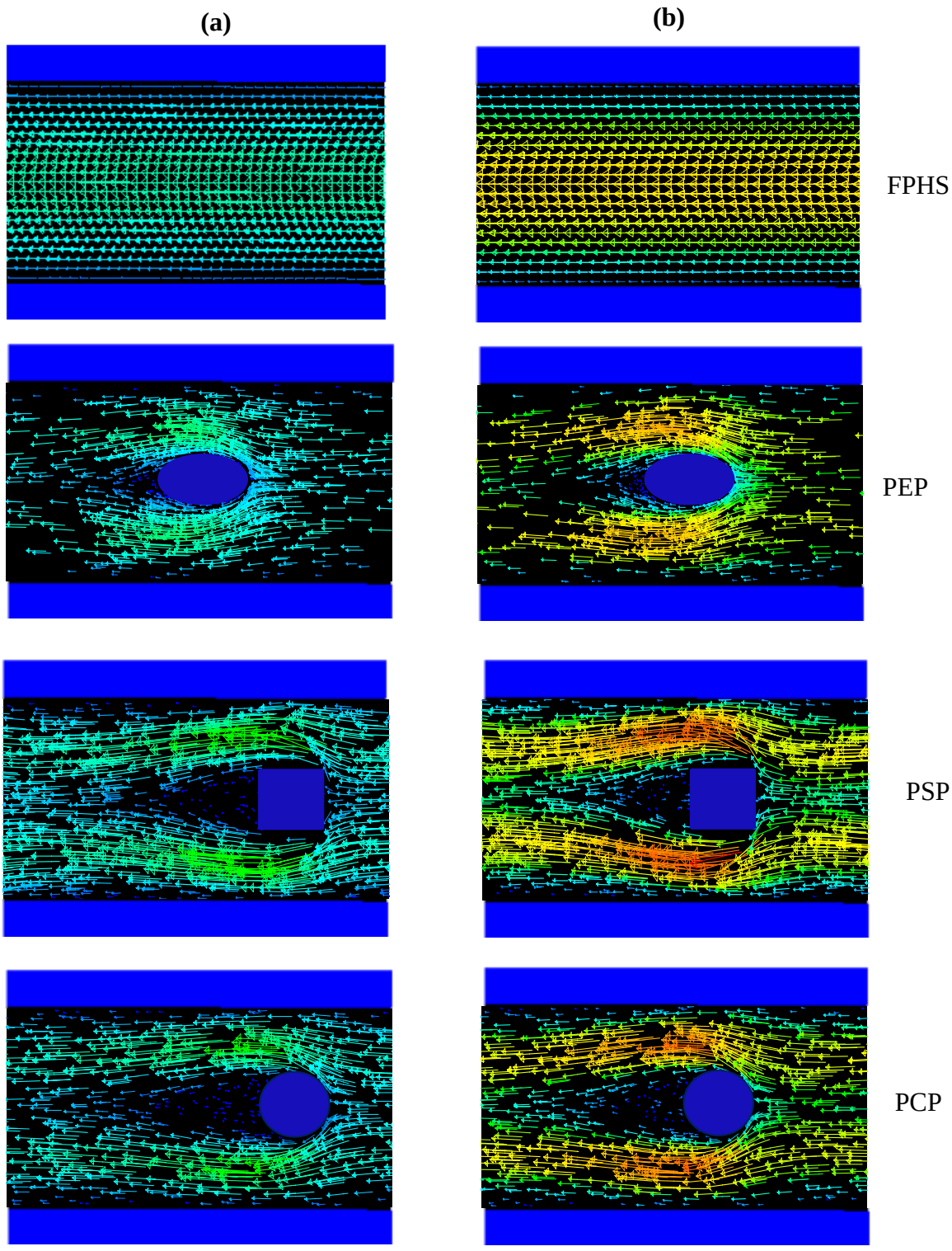

Figure 4-3: velocity vector for CHSs with *Re*=200 (a) pure water & (b) **Φ**=5% for *Re*=200 displaying vortices behind pins

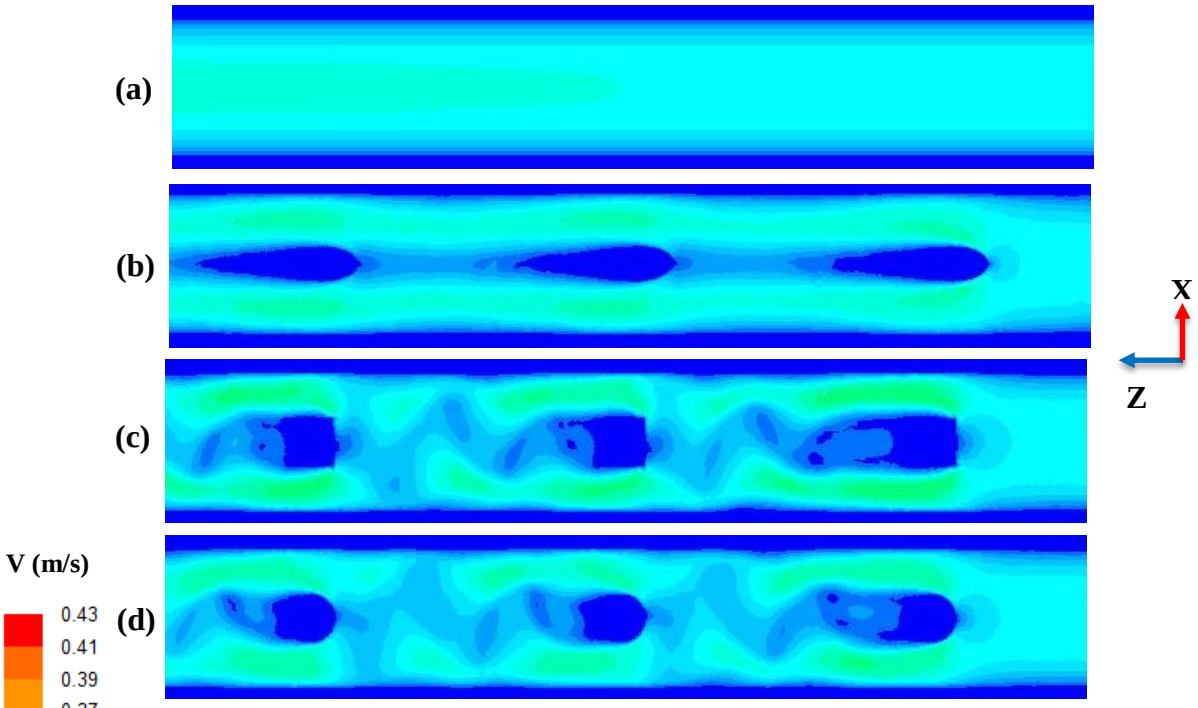

Figure 4-4: Stream wise velocity contour for water flow in Pinned Plate – Fin heat sink with *Re*=800 (a) FPHS (b) PEP (c) PSP (d) PCP

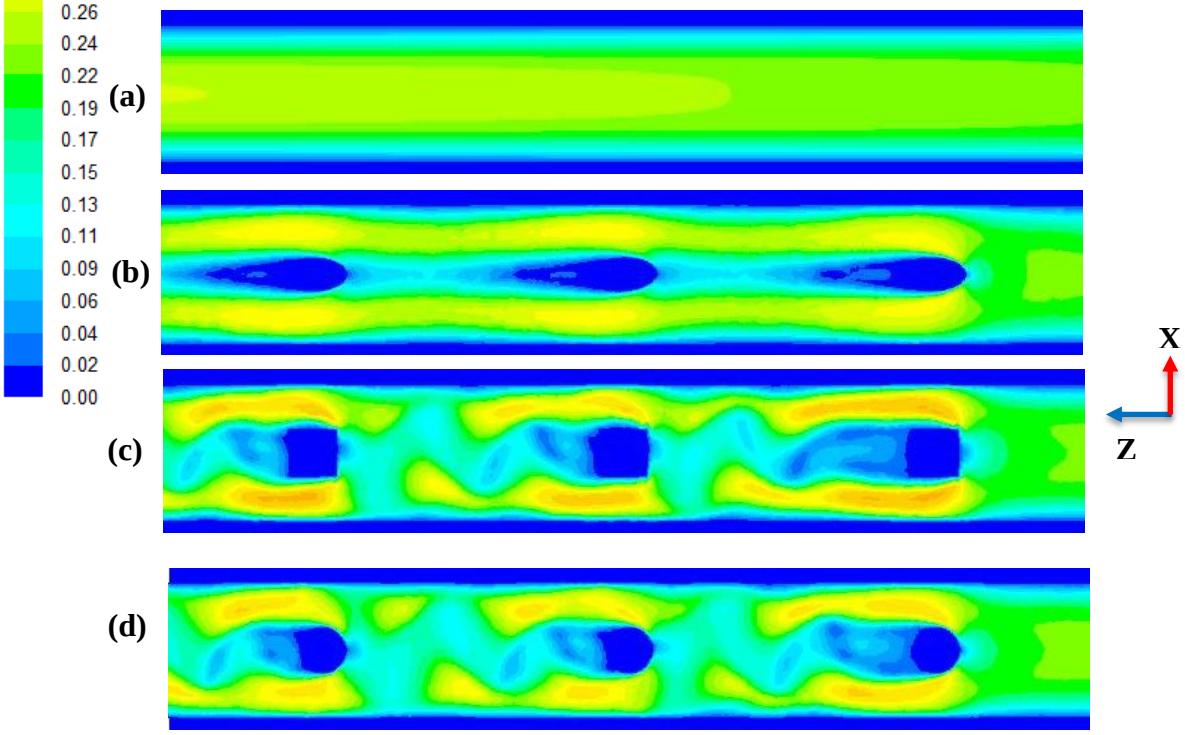

Figure 4-5: Stream wise velocity contour for nanofluid flow in Pinned Plate – Fin heat sink with

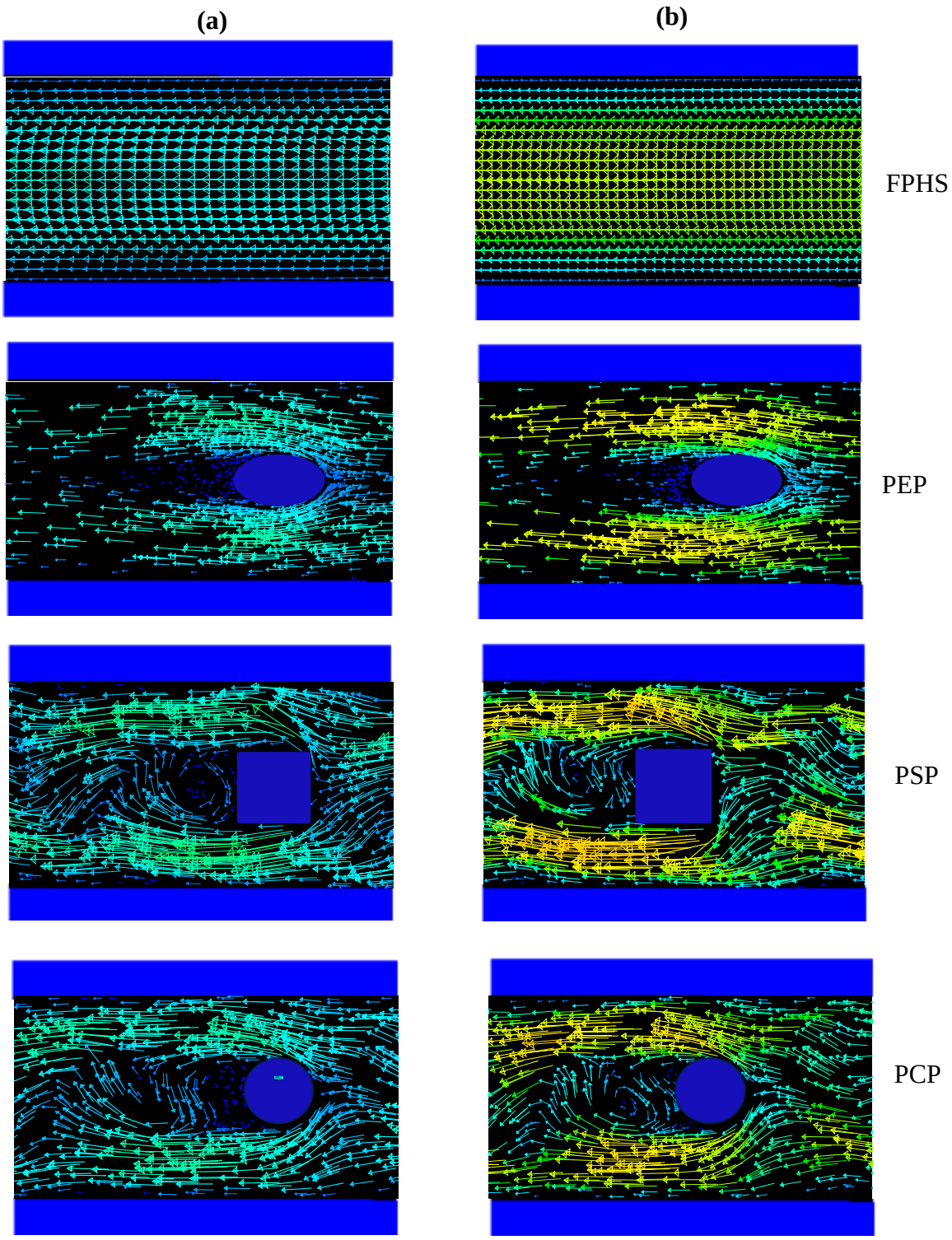

Figure 4-6: velocity vector for CHSs with *Re*= 800 (a) pure water & (b) Φ=5% for *Re*= 800

4.3 Effect of nano-particles volume fraction

Figure 4-7 (a-d) shows the relationship between the pressure drop (ΔP) and the Reynolds number (Re) with different volume fraction of nanofluid from 0 to 5% for four different heat sinks shapes. It is noted that whenever Reynolds number increases, the pressure drop goes up due to the increase of the velocity gradient at the walls of the channel. Furthermore, the increase of the SiO_2-water nanoparticles concentrations causes increasing the viscosity of the SiO_2-water nanofluid. This leads to grow the pressure drop along heat sinks. The lowest pressure drop values are for FPHS (Figure 4-7-a) because the path of flow is empty from any pins as obstacles. However, the highest values of pressure drop are for the PSP (Figure 4-7-b) compared with other shapes because the geometry of square pins has sharp edges and largest vortices that cause the largest obstacle to the fluid flow. These findings are confirmed with the experimental and numerical data of previous studies.

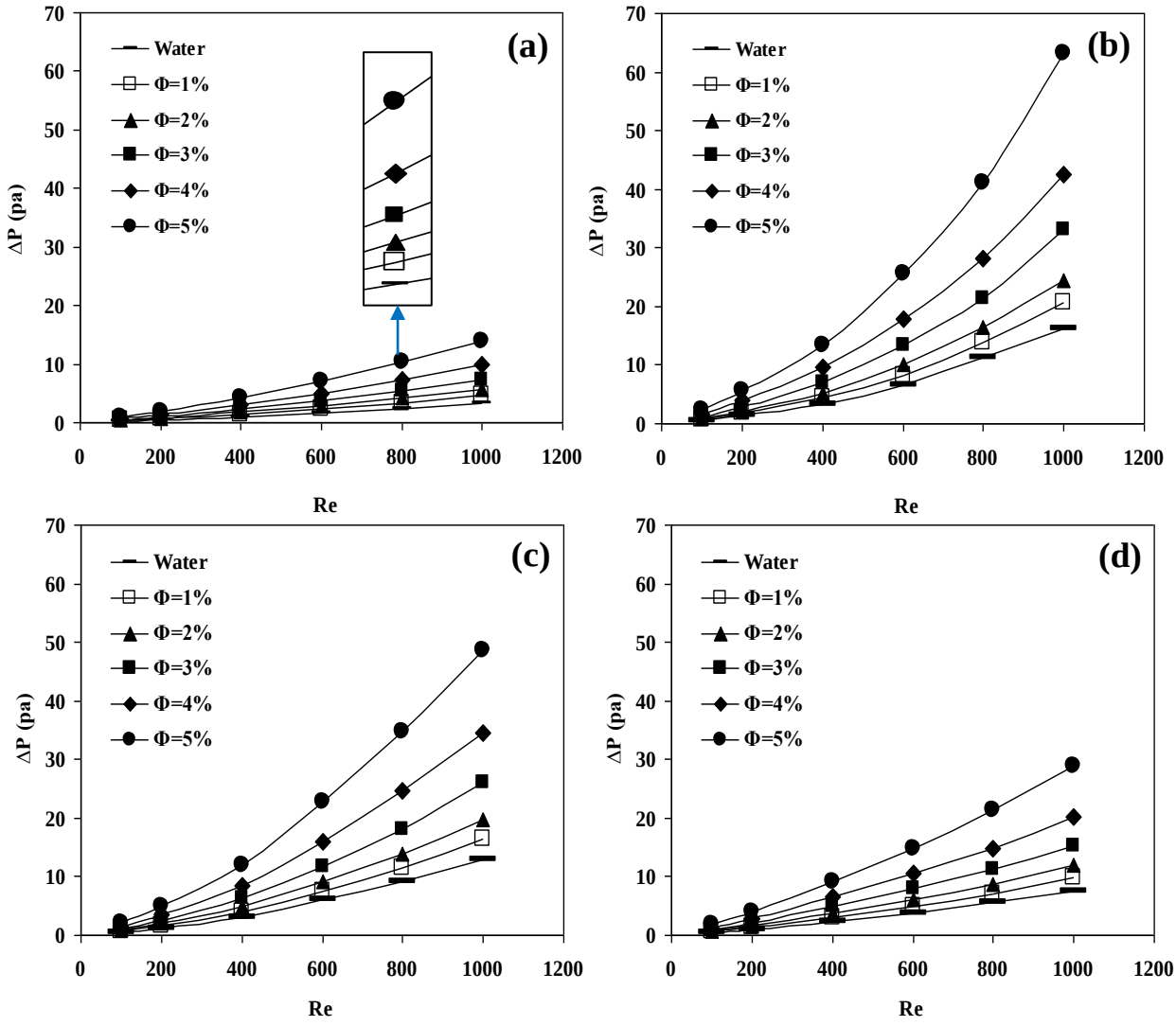

Figure 4-7: Effect of nanofluids volume fraction on *ΔP* of (a) FPHS (b) PSP (c) PCP (d) PEP

Figure 4-8 (a-d) illustrates the effect of nanoparticle volume fraction on the average Nusselt number ($\overline{Nu}$) values with different heat sinks and Reynolds number. It can be shown clearly that the $\overline{Nu}$ for all different heat sink shapes has similar behaviour with increasing *Re* and nanofluid concentrations. The average Nusselt number enhances with increasing *Re* at a given concentration of nanofluid. This enhancement occurs because the temperature gradient increases and the thermal boundary layer thickness reduces along the heat sink; for these reasons, the heat transfer rate improves. As nanofluid concentration increases, the Nusselt number enhances at a given Reynolds number. This is because of the Brownian motion of nanofluid particles, which means improvement in the thermal conductivity and specific heat of nanofluid compared with pure water. The data are consistent with the experimental and numerical data of previous studies.

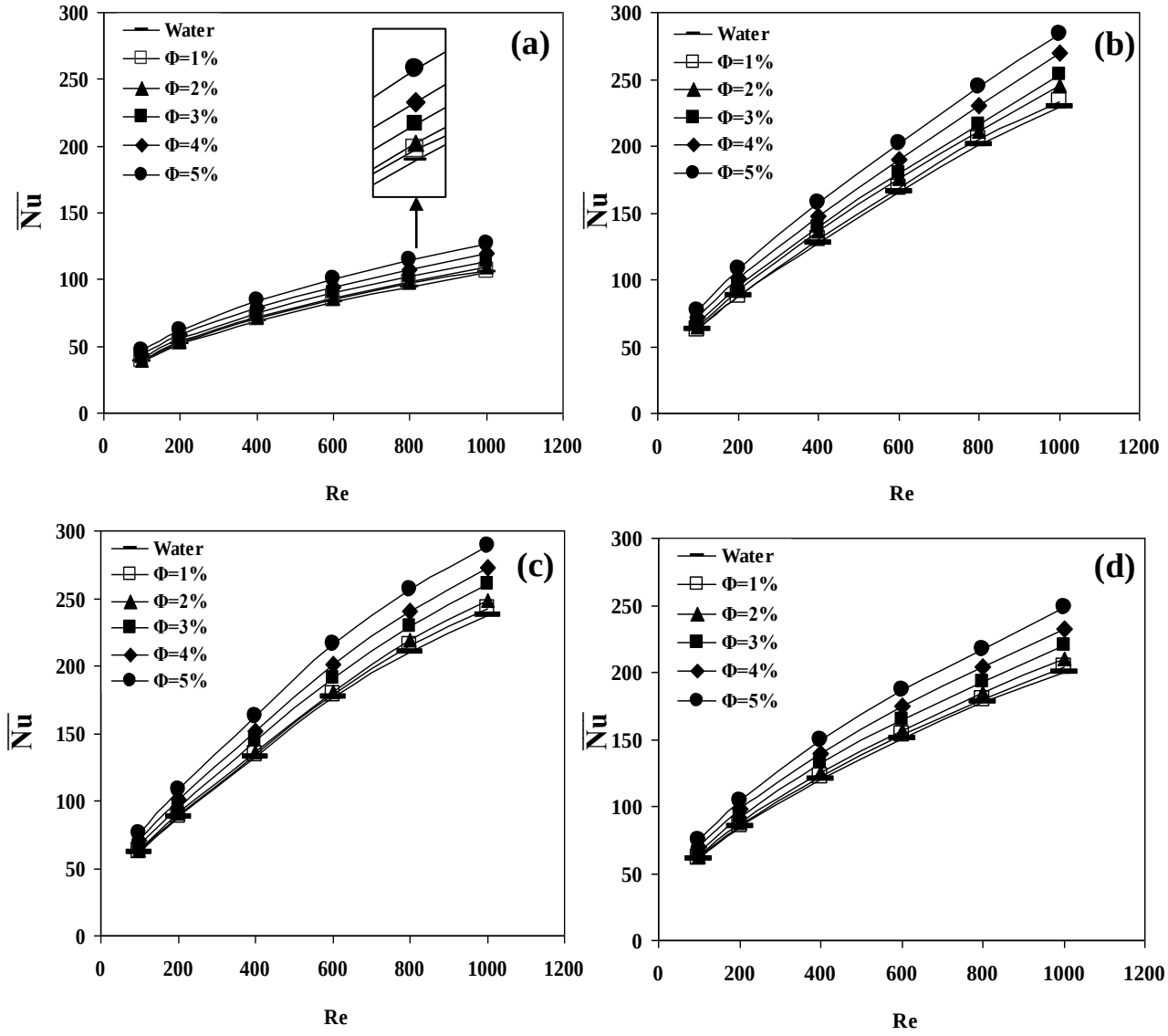

Figure 4-8: Effect of nanofluids volume fraction on $\overline{Nu}$ of (a) FPHS (b) PSP (c) PCP (d) PEP

Figure 4-9 (a-d) explains the effect of nanofluid concentrations and Reynolds number on the base temperature (T_b) of the heat sinks. For all Cases of the heat sink, the base temperature of heat sinks drops as Reynolds number increases due to increasing the cooling rate with growing the velocity gradient. Thus, the turbulence of fluid flow enlarges with increasing *Re*, which leads to reducing the thermal boundary layer along heat sinks. Additionally, the base temperature of heat sink is reduced with increasing the volume fractions concentration of nanofluid due to the enhancement in the effective thermal conductivity of the base fluid (Brownian motion). The Pinned Plate – Fin heat sinks shapes (b, c, and d) have a lower T_b compared with FPHS shape. This is due to the presence of pins in the heat sink channel, producing the re-circulation flow and enhancement in mixing fluid layers. These findings are confirmed with the experimental and numerical data of previous studies.

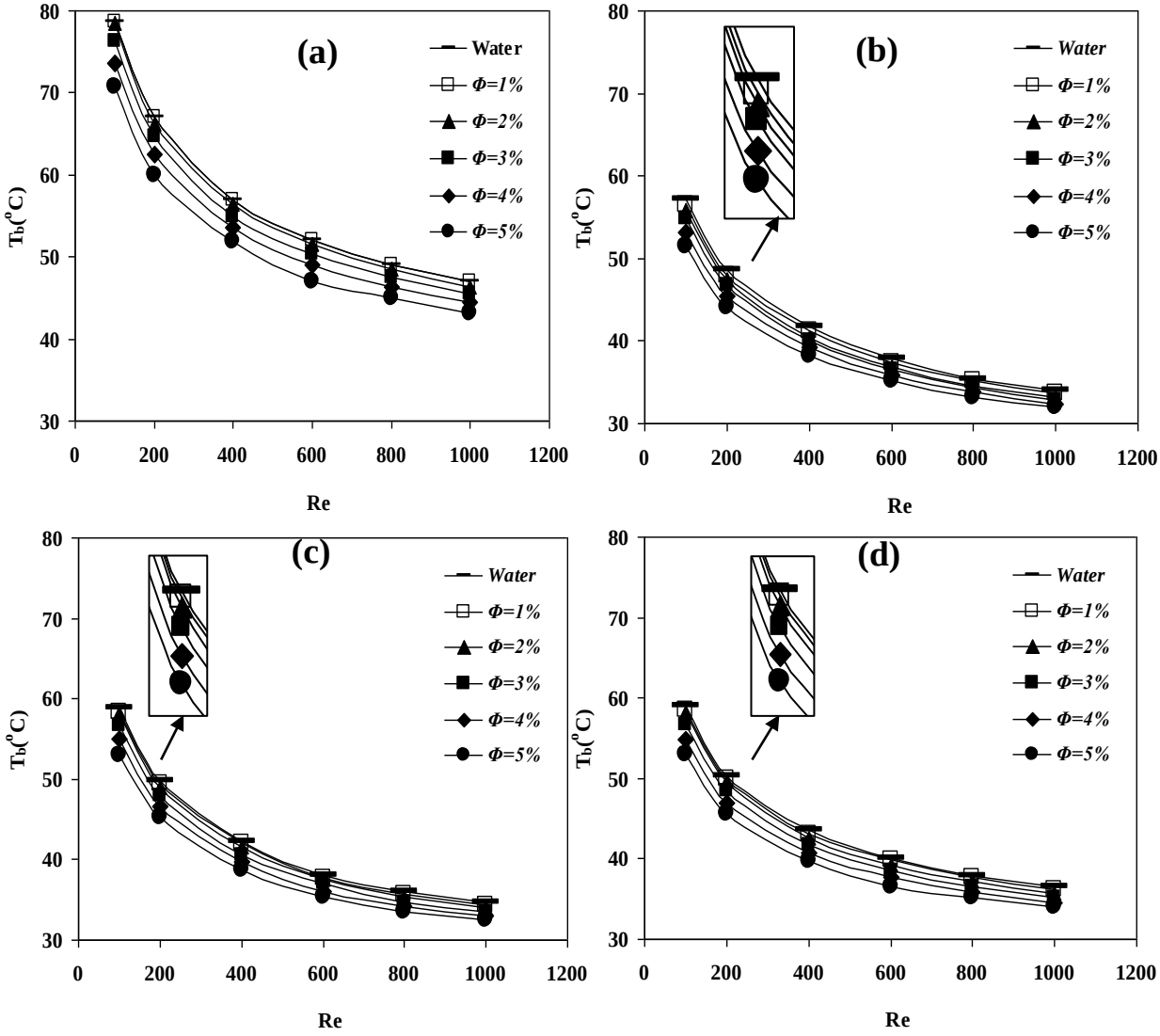

Figure 4-9: Effect of nanofluids volume fraction on T_b of (a) FPHS (b) PSP (c) PCP (d) PEP

Figure 4-10 (a-d) shows the effect of nanoparticle volume fraction on the total entropy generation values (S_{gen}) for different Pinned Plate – Fin heat sinks shapes with various Reynolds number. As mentioned early, the total entropy generation includes two effects; fluid flow friction and heat transfer. It is found that the entropy generation reduces as Reynolds number goes up. The main reason is that the heat transfer rate augments and the base temperature reduces with increasing Reynolds number. Thus, the irreversibility between the heat sink and fluid flow decreases with increasing Reynolds number. In other words, the thermal entropy generation is more effective on the total entropy generation compared with the frictional entropy generation. Furthermore, the entropy generation drops as the volume fraction of SiO_2-water nanofluid increases from 0% to 5%. This is because the nanofluid has lower specific heat capacity and higher thermal conductivity than that of pure water (Brownian motion of nanofluid). The behaviour of the findings is an agreement with the experimental and numerical data of previous studies. Additionally, the Pinned Plate–Fin heat sinks have the lowest entropy generation compared with the traditional heat sinks.

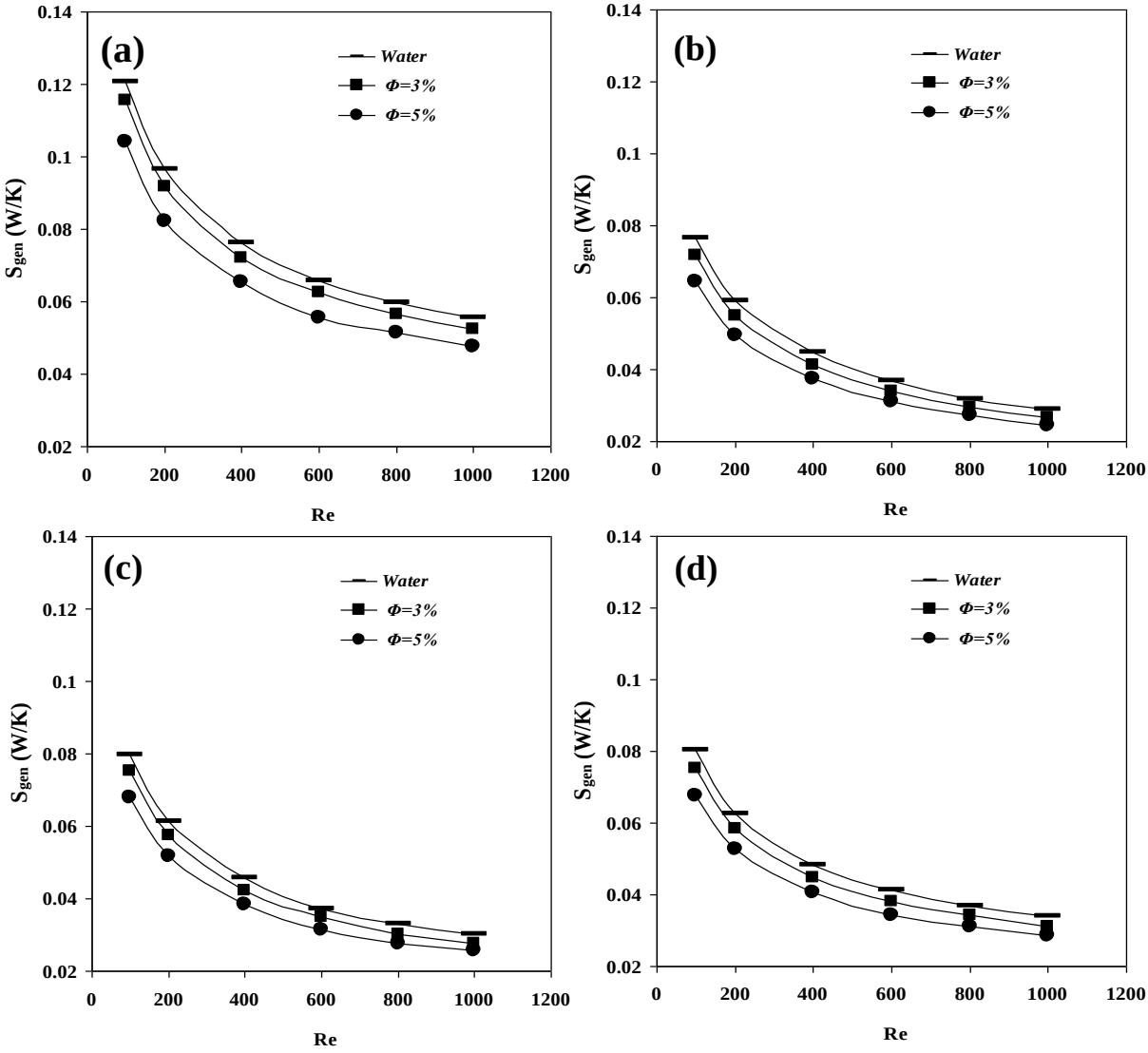

Figure 4-10: Effect of nanofluids volume fraction on S_{gen} of (a) FPHS (b) PSP (c) PCP (d) PEP

4.4 Comparison of Temperature Management of Heat Sinks shapes

Figures 4-11 to 4-12 display the Pinned Plate–Fin heat sink temperature contours of different pins cross-section with *Re*= 200 and 800 using pure water and 5% SiO_2-water nanofluid concentration to achieve the significant heat sink of electronic cooling applications.

Figure 4-11 shows the Pinned Plate – Fin heat sinks temperature contour for water base fluid and 5% SiO_2-water at *Re*= 200. Note that the Pinned Plate – Fin heat sinks have lower temperature distribution from nearly 25.8^{o}C to 51.7^{o}C compared with the surface temperature distribution of flat plate heat sink between approximately 38.6^{o}C and 70.4^{o}C for pure water. This is because the thickness of thermal boundary layer reduces along heat sinks due to presence pins as tabulators. For 5% SiO_2-water nanofluid concentration at the same Reynolds number, the surface temperature distribution reduces for all kinds of heat sinks. The Pinned Plate–Fin heat sinks still have lower temperature distribution from nearly 23.5^{o}C to 46.6^{o}C while the surface temperature distribution of flat plate heat sink is between approximately 34.5^{o}C and 62.5^{o}C. This behaviour happens because the nanofluid increases the value of thermal conductivity for base fluid (Brownian motion) and the heat transfer rate enhances from solid domain to fluid flow filed.

When the Reynolds number increases to 800, as shown in Figure 4-12, the temperature range is lower than that of low Reynolds number at 200 for all types of heat sinks shapes. Therefore, it means that the cooling is rate improved with increasing *Re*. Note that the temperature distribution range drops for both the Pinned Plate – Fin and traditional heat sinks. The temperature distribution of Pinned Plate – Fin heat sinks is from nearly 21.6^{o}C to 38^{o}C and from 21^{o}C to 35^{o}C for pure water and 5% SiO_2-water nanofluid, respectively. While the surface temperature distribution of traditional heat sink is from approximately 28^{o}C to 51^{o}C and 26^{o}C and 46.5^{o}C for pure water and 5% SiO_2-water nanofluid, respectively. This is because increasing Reynolds number leads to an increase in the velocity gradient and demolishing the thickness of the thermal boundary layer along the heat sinks channel.

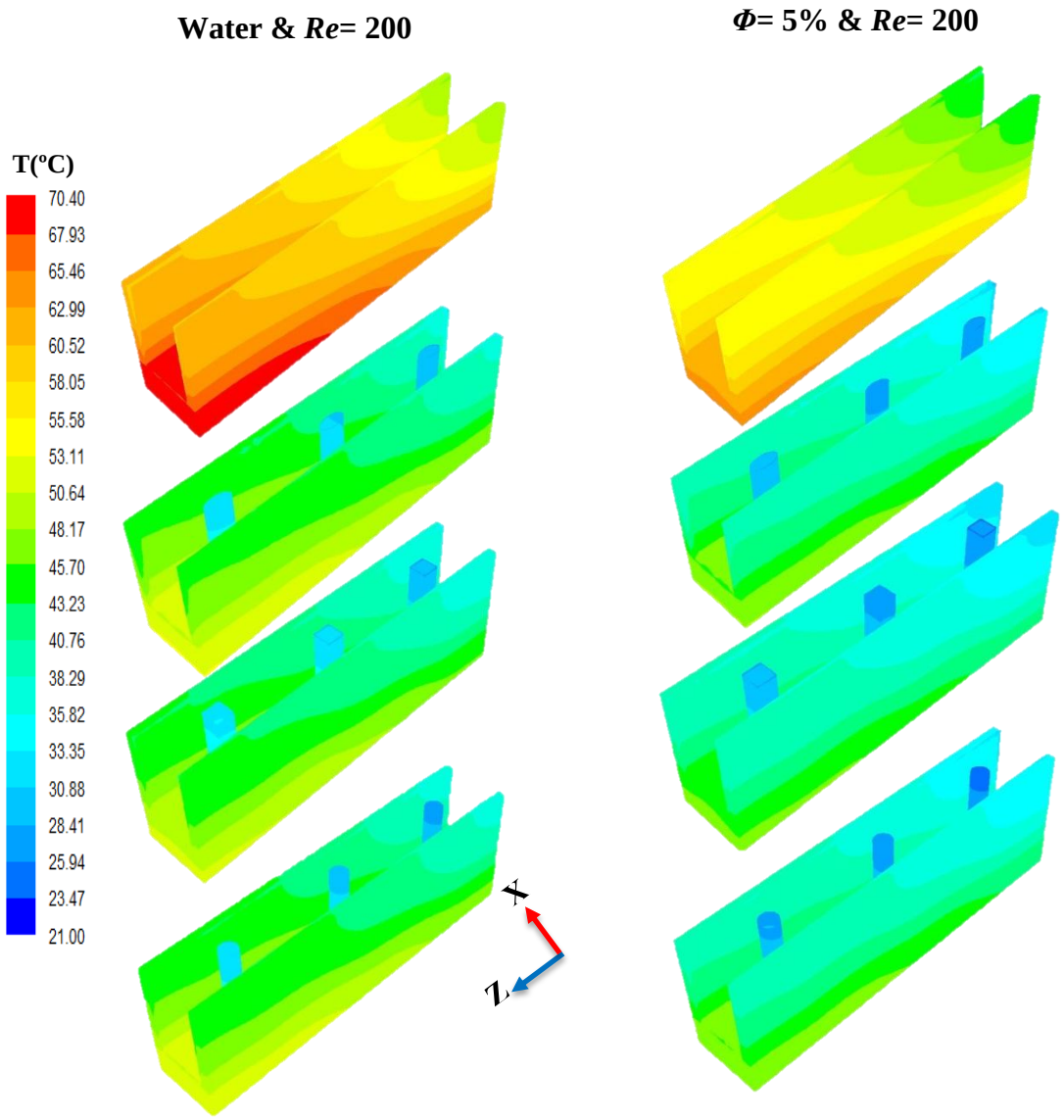

Figure 4-11: Isotherms contour of Pinned Plate – Fin heat sinks with different pin cross section at *Re*= 200 with water and 5% SiO_2-water

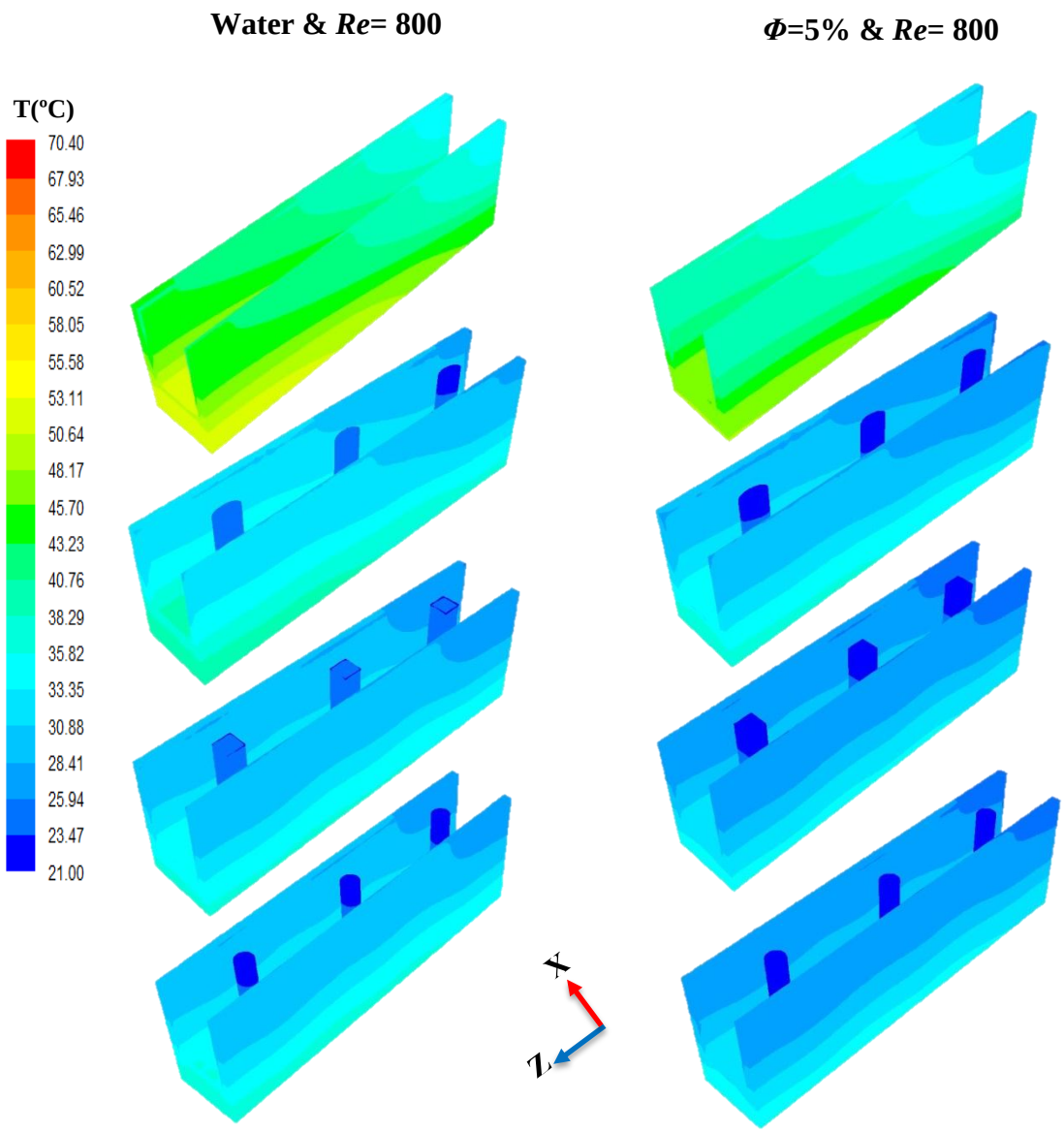

Figure 4-12: Isotherms contour of Pinned Plate – Fin heat sinks with different pin cross section at *Re*= 800 with water and 5% SiO_2-water

4.5 Comparison between Heat Sinks shapes

The effect of different heat sink shapes on the hydrothermal characteristics is shown in Figures 4-13 to 4-17. Three different Pinned Plate – Fin heat sink shapes that are plate-circular pins (PCP), plate-square pins (PSP), and plate-elliptic pins (PEP) heat sinks are compared with the flat-plate heat sink (FPHS) as a traditional shape, with pure water and 5% of SiO_2-water for discovering the substantial heat sink for electronic cooling applications.

In Figure 4-13 (a-b), the pressure drop (ΔP) grows, at any given shape, with increasing Reynolds number due to the rise in the velocity gradient at the internal wall of the channel. In addition, the pressure drop of Pinned Plate – Fin heat sinks is larger than that of the traditional heat sink at any Reynolds number. This is because the presence of pins obstructs the fluid flow path across the heat sink channels. The PEP has a lower increasing in pressure drop by about 2.6 and 2 times for water and 5% SiO2-water respectively, than the traditional heat sinks. While the significant growing of pressure drop was for PSP by approximately 3.7 and 3.25 times for water and 5% SiO_2-water, respectively, compared with the traditional heat sinks. because the shape of the square pin has a large drag force and obstruction for fluid flow path compared with PCP and PEP, which are more aerodynamic shapes.

Figure 4-14 (a-b) displays that the average Nusselt number ($\overline{Nu}$) has similar behaviour for all kinds of heat sinks. The average Nusselt number is remarkably enhanced with increasing Reynolds number due to increase the temperature gradient and reducing the thermal boundary layer thickness along the heat sinks channels leads to enhancement of heat transfer rate. The Pinned Plate – Fin heat sinks have a larger $\overline{Nu}$ than that of the flat plate heat sink for any given Reynolds number. This is because the presence of pins produces vortics and re-circulation fluid flow leads to an improvement in the mixing of fluid layers. Thus, the highest average Nusselt number for PCP is around 93% and 100% for pure water and 5% SiO_2-water, respectively compared with other Pinned Plate – Fin heat sinks.

The base temperature of heat sinks (T_b) has the same behaviour for all types of heat sinks, as shown in Figure 4-15 (a-b). It is found that the base temperature goes down

with increasing Reynolds number due to vanishing the boundary layers thickness which leads to improvement the cooling rate. For any given Reynolds number, the Pinned Plate – Fin heat sinks have a lower T_b than that of the flat plate heat sink because of the presence of pins, as mentioned earlier. Furthermore, pins are represented as obstacles development the thermal boundary layer across the heat sink channels. Therefore, the PCP and PSP have the lowest T_b nearly 25% for pure water and 5% nanofluid.

Figure 4-16 (a-b) illustrates that the total entropy generation (S_{gen}) has the same pattern for all types of heat sinks. The total entropy generation significantly reduces with increasing Reynolds number due to the enhancement in cooling rate of heat sinks, as mentioned early. The PCP and PSP have the smallest entropy generation approximately 42% for pure water and 5% SiO_2-water among other heat sinks. However, the highest entropy generation is for PF heat sink for water and 5% SiO_2-water. The main reason is that the PCP and PSP have the largest heat transfer enhancement and the smallest reduction in the base temperature among other heat sinks. Thus, the irreversibility of PCP and PSP is lower than that of other heat sinks. This means that the thermal entropy generation dominates on the total entropy generation higher than the frictional entropy.

The hydrothermal performance of heat sinks (*HTP*) is higher than unity and the *HTP* improves as the Reynolds number increases for all kinds of Pinned Plate – Fin heat sinks shapes, as shown in Figure 4-17 (a-b). This is because the enhancement in the average Nusselt number is more substantial than increasing in the pressure drop along heat sinks. Generally, the *HTP* of using nanofluid is more than that of pure water because the cooling rate augmentation for using nanofluid is larger than that of using just pure water. Furthermore, the increasing in the pressure drop of nanofluid is higher than that of pure water. For $Re < 400$ and $Re > 800$, the PEP has the highest hydrothermal performance. However, as $400 \leq Re \leq 800$, the PCP has the highest hydrothermal performance. The maximum *HTP* of PEP is 1.44 and 1.52 for water and SiO_2-water, respectively at $Re = 1000$. While, the greatest *HTP* of PCP is 1.44 and 1.50 for water and SiO_2-water, respectively at $Re = 800$.

According to the previous findings, circular pins (PCP) with flat plate fins achieves the desirable enhancement in hydrothermal performance and the total entropy generation. Furthermore, the PCP heat sink has the most significant Nusselt number, the lowest base temperature, and acceptable pressure drop as well as ease of manufacturing. Thus, the plate-circular pins heat sink (PCP) is chosen to test the effect of the location, number and diameter of pins on the hydrothermal characteristics of the heat sink.

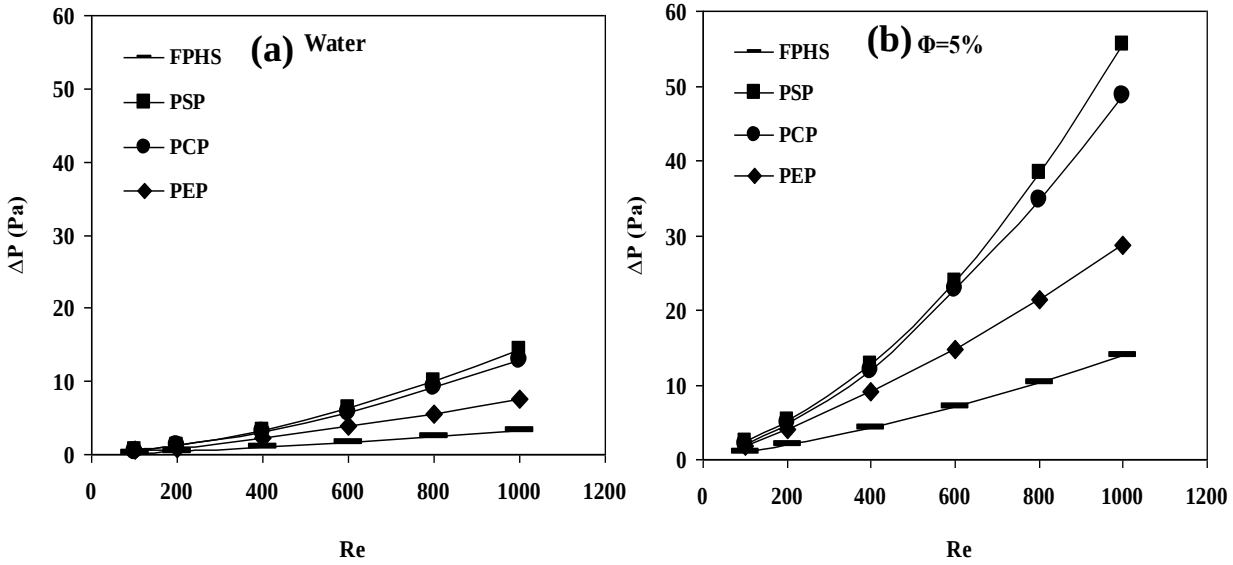

Figure 4-13: Comparison ΔP of heat sinks shape for (a) water (b) Φ=5% SiO_2-water

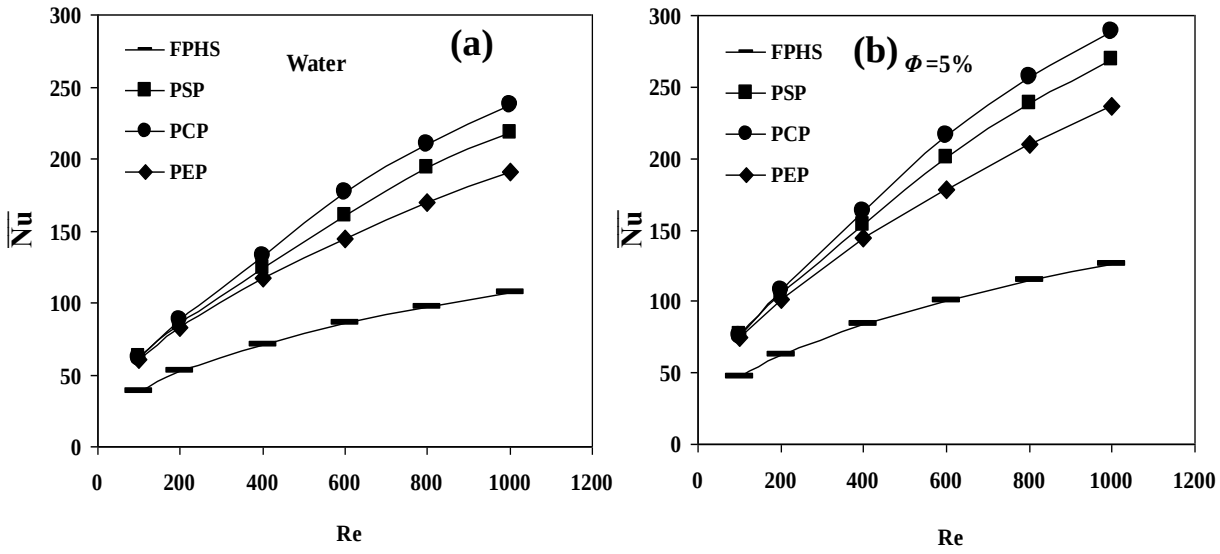

Figure 4-14: Comparison $\overline{Nu}$ of heat sinks shape for (a) water (b) Φ=5% SiO_2-water

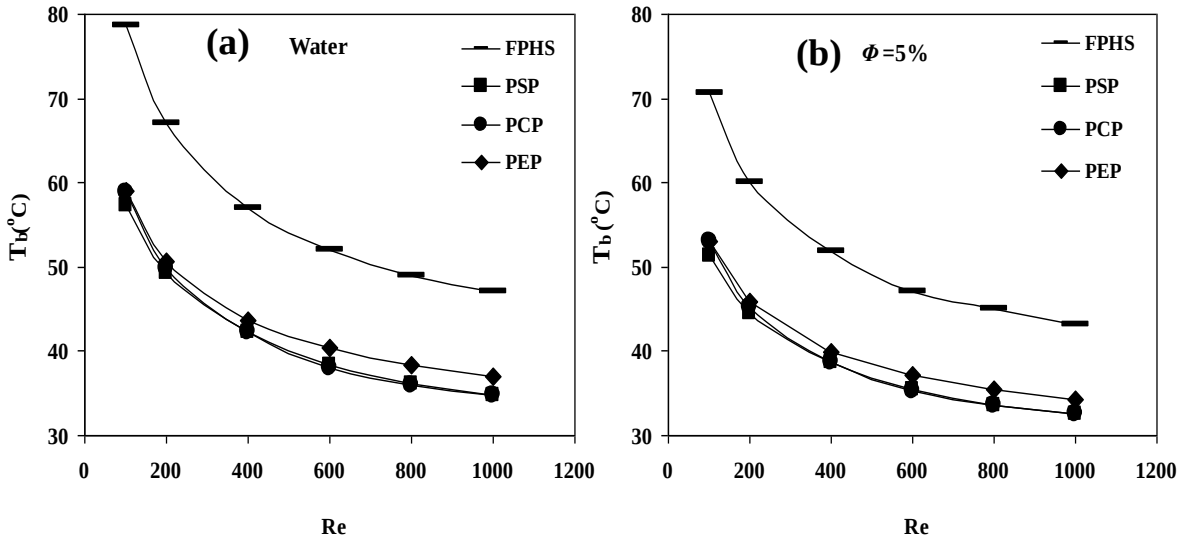

Figure 4-15 : Comparison T_b of heat sinks shape for (a) water (b) Φ=5% SiO_2-water

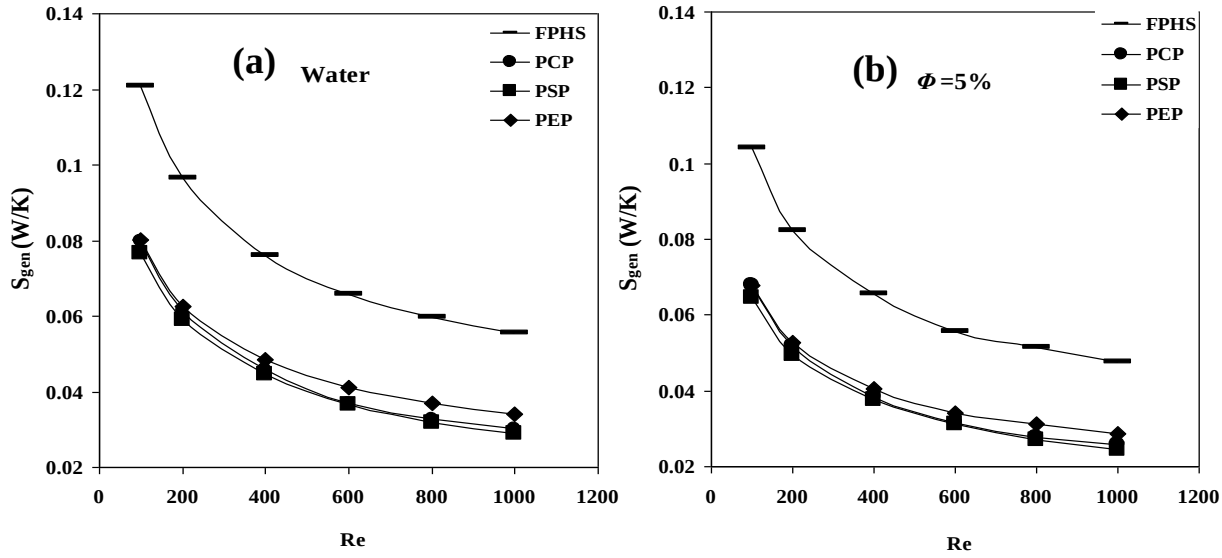

Figure 4-16: Comparison S_{gen} of heat sinks shape for (a) water (b) Φ=5% SiO_2-water

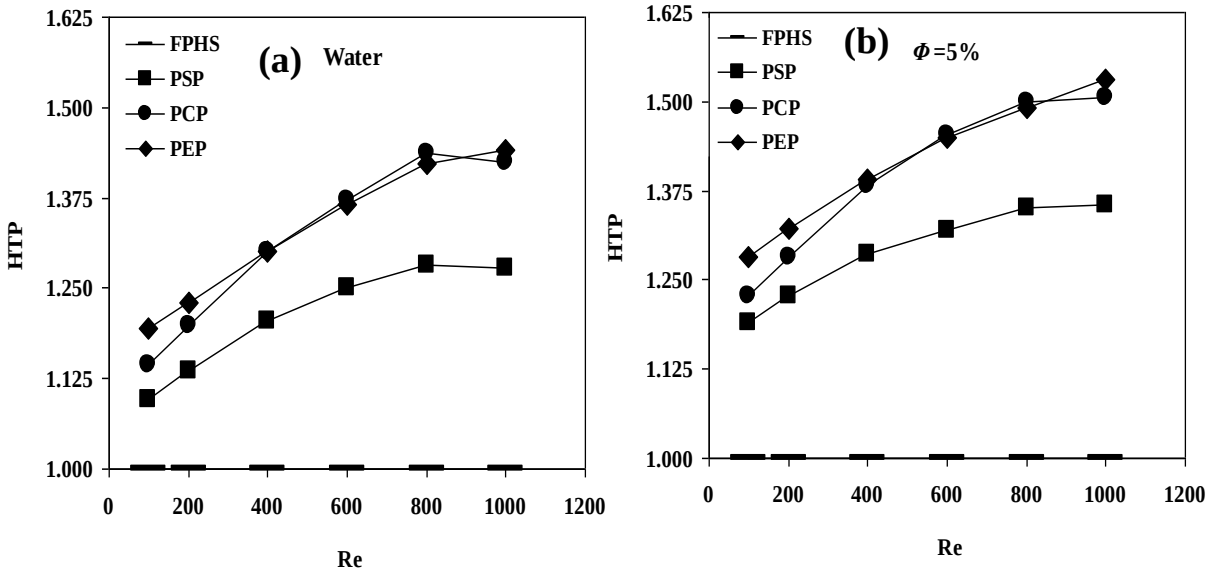

Figure 4-17: *HTP* for Comparison heat sinks shape at (a) water (b) Φ= 5% SiO_2-

4.6 Effect of circular pins location and number

Since the circular pins with flat plate fins obtain the recommended enhancement in hydrothermal performance, the plate-circular pins heat sink (PCP) is chosen to test the effect of the location and number of pins on the hydrothermal characteristics and the total entropy generation of the heat sinks.

4.6.1 One circular pin

Figure 4-18 shows the locations of one circular pin at [Case 1 (Z_1= 7/42), Case 2 (Z_2 = 21/42) and Case 3 (Z_3 = 35/42)] along the Pinned Plate – Fin heat sinks. Figure 4-19 (a-d) explains the effect of one circular pin locations across the heat sink channel on the ΔP, Nu, T_b and S_{gen} with pure water and 5% volume fraction of SiO_2-water.

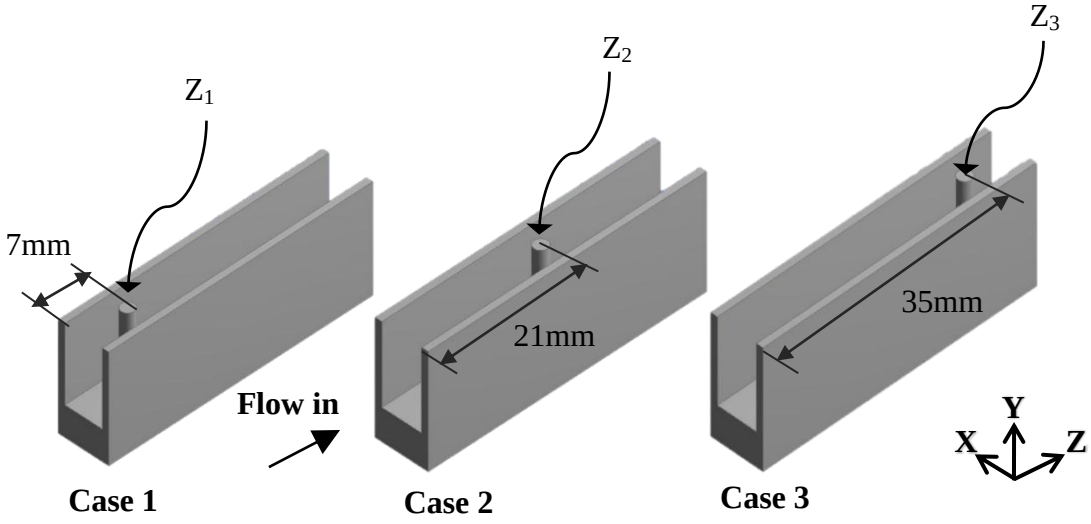

Figure 4-18: The locations of one circular pin across the Pinned Plate – Fin heat sinks channels

It can be shown in Figure 4-19 (a) that the behaviour of pressure drop is similar for all kinds of heat sink shapes. It is noticeable that the pressure drop increases when the Reynolds number increases for any location of pin. The effect of the change of a pin location is less significant on the pressure drop across heat sinks for water and 5% of SiO_2-water since the blockage of fluid flow by a single pin is the same even though the location of pin is changed along the channel of heat sinks.

Figure 4-19 (b) shows that that the average Nusselt number ($\overline{Nu}$) has similar behaviour for all types of heat sinks. It is understandable that the average Nusselt number improves when the Reynolds number goes up for any pin location. When the nanofluid concentration is used, the average Nusselt number enhances. Additionally, when a single pin is at the Case1 of the heat sink channel, it is obtained that the largest average Nusselt number value is nearly 6% and 8% for water and SiO_2-water, respectively. This is probably because of the enhancement in the mixing fluid layers at this location rather than the other locations. Furthermore, the pin at the Case1 location channel might delay the development of boundary layer more than the other locations and this location eliminate the boundary layer.

The patterns of base temperature (T_b) have the same for all types of heat sinks, as shown in Figure 4-19 (c). The base temperature reduces when the Reynolds number increases for any pin location. When the nanofluid concentration is applied instead of pure water, the base temperature of heat sinks reduces. It can be remarked that the T_b values are a lower for the pin at the Case 1 and Case 2 locations than that of the pin at the Case 3 channel for water and 5% of SiO_2-water, for the same previously mentioned reasons in the above section of the Nusselt number. This reduction in the T_b is closely 1% and 2% for water and 5% of SiO2-water, respectively.

Figure 4-19(d) explains that the total entropy generation (S_{gen}) reduces when the Reynolds number grows up. When the nanofluid concentration increases, the entropy generation decreases due to the effect of Brownian motion of nanofluid. It can be noted that the total entropy generation for the pin at the Case 1 and Case 2 locations are slightly lower than that of the pin at the Case 3 channel of heat sinks for water and 5% of SiO_2-water. The decrease in the S_{gen} is about 2% and 3% for water and 5% of SiO_2-water, respectively. This is because the single pin at the Case 1 and Case 2 locations of heat sink have the highest average Nusselt number and the lowest reduction in the base temperature among other heat sinks. Moreover, the irreversibility of this kind of heat sinks is lower than that of other heat sinks.

The hydrothermal performance (*HTP*) of heat sinks enhances when the Reynolds number goes up for any pin location, as shown in Figure 4-20. With applying the

nanofluid concentration for any pin location, the *HTP* is enhanced due to the ratio ofaverage Nusselt number improvement which is larger than the ratio of augmentation in pressure drop. The superior *HTP* values are enlarged of the pin at the Case 1 of the heat sink for pure water and 5% of SiO_2-water. This is because the largest *Nu* is for the pin at the Case 1 location of channel and the single pin at this location as obstacle can reduce the boundary layer thickness more than the other locations leads to delaying the growth of the boundary layer at this region, as mentioned earlier.

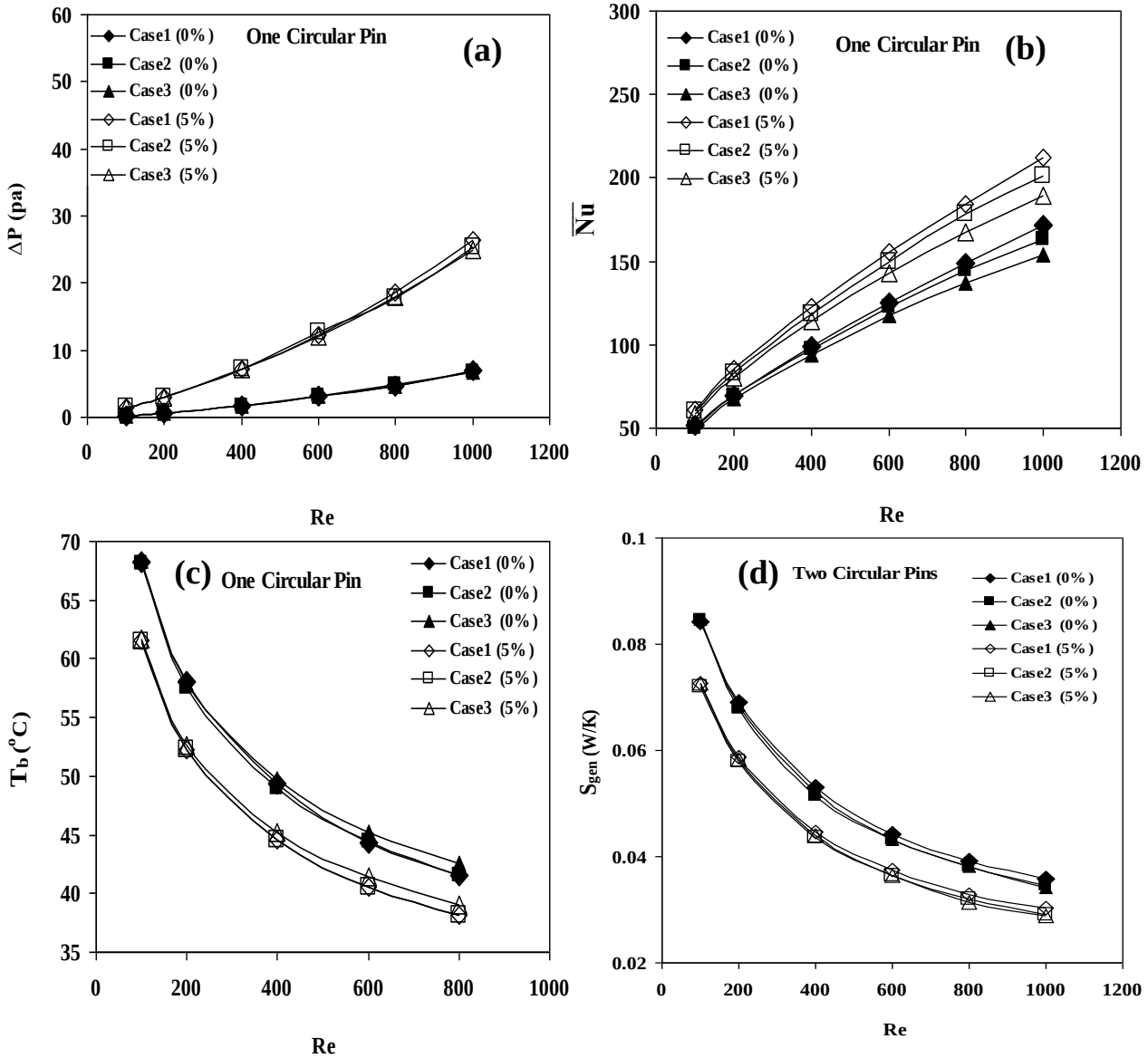

Figure 4-19: Effect of one circular pin location on (a) ΔP (b) *Nu* (c) T_b and (e) S_{gen} for pure water and 5% SiO_2-water

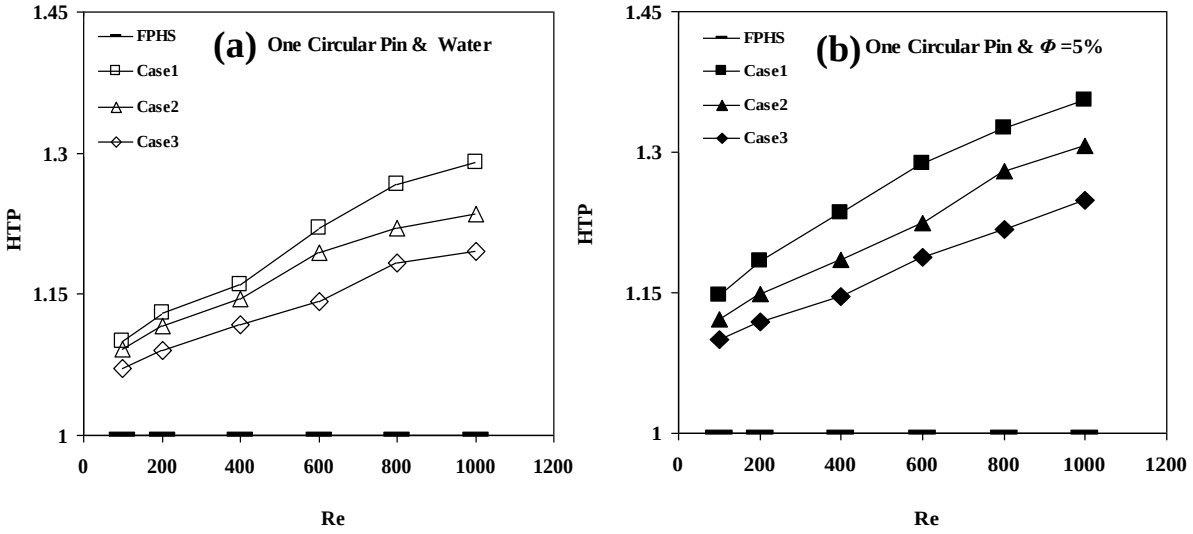

Figure 4-20: Effect of one circular pin location on *HTP* with (a) pure water and (b) 5% SiO_2-water

4.6.2 Two Circular Pins

Figure 4-21 shows the locations of double circular pins at Case 1, Case 2and Case 3 along the Pinned Plate – Fin heat sinks channels. The effect of double circular pins location at channel [Case 1 (Z_1, Z_2), Case 2 (Z_1, Z_3) and Case 3 (Z_2, Z_3)] of the heat sink channel on the ΔP, Nu, T_b and S_{gen} with pure water and 5% volume fraction of SiO_2-water, as shown in Figure 4-22 (a-d).

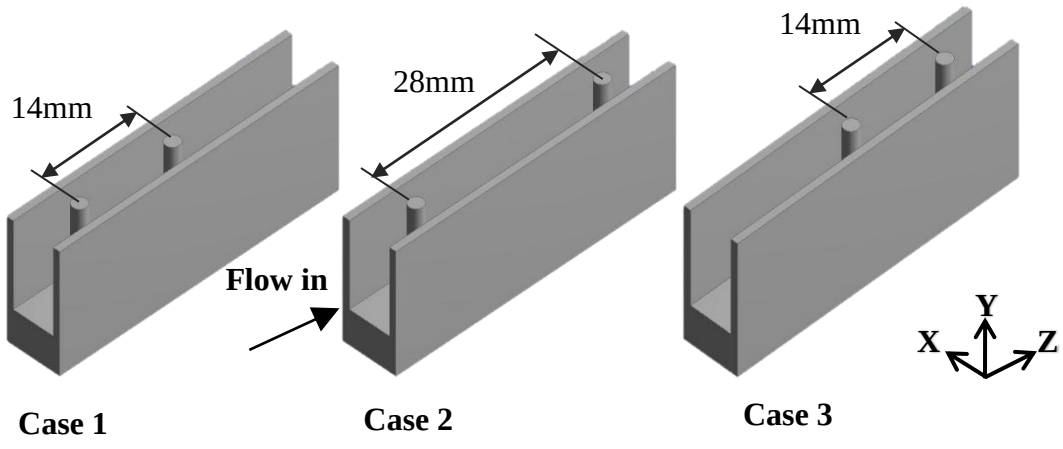

Figure 4-21: The locations of double pins along Pinned Plate – Fin heat sinks channels

It can be noticed that the pressure drop has the same behaviour for all kinds of heat sink shapes, as presented in Figure 4-22 (a). The pressure drop (ΔP) increases when the Reynolds number increases. When the nanofluid concentration is used, the pressure drop goes up as well. It can be noted that the pressure drop values very close even though pins have different locations for water and SiO_2-water. This is because, as mentioned early, the obstruction of fluid flow by double pins is same even though the location of pins is changed along the channel of heat sinks.

The trend of average Nusselt number ($\overline{Nu}$) is similar for all types of heat sink shapes, as illustrated in Figure 4-22 (b). The average Nusselt number improves as increasing the Reynolds number for any pins location. When the nanofluid is used, the average Nusselt number increases, as mentioned early. Moreover, the largest value of Nu is nearly 5% when the double pins are located at the Case 2 and the Case 1 channel compared with the Case 3 location of pins for the base fluid and nanofluid concentration. For the same previous reasons are mentioned, that the enhancement in the mixing fluid layers at these locations are better than as the double pins are at the Case 3 location of the channel. Furthermore, the pins at the Case 1 and Case 2 locations of the channel might delay and destroy the growth of the boundary layer more than when the pins are at the Case 3 location.

Figure 4-22(c) illustrates that the base temperature (T_b) has similar pattern for all kinds of heat sink shapes. The base temperature drops with increasing the Reynolds number, for any pins location. Also, the base temperature decreases as using SiO_2-water instead of pure water. It can be detected that the T_b values are a few lower for the pins at the Case 2and the Case 1 locations than that of pins at the Case 3 channel for water and SiO_2-water, for the same previously mentioned reasons. This dropping in the T_b is around only by 1% for water and 5% of SiO2-water.

The manner of the total entropy generation (S_{gen}) is the same for all types of heat sink shapes, as shown in Figure 4-22(d). It is noticed that the total entropy generation decreases when the Reynolds number increases due to increasing cooling rate from heat sink to fluid flow. When the nanofluid concentration increases, the entropy generation drops due to the Brownian motion of SiO_2-water. It can be obvious that

the total entropy generation for the double pins at the Case 1 and Case 2locations are slightly lower than that of pins at the Case 3 channel of heat sinks for water and 5% of SiO_2-water. The reduction of entropy generation is nearly 2% for water and 5% of SiO_2-water. This is because the double pins at the Case 1 and Case 2locations of heat sink have the largestaverage Nusselt number and the lowest reduction in the base temperature to some extent compared with the double pins at the Case 3 of the channel. Moreover, the irreversibility of this kind of heat sinks is lower than that of other heat sinks.

Figure 4-23 explains that the hydrothermal performance *HTP* enhances as the Reynolds number goes up. When SiO_2-water is used instead of pure water, the *HTP* of heat sinks improves due to the heat transfer rate enhancement is greater than the pressure drop growing. The greater *HTP* value is for the double pins at the Case 1 of the channel for the base fluid and SiO_2-water. Since the highest *Nu* is for the double pins at the Case 1 of the channel as well as the boundary layer thickness reduces more than as the pins are at the other locations, as mentioned earlier.

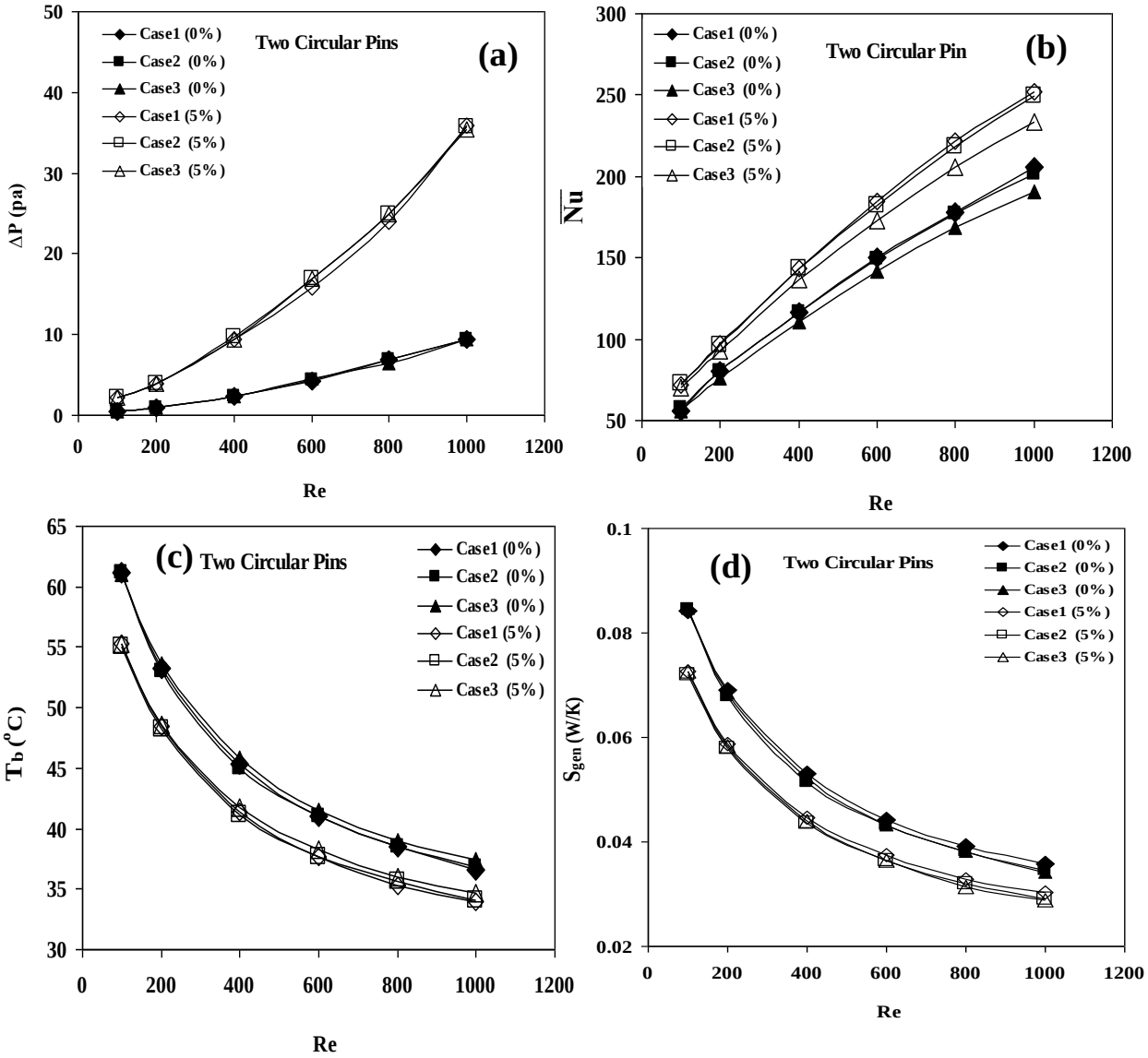

Figure 4-22: Effect of double circular pins locations on (a) ΔP (b) Nu (c) T_b and (d) S_{gen} with pure water and 5% SiO_2-water

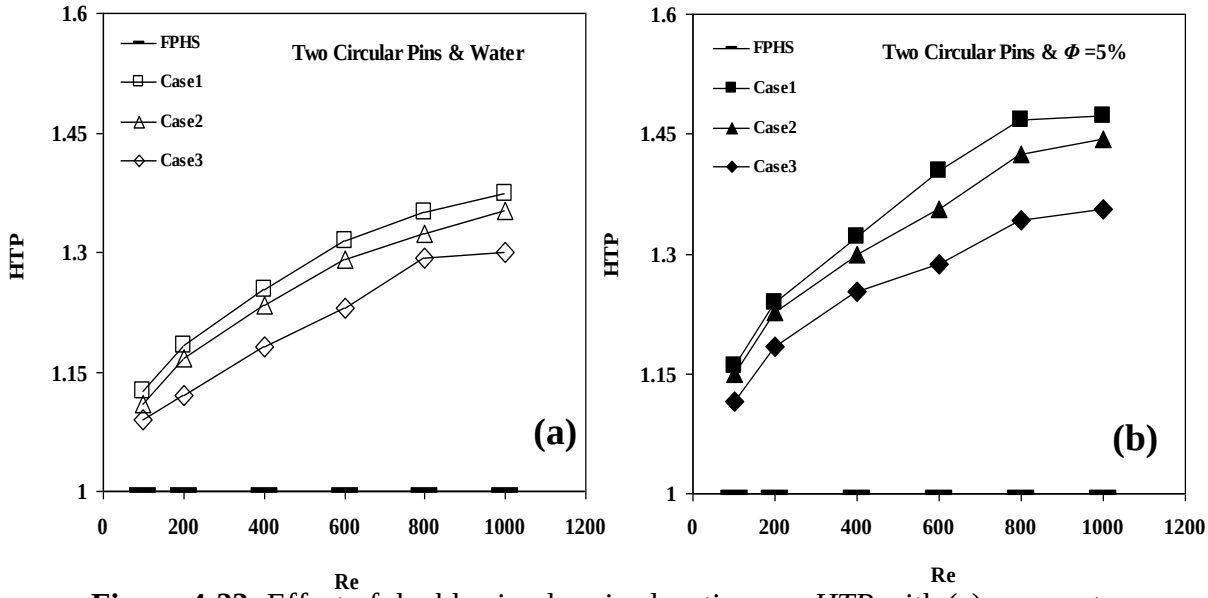

Figure 4-23: Effect of double circular pins locations on *HTP* with (a) pure water and (b) 5% SiO_2-water

4.7 Comparison between One, Two and Three Circular Pins

The S_{gen} and *HTP* of the plate-circular pins heat sink (PCP) with Case 1 single circular pin, Case 1 double and three circular pins are compared together to obtain the remarkable heat sink for electronic cooling applications.

Figure 4-24 (a-b) illustrates the relationship between the total entropy generation (S_{gen}) and Reynold number with a different number of pins for pure water and 5% SiO_2-water nanofluids. It is indicated that the total entropy generation has the same trend for all configuration of pins numbers. The total entropy generation significantly reduces with developing Reynolds number due to the enhancement in cooling rate of heat sinks, as mentioned early. It is clear that the three circular pins have the smallest entropy generation, approximately 24% for both pure water and 5% SiO_2-water among other pins numbers. However, the highest entropy generation is for one pin for water and 5% SiO_2-water. The main reason is that the three circular pins have the maximum heat transfer enhancement and the lowest reduction in the base temperature compared with another number of pins.

The behaviour of the hydrothermal performance (*HTP*) of plate-circular pins heat sink with Reynolds number for a different number of pins for pure water and 5% SiO_2-water nanofluids are explained in Figure 4-25 (a-b). The hydrothermal performance is over one and the *HTP* improves as the Reynolds number increases for all numbers of circular pins. This is because the enhancement of theaverage Nusselt number is more substantial than increasing in the pressure drop along heat sinks. It is noted that the highest hydrothermal performance is for three circular pins for both pure water and 5% SiO_2-water among other pins numbers.

Since the three circular pins with plate fins heat sink has the lowest entropy generation and the highest hydrothermal performance. Consequently, it is recommended to use this kind of heat sinks for an electronic cooling system.

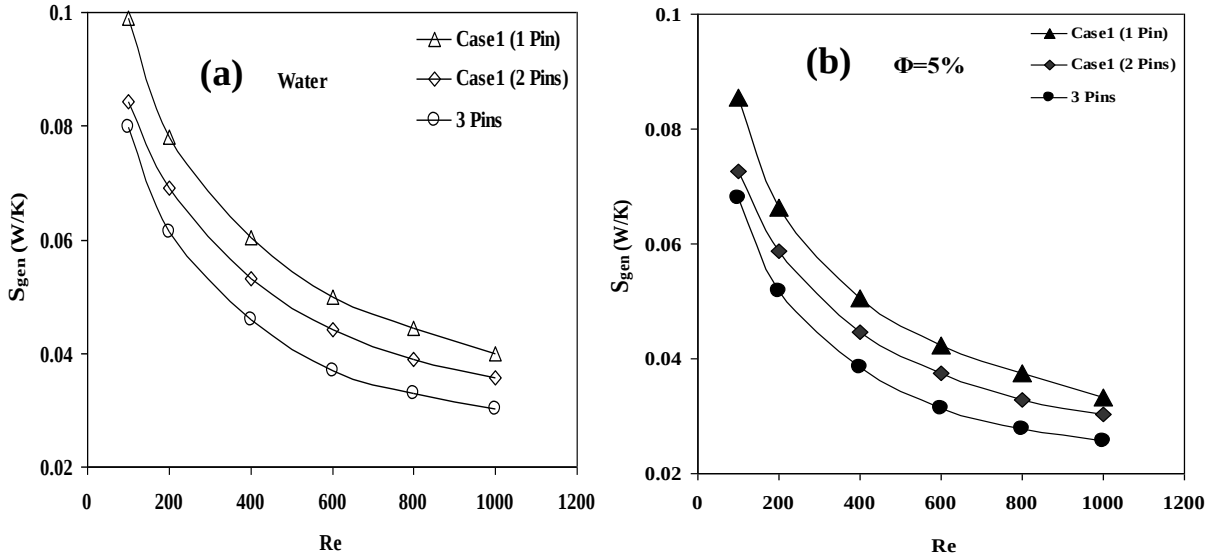

Figure 4-24: Comparison S_{gen} of single, double and three circular pins locations with (a) pure water and (b) 5% SiO_2-water

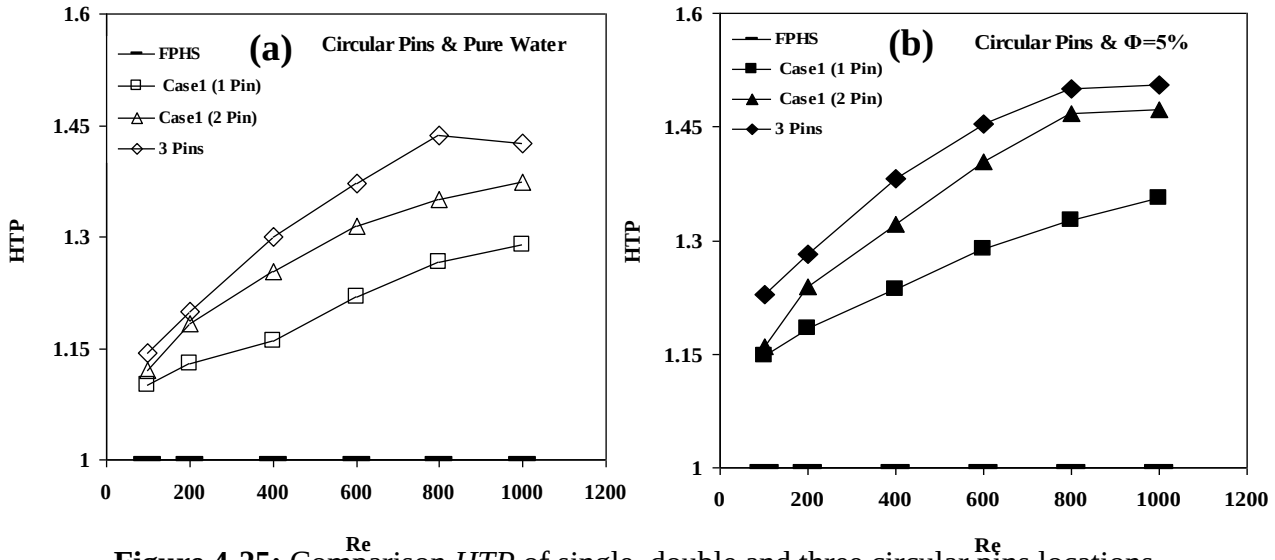

Figure 4-25: Comparison *HTP* of single, double and three circular pins locations with

4.8 Pins Diameter Effect

The behaviour of pin diameter on the characteristics of heat transfer and fluid flow shows in Figure 4-26 (a-d). Three different circular pin diameters are investigated; 1 mm, 2 mm and 3 mm for pure water and 5% nanofluid concentration.

In Figure 4-26 (a), the pressure drop (ΔP) grows when Reynolds number goes up due to the increment of velocity gradient at the internal wall of the channel. Thus, the pressure drop goes up with increasing the diameter of pins for any given Reynolds number. This is because the increase in diameter causes a narrow flow of fluid in the channel results in increase the pressure drop. The pressure drop increases with replacing pure water by 5% nanofluid concentration due to the increase of base fluid viscosity.

The average Nusselt number ($\overline{Nu}$) enhances with increasing Reynolds number increases due to the increasing of temperature gradient and reducing the thickness of boundary layer, as shown in Figure 4-26 (b). The average Nusselt number augments as the pin diameters increases. Thus, the average Nusselt number of 3 mm pin diameter improves about 32% for pure water and SiO_2-water compared with 1mm of the pin diameter. As mentioned early, the surface area of heat transfer enlarges, the

enhancement of conduction heat transfer and proper fluid mixing along the heat sink. The $\overline{\mathrm{Nu}}$ enhances when pure water is replaced by 5% of SiO_2-water due to enhancement in the effective thermal conductivity of the base fluid.

Figure 4-26 (c) shows that the base temperature (T_b) decreases with increases Reynolds number due to the enhancement of heat transfer and cooling rate. When the diameter of pins enlarges, the base temperature decreases. The 3 mm of pin diameter has lower T_b which is nearly 17% for water and SiO_2-water compared with 1mm of pins diameter due to the augmentation in the surface area of heat transfer and proper fluid mixing across the heat sink. The T_b of heat sinks decreases with replacing pure water by 5% nanofluid concentration due to the increase the thermal conductivity effectiveness of base fluid (Brownian motion).

Figure 4-26 (d) shows that the total entropy generation (S_{gen}) goes down when the Reynolds number goes up due to the enhancement in the cooling rate of heat sinks. When the diameter of the pin enlarges, the entropy generation decrease because the heat transfer rate enhances and the base temperature of heat sinks drops with enlargement of pin diameter. The entropy generation decreases with replacing pure water by 5% nanofluid concentration because of the Brownian motion of nanofluid. The 3 mm diameter of pins has the lowest entropy generation which is nearly 32% for both coolant fluids compared with 1mm pins diameter.

The hydrothermal performance (*HTP*) improves as the Reynolds number goes up due to the ratio of average Nusselt number enhancement which is larger than that of pressure drop, as shown in Figure 4-27. As $Re > 200$, the superior case is for 2 mm of pin diameter because it has the excellent balance between the increasing pressure drop and the average Nusselt number enhancement ratio compared with the case 1 mm and 3 mm of pin diameters. The *HTP* increases with replacing pure water by 5% nanofluid concentration because the ratio of increasing in average Nusselt number values is more remarkable than the growth in the pressure drop.

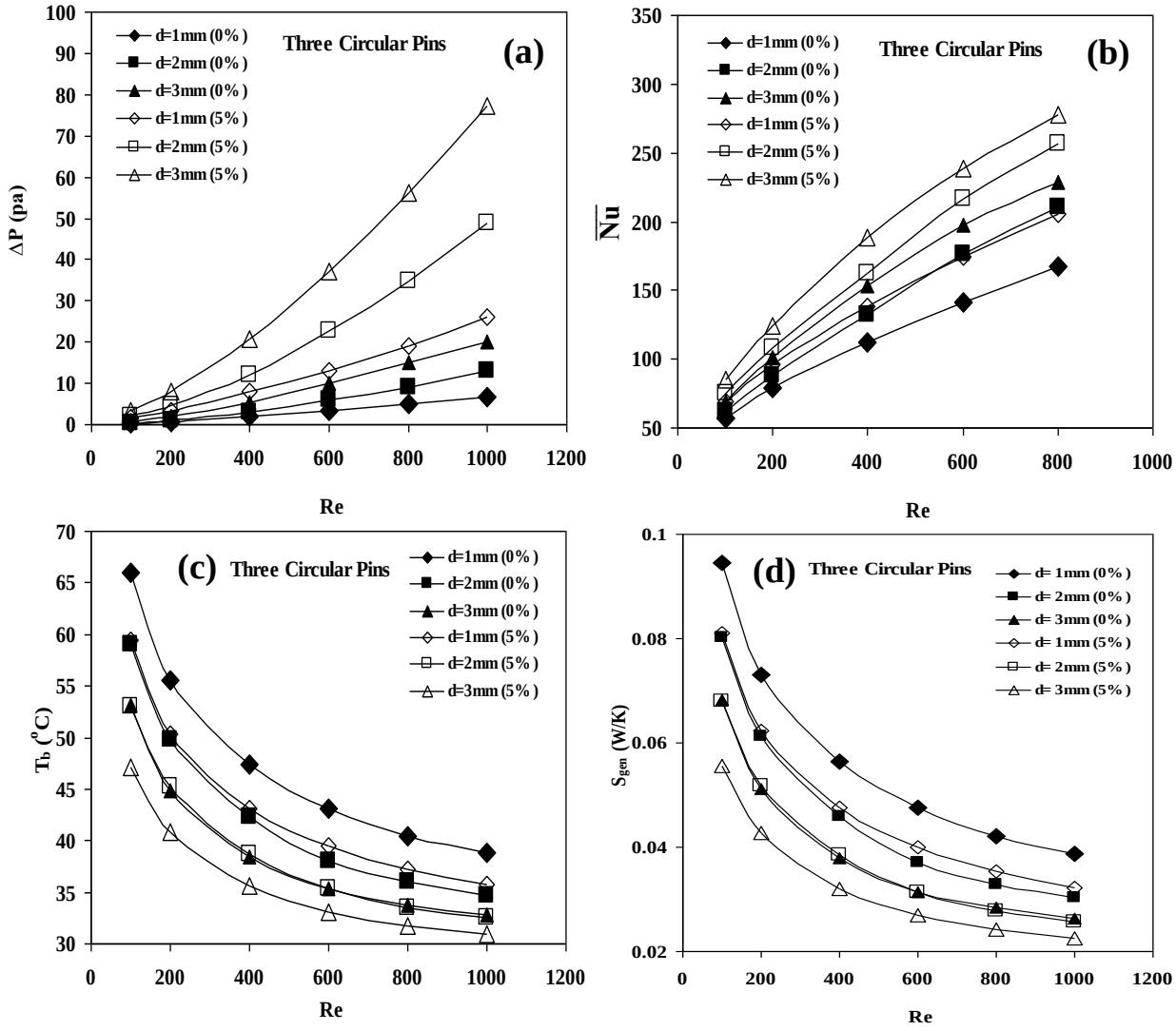

Figure 4-26 : Effect of pin diameter on (a) ΔP (b) $\overline{Nu}$ (c) T_b (d) S_{gen} for pure water and 5% SiO_2-water

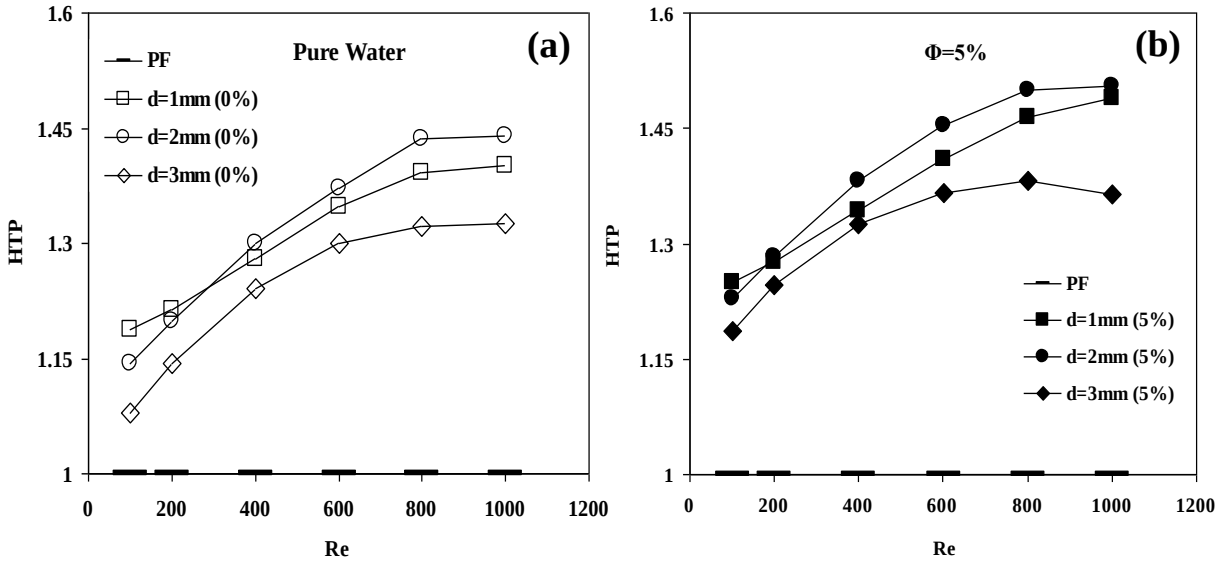

Figure 4-27 : Effect of pin diameter on *HTP* with (a) pure water and (b) 5% SiO_2-water

CHAPTER FIVE

Conclusion and Recommendations

5.1 Conclusions

In the current research, the computational investigation of laminar forced convection and the total entropy generation in a Pinned Plate – Fin heat sink using SiO_2-Water nanofluids as a coolant is considered. The ANSYS-FLUENT 14.5 package program is applied with various range of Reynolds numbers of (100-1000) and 0, 1, 2, 3, 4 and 5% SiO_2-Water nanofluids concentration as 20 nm SiO_2 particle diameter. Three different geometries of Pinned Plate – Fin heat sinks such as plate-square pins heat sink (PSP), plate-circular pins heat sink (PCP) and plate-elliptic pins heat sink (PEP) are compared with the traditional flat plate fins heat sink (FPHS) as a traditional case. Also, the location and the number of circular pins are assessed. Thus, the diameter of the circular pins of Pinned Plate – Fin heat sinks is tested. Furthermore, the findings of the present work are compared with the previous numerical and experimental studies to validate the used package accuracy. Moreover, the grid independence test (GIT) is achieved to estimate the mesh quality in the present study.

The following points outline briefly the summary of the main results of this study:

1. The hydrothermal performance, pressure drop and average Nusselt number are increased while the total entropy generation and the base temperature of heat sink are reduced with increasing the SiO_2-water nanofluids concentration and Reynolds number for all heat sinks shapes.

2. The highest average Nusselt number of PCP is around 93% and 100% for pure water and 5% SiO_2-water, respectively, compared with other Pinned Plate – Fin heat sinks.

3. The PCP and PSP have the lowest base temperature, which is nearly 25% for pure water and 5% nanofluids.

4. The highest hydrothermal performance for PEP is 1.44 and 1.52 for water and SiO_2-water, respectively, as *Re*= 1000. While, the most magnificent hydrothermal performance for PCP is 1.44 and 1.50 for water and SiO2-water, respectively, as *Re*= 800.

5. The PCP and PSP have the smallest total entropy generation, approximately 42% for pure water and 5% SiO_2-water among other heat sinks.

6. The plate-circular pins heat sink (PCP) produce a significant enhancement in hydrothermal performance and the total entropy generation. Thus, it has the most substantial Nusselt number, the lowest the base temperature, acceptable pressure drop as well as ease of manufacturing.

7. Concerning the location and number of pins, the lowest entropy generation and the highest hydrothermal performance are for three circular pins (PCP).

8. Based on the diameter of pins, the superior case is for 2mm of pins diameter as *Re* > 200, because it has the preferable balance between the increase of pressure drop and the average Nusselt number enhancement ratio compared with the case 1 mm and 3 mm of pin diameters.

In General, the results show that using the plate-circular pins heat sink (PCP) with SiO_2-water nanofluid instead of the traditional base fluid can produce a considerable improvement in the hydrothermal and total entropy generation performance of heat sinks. Thus, it is recommended to use this kind of heat sinks for an electronic cooling systems.

5.2 Recommendations for Future Studies

According to the results of the current numerical study, it can be performed investigations that given for the future as follows:

1. An experimental study to examine the hydrothermal performance and the entropy generation of suggested Pinned Plate – Fin heat sinks.

2. Other extended surface as turbulators geometries such as twisted pins, winglets, rings, twisted pins, baffles, vortex generator, and obstacles could be numerically and experimentally performed.

3. The turbulent nanofluids flow over Pinned Plate – Fin heat sinks with different shapes of pins cross-section can be experimentally and numerically investigated.

4. The unsteady flow effects could be demonstrated for future consideration.

5. The effect of vibration and noise on the hydraulic and thermal characteristics as well as the entropy generation of Pinned Plate – Fin heat sinks could be tested.

6. It is recommended to examine the experimental and numerical of natural convection heat transfer, fluid flow and entropy generation for this kind of heat sink shapes.

7. It could be experimentally applied the Pinned Plate – Fin heat sinks for PV panels, turbine blades, LED lighting system, solar collectors and other applications.

References

[1] L. T. Yeh, "Review of Heat Transfer Technologies in Electronic Equipment," Journal of electronic packaging, vol. 117, pp.333–339, 1995.

[2] Y. K. Prajapati, "Influence of fin height on heat transfer and fluid flow characteristics of rectangular microchannel heat sink," International Journal of Heat and Mass. vol. 137, pp. 1041–1052, 2019.

[3] A. J. Chamkha, M. Molana, A. Rahnama, and F. Ghadami, "On the nanofluids applications in microchannels: A comprehensive review," Powder Technol. vol. 332, pp. 287-322, 2018.

[4] Y. Yang and H. Peng, "Investigation of planted pin fins for heat transfer enhancement in plate fin heat sink," Microelectronics Reliability. vol. 49, no. 2, pp. 163–169, 2009.

[5] S. Lee, "Measuring Thermal Conductivity of Fluids Containing Oxide Nanoparticles," Journal of Heat Transfer, vol. 121, pp. 280-289, 1999.

[6] Y. Xuan and Q. Li, "Heat transfer enhancement of nanofluids," *International Journal of heat and fluid flow*, vol. 21, pp. 58–64, 2000.

[7] A. Al-damook and F. Saleh, "Heat transfer and air flow characteristics enhancement of compact plate-pin fins heat sinks – a review," Propulsion and Power Research, vol. 7, no. 2, pp. 138–146, 2018.

[8] G. Xie, Z. Chen, B. Sunden, and W. Zhang, "Numerical Predictions of the Flow and Thermal Performance of Water-Cooled Single-Layer and Double-Layer Wavy Microchannel Heat Sinks," Numerical Heat Transfer, Part A : Applications, vol. 63, no. 3, pp. 37– 41, 2013

[9] H. E. Ahmed and M. I. Ahmed, "Optimum thermal shape of triangular, trapezoidal and rectangular grooved microchannel heat sinks," International Communications in Heat and Mass Transfer. vol. 66, pp. 47– 57, 2015.

[10] B. Fani, A. Abbassi, and M. Kalteh, "Effect of nanoparticles size on thermal performance of nanofluid in a trapezoidal microchannel-heat-sink," International Communications in Heat and Mass Transfer. vol. 45, pp. 155–161, 2013.

[11] C. Chen and C. Ding, “Study on the thermal behavior and cooling performance of a nanofluid-cooled microchannel heat sink,” International Journal of Thermal Sciences., vol. 50, no. 3, pp. 378–384, 2011.

[12] T. Hung, W. Yan, X. Wang, and C. Chang, “Heat transfer enhancement in microchannel heat sinks using nanofluids,” International Journal Heat Mass Transf., vol. 55, pp. 2559–2570, 2012.

[13] A. A. Alfaryjat, D. Stanciu, A. Dobrovicescu, V. Badescu and M. Aldhaidhawi, “Numerical investigation of entropy generation in micro- channels heat sink with different shapes,” In IOP conference series: materials science and engineering, vol. 147, no. 1, p.012134. IOP Publishing, 2016.

[14] A. A. Alfaryjat, A. Dobrovicescu, and D. Stanciu, “Influence of heat flux and Reynolds number on the entropy generation for different types of nanofluids in a hexagon microchannel heat sink,” Chinese Journal of Chemical Engineering. vol. 27, no. 3, pp. 501-513, 2019.

[15] A. Shalchi-tabrizi and H. Reza, “Analysis of entropy generation and convective heat transfer of Al_2O_3 nanofluid flow in a tangential micro heat sink,” International Journal of Heat and Mass Transfer. vol. 55, pp. 4366–4375, 2012.

[16] C. J. Ho, L. C. Wei, and Z. W. Li, “An experimental investigation of forced convective cooling performance of a microchannel heat sink with Al2O3/water nanofluid,” Applied Thermal Engineering. vol. 30, pp. 96–103, 2010.

[17] W. Duangthongsuk, S. Dalkilic, and S. Wongwises, “Convective Heat Transfer of Al_2O_3-water Nanofluids in a Microchannel Heat Sink,” Current Nanoscience, vol. 8, pp. 317–322, 2012.

[18] S. M. Hassani, M. Khoshvaght-aliabadi, and S. H. Mazloumi, “Influence of chevron fin interruption on thermo-fluidic transport characteristics of nanofluid-cooled electronic heat sink,” Chemical Engineering Science. vol. 191, pp. 436–447, 2018.

[19] S. Halelfadl, A. M. Adham, N. Mohd-ghazali, T. Maré, P. Estellé, and R. Ahmad, “Optimization of thermal performances and pressure drop of rectangular microchannel heat sink using aqueous carbon nanotubes based nanofluid,” Applied Thermal Engineering. vol. 62, no.2, pp. 492–499, 2014.

[20] E. Manay, E. F. Akyürek, and B. Sahin, “Entropy generation of nanofluid flow in a microchannel heat sink,” Results in Physics. vol. 9, pp. 615-624, 2018.

[21] A. Ijam, R. Saidur, and P. Ganesan, “Cooling of minichannel heat sink using nanofluids,” International Communications in Heat and Mass Transfer. vol. 39, no. 8, pp. 1188–1194, 2012.

[22] S. Mohammad, H. Hashemi, S. A. Fazeli, H. Zirakzadeh, and M. Ashjaee, “Study of heat transfer enhancement in a nanofluid-cooled miniature heat sink,” International Communications in Heat and Mass Transfer. vol. 39, no. 6, pp. 877–884, 2012.

[23] S. A. Jajja, W. Ali, H. M. Ali, and A. M. Ali, “Water cooled minichannel heat sinks for microprocessor cooling: Effect of fin spacing,” Applied Thermal Engineering. vol. 64, pp. 76–82, 2014.

[24] P. Naphon and L. Nakharintr, “Heat transfer of nanofluids in the mini-rectangular fin heat sinks,” International Communications in Heat and Mass Transfer. vol. 40, no. 1, pp. 25–31, 2013.

[25] S. M. Hassani and S. H. Mazloumi, “Performance enhancement of straight and wavy miniature heat sinks using pin-fin interruptions and nanofluids,” Chemical Engineering and Processing, vol. 122, pp. 90–108, 2017.

[26] S. A. Fazeli, S. Mohammad, H. Hashemi, H. Zirakzadeh, and M. Ashjaee, “Experimental and numerical investigation of heat transfer in a miniature heat sink utilizing silica nanofluid,” Superlattices Microstructures. vol. 51, no. 2, pp. 247–264, 2012.

[27] M. Saeed and M. Kim, “Heat transfer enhancement using nanofluids (Al_2O_3-H_2O) in mini-channel heatsinks,” International Journal of Heat and Mass Transfer. vol. 120, pp. 671–682, 2018.

[28] M. R. Sohel, R. Saidur, S. S. Khaleduzzaman, and T. A. Ibrahim, “Cooling performance investigation of electronics cooling system using Al_2O_3-H_2O nano fluid,” International Communications in Heat and Mass Transfer. vol. 65, pp. 89–93, 2015.

[29] C. J. Ho and W. C. Chen, “An experimental study on thermal performance of Al_2O_3/water nanofluid in a minichannel heat sink,” Applied Thermal Engineering. vol. 50, pp. 516–522, 2013.

[30] M. I. Hasan, “Investigation of flow and heat transfer characteristics in micro pin fin heat sink with nanofluid,” Applied Thermal Engineering. vol. 63, no. 2, pp. 598–607, 2014.

[31] J. F. Tullius, T. K. Tullius, and Y. Bayazitoglu, “Optimization of short micro pin fins in minichannels,” International Journal of Heat and Mass Transfer. vol. 55, pp. 3921–3932, 2012.

[32] W. Duangthongsuk and S. Wongwises, “An experimental study on the thermal and hydraulic performances of nanofluids flow in a miniature circular pin fin heat sink,” Experimental Thermal and Fluid Science. vol. 66, pp. 28–35, 2015.

[33] W. Duangthongsuk and S. Wongwises, “A Comparison of the Heat Transfer Performance and Pressure Drop of Nanofluid-Cooled Heat Sinks with Different Miniature Pin Fin Configurations,” Experimental Thermal and Fluid Science. vol. 69, pp. 111–118, 2015.

[34] M. Khoshvaght-Aliabadi, S. Deldar, and S. M. Hassani, “Effects of pin-fins geometry and nanofluid on the performance of a pin-fin miniature heat sink (PFMHS),” International Journal of Mechanical Sciences. vol. 148, pp. 442–458, 2018.

[35] A. H. Muhammad and W. Arshad, “Effect of channel angle of pin-fin heat sink on heat transfer performance using water based graphene nanoplatelets nanofluids,” International Journal of Heat and Mass Transfer. vol. 106, pp. 465–472, 2017.

[36] R. Vinoth and D. Senthil Kumar, “Channel cross section effect on heat transfer performance of oblique finned microchannel heat sink,” International Communications in Heat and Mass Transfer. vol. 87, pp. 270–276, 2017.

[37] H. Shafeie, O. Abouali, K. Jafarpur, and G. Ahmadi, “Numerical study of heat transfer performance of single-phase heat sinks with micro pin-fin structures,” Applied Thermal Engineering. vol. 58, pp. 68–76, 2013.

[38] T. Ambreen and M. H. Kim, “Effect of fin shape on the thermal performance of nanofluid-cooled micro pin-fin heat sinks,” International Journal of Heat and Mass Transfer. vol. 126, pp. 245–256, 2018.

[39] Y. Jia, G. Xia, Y. Li, D. Ma, and B. Cai, “Heat transfer and fluid flow characteristics of combined microchannel with cone-shaped micro pin fins,” International Communications in Heat and Mass Transfer. vol. 92, pp. 78–89, 2018.

[40] M. Roshani, S. Z. Miry, P. Hanafizadeh, and M. Ashjaee, “Hydrodynamics and Heat Transfer Characteristics of a Miniature Plate Pin-Fin Heat Sink Utilizing Al_2O_3–Water and TiO_2–Water Nanofluids,” Journal of Thermal Science and Engineering Applications vol. 7, no. 3, pp. 031007, 2015.

[41] H. Zirakzadeh, A. Mashayekh, H.N. Bidgoli, M. Ashjaee, “Experimental investigation of heat transfer in a novel heat sink by means of alumina nanofluids,” Heat Transfer Research, vol. 43, no. 3, pp. 709–720, 2012.

[42] ANSYS FLUENT V 14.5 User’s Guide, 2012

[43] R.W. Serth, “Process heat transfer”. Academic press; ” 2nd Edition. 2014

[44] J.D., Anderson J., Wendt, “Computational fluid dynamics,”. *New York: McGraw-Hill*. 1995.

[45] M. Corcione, “Heat transfer features of buoyancy-driven nanofluids inside rectangular enclosures differentially heated at the sidewalls,” International Journal of Thermal Sciences. vol. 49, no. 9, pp. 1536–1546, 2010.

[46] R. S. Vajjha and D. K. Das, “Experimental determination of thermal conductivity of three nanofluids and development of new correlations,” International Journal of Heat and Mass Transfer. vol. 52, pp. 4675–4682, 2009.

[47] A. Al-damook, N. Kapur, J. L. Summers, and H. M. Thompson “Computational Shape and Optimisation of Pin Fin Heat Sinks with Rectangular Perforations,” Applied Thermal Engineering. vol. 105, pp. 691–703, 2016.

[48] Khan, W. A., Culham, J. R., and Yovanovich, M. M. "Optimization of pin-fin heat sinks using entropy generation minimization." IEEE Transactions on Components and Packaging Technologies vol.28, no. 2, pp. 247-254, 2005.

[49] W. Guo, G. Li, Y. Zheng, and C. Dong, “Numerical study of nanofluids thermal and hydraulic characteristics considering Brownian motion effect in micro fin heat sink,” Journal of Molecular Liquids. vol. 264, pp. 38–47, 2018.

الخلاصة

من اهم التحديات التي تواجه الصناعات الحديثة هي مشكلة ارتفاع درجة الحرارة في الاجهزة الالكترونية والمحولات الكهربائية والمحركات الميكانيكية بكافة انواعها. ان ارتفاع درجة الحرارة اكثر من الحد المسموح به يسبب تلف في اجزاء تلك الاجهزة و تعطيلها، لذلك تحتاج تلك الاجهزة والمكائن تبريداً جيداً وابقاءها عند درجة حرارة محددة لكل جهاز بالاستعانة بطرق التبريد المتعددة. تعد الاحواض الحرارية واحد من تلك الطرق المتاحة وغير مكلفة لتبريد تلك الاجهزة و تشتيت الحرارة المتولدة منها.

يستخدم في هذا البحث الاحواض الحرارية المدمجة (زعانف مسطحة مع الزعانف الوتدية مدمجة معاً في حوض حراري واحد) مع استخدام تقنية التبريد بالموانع النانوية مستخدماً سليكا اوكسيد للمائع النانوي المذاب بالماء كمائع تشغيل لتحسين الاداء الهايدروحراري و توليد للاعشوائية في الحوض الحراري. ان عملية اجراء الحسابات النظرية والمحاكات للحوض الحراري المدمج تمت بواسطة استخدام تقنية CFD متطور هو ANSYS-FLUENT14.5 الذي يملك قدر كبير لاجراء الحسابات المعقدة بكفاءة ودقة عاليتين. تقوم هذه التقنية بحل معادلات انتقال الحرارة وجريان المائع الطباقي باستخدام طريقة الحجوم المحددة وخوارزمية SIMPLE. شملت الاحواض الحرارية ثلاثة انواع مختلفة من المقاطع العرضية للزعانف الوتدية دائرية (PCP) ومربعة (PSP) وبيضاوية (PEP) وبالاضافة الى الحوض الحراري المسطح بدون زعانف وتدية (FPHS) كحالة قياسية للمقارنة بين الانواع. تم اختبار تأثيرتركيز المائع النانوي (السليكا-ماء) بعدة مقادير ٠,١,٢,٣,٤,٥% مع ٢٠ نانومتر قطر الجسيمات النانوية المتناهية في الصغر ولمدى رقم رينولد يتراوح من ١٠٠الى ١٠٠٠. يتم اختبار تأثير عدد الزعانف الوتدية (١,٢,٣) وموقعها وكذلك اقطار تلك الزعانف الوتدية (١,٢,٣ ملم) كلها عند فيض حراري ثابت بمقداره ١٠^{5} واط لكل متر مربع.

أظهرت النتائج الرئيسية أن أعلى رقم نسلت هو لـ PCP بحوالي ٩٣% مقارنةً مع الماءالنقي و ١٠٠% عند تركيز٥% للمائع النانوي مقارنة مع FP. يتمتع كل من الزعانف الوتدية دائرية المقطع و مربعة المقطع بأدنى درجة حرارة عند قاعدة الحوض الحراري، حوالي ٢٥% للماء النقي و ٥% للسائل النانوي. أضافة الى ذلك، فإن أعلى أداء هايدروحراري هو للزعانف الوتدية بيضوية المقطع بمقدار ١,٤٤ و ١,٥٢ للماء و للمائع النانوي على توالي عند رقم رينولد ١٠٠٠. بينما، عند رقم رينولد ٨٠٠ ، فان الأداء الهايدروحراري الأكثر قيمة هو للزعانف الوتدية دائرية المقطع بمقدار ١.٤٤ و ١.٥٠ للمياه وللمائع النانوي على التوالي. علاوةً على ذلك، فان الزعانف الوتدية دائرية المقطع بعدد ثلاثة زعانف مع قطر كل زعنفة ٢ملم لها اكبر اداء هايدروحراري. بالاضافة الى ذلك، فإن الزعانف الوتدية دائرية المقطع و مربعة المقطع لديهما اقل توليد للاعشوائية بحوالي ٤٢% للماء النقي و ٥ % للمائع النانوي مقارنة مع الأحواض الحرارية الأخرى. وبالتالي ،يوصى باستخدام هذا النوع من أحواض الحرارة مع الموائع النانوية بدلاً من سائل التبريد التقليدي لتبريد نظام إلكتروني.

جمهوريـــــــــة العـــــــــراق
وزارة التعليم العالي والبحث العلمي
جـامعـــة الأنبـــار- كـلـية الـهـندســة
قســـــــم الهندســـــة الميكانيكيـــة

تحسين الأداء الهايدروحراري للأحواض الحرارية وتدية – مستوية الزعانف باستخدام السوائل النانوية

رسالة مقدمة إلى مجلس
كلية الهندسة – جامعة الأنبار
وهي جزء من متطلبات نيل درجة الماجستير
في علوم الهندسة الميكانيكية
من قِبل

أحمد مفيد فاضل
(بكالوريوس هندسة ميكانيكية – ٢٠١٤)

بإشراف

م.د. وسام هاشم خليل
م.د. عامر جميل شريف

١٤٤١ هـ ٢٠١٩ م